EVALUATION AND OPTIMISATION OF SURFACE ROUGHNESS AND TOOL WEAR IN TURNING AISI 304 ALLOY STEEL USING FORMULATED CUTTING FLUIDS

BY

AWODE, Emmanuel Imhanote

PhD/SEET/2016/841

FEDERAL UNIVERSITY OF TECHNOLOGY, MINNA, NIGERIA
MECHANICAL ENGINEERING (INDUSTRIAL AND PRODUCTION ENGINEERING)

OCTOBER, 2021

ABSTRACT

Cutting fluids play a major role in machining operations. They have shown to be instrumental to achieving better machining performance–minimal tool wear, minimal surface roughness and better machining finished product. These characteristics can be attributed to their ability to act as coolant, lubricant and flush away chip formation. The recent trend in the development of cutting fluids is tending towards use of non-edible vegetable based-oil which could be seen as satisfying requirement imposed by health, safety and environmental pollutions and food scarcity. In this work, the development, characterisation and machining parameter optimisation of two non-edible oil base cutting fluid is reported. The non-edible oil extracted from Jatropha and Neem seed –here in referred to as Jatropha seed oil (JSO) and Neem seed oil (NSO) were extracted through cold press process. The characterisation of JSO and NSO showed a viscosity values of 21.30 and 25.10 respectively; pour point values of 260 and 238, and specific gravity of 0.907 and 0.919. In addition, the analysis of Fatty Acid Composition (FAC) of JSO showed a composition approximately 21.6% with Palmitic acid (14.2%) as constituent, while NSO showed composition of 37.0% constituted by palmitic acid (18.0%) and stearic acids (18.0%).
The characterisation of Jatropha oil-based cutting fluid (JBCF) and Neem oil-based cutting fluid (NBCF) (hereafter referred to as vegetable cutting fluids) were conducted to establish the physicochemical properties and FAC. JBCF and NBCF showed pH value of 8.36 and 8.67 respectively and viscosity value of 0.52 mm^2/s and 0.50 mm^2/s. The anticorrosion test (which was based on iron filling method) as well as stability test showed good resistance to corrosion and good stability respectively. The performance of the JBCF and NBCF on turning of AISI304 alloy steel using tungsten carbide cutting tool was further evaluated and optimised using Grey Relational Analysis (GRA). The S/N result showed that an optimal surface roughness of 0.740µm were reached at cutting speed of 1250 m/min (level 5), feed rate of 1.15 mm/rev (level 5), depth of cut of 0.65mm (level 3) for JBCF, and at cutting speed of 1000 m/min l4, feed rate of 0.52 mm/rev (level 1), and depth of cut of 0.1mm (level 1) for NBCF. Similarly, the optimum tool wear of 0.800mm was reached at cutting speed of 500 m/min (level 1), feed rate of 1.15 mm/rev (level 5), depth of cut of 0.65mm (level 3) for the JBCF, and at cutting speed of 630 m/min (level 2), feed rate of 1.0 mm/rev (level 4), depth of cut of 0.10 mm (level 1) for the NBCF. Based on the ANOVA, the cutting speed and depth of cut had significant contribution of 62.73% and 37.26% respectively on the surface roughness and 70.83% and 40.41% respectively on tool wear under both JBCF and NBCF. The experimental result s show NBCF compare favourably to JBCF and MBCF, however, JBCF exhibit minimal surface roughness, minimal tool wear and overall better performance when compared to NBCF and MBCF.

TABLE OF CONTENTS

LIST OF TABLES

LIST OF FIGURES

Figure **Page**

LIST OF PLATES

ABBREVIATIONS

GRA	Grey relational analysis
GRC	Grey relational coefficient
GRG	Grey relational generation
R-sq	Root square
R-sq (adj)	Root square adjusted
(μm)	Micrometre
Mm	Millimetre
m/min	Metre per minute
S/N	Signal-to-noise ratio
Log	Logarithm
OSI	Oxidative stability index
ASTM	American standard test measurement
EPA	Extreme pressure addictive
rev/min	Revolution per minute
mm/rev	Millimetre per revolution
CNC	Computer numerical control
AISI	American iron and steel institute
SAE	Society of automotive engineering
ANOVA	Analysis of variance
MQL	Minimum quantity of lubrication
BUE	Built up edge
RSM	Response surface methodology
FAC	Fatty acid composition
GCMS	Gas chromatography mass spectrum

SYMBOLS

$\tilde{\lambda}$	The distinguishing coefficient, $\beta \in [0, 1]$.
Σ	Sum of individual response
Vc	Cutting velocity
Ra	Arithmetic average of surface roughness
η	Dynamic viscosity
µm	Micro-metre
%	Percentage
K	Ball constant
ρ_1	Ball density
ρ_2	Fluid density

CHAPTER ONE

1.0 INTRODUCTION

1.1 Background to the Study

Several times cutting fluids have been employed during machining process to influence workpiece, tool and chip characteristics to the desired form. The earliest report of machining using water as coolant was presented in 1907 by Taylor; while cutting speed increase by 40%, it enabled high speed steel to machine steel materials (Taylor, 1907). The vegetable oil-based cutting fluids have been the widely accepted options to mineral oil-based cutting fluids owing to some existing properties that are chemical in nature plus the ability to biodegrade. The results of Machining processes have shown and proven why formulated vegetable oil based cutting fluids have highly performed better than mineral oil-based cutting fluids (Lawal *et al.*, 2012). This work evaluates and optimizes the significance of Jatropha oil-based cutting fluid, neem oil-based cutting fluid and mineral oil-based cutting fluid on surface roughness and tool wear in turning of AISI 304 alloy steel with coated carbide inserts using RSM method. One of the main reasons for this work is to find equilibrium that meet scientific and environmental demand for the new cutting fluid during machining process. Therefore, the process for the vegetable cutting fluids formulation requires components selection that are not harmful to both the workers and the environment (Lawal *et al.*, 2014). These formulated cutting fluids are of high importance to the machining industry.

Machining industry has achieved tremendous feat beginning from raw material processing to finished products which involve the application of cutting fluid, technology and certain mathematical model. There are high expectations in the machining industry to minimise both tool wear and surface roughness. In recent times, technological advancement had made it possible to achieve high dimensional accuracies with complex geometry (Taga *et al.*, 2015).

The cutting speed, feed rate and depth of cut are the common parameters that are usually considered during machining experimentation, evaluation and optimisation (Patnaik *et al,* 2020). These parameters have great influence on the machining process. Optimisation of these parameters requires combining the multiple responses obtained from these input factors during machining process, while simultaneously considering constraints like cutting forces and tool wear (Khandey, 2008). Various research and investigations have shown that the optimum process environment that satisfies both quality and productivity during machining operation, considers cutting tool flank wear reduction. The growing demand for productivity improvement plays a major role towards cutting tools invention in relation to material and design (Bhateja *et al*., 2013, Huang & Liang, 2005 & Ghani *et al.*, 2004). The past one hundred years have shown that there have been a lot of consistent development in the performance of cutting fluids as a result of wide range of research and discoveries. For example, there are difficulty in laying claims to the real values obtained for temperature; one of the key component in measuring wear rate for all tool materials is the temperature obtained from machining operation. However, the needed parameters for such calculations have been difficult to establish.

Surface roughness is one major response that cannot be overlooked when considering machining operation on a workpiece. Therefore, deflections and flexing movement must be minimised to get the needed workpiece quality or precision (Khandey, 2008). The suitable combination of distinct corrosion resistance, high level of strength including retention of strength at a well improved temperatures, an attractive and suiting outlook with a good formability, have placed materials from stainless steel as an excellent choice for varieties of application, including boiling water nuclear reactors and piping components to certain kitchen sink (Machado *et al.*, 2006). A lot of existing work have proven that the major wear mechanisms comes from chipping operation, abrasion, fatique, adhesion, oxidation and

diffusion when considering one or more layer coated tool (An *et al.* (2014), Chinchanikar & Choudhury (2013), Sahoo & Sahoo (2012).

Shearing process and friction generate heat coming majorly between workpiece and the tool. The chips carry majority of the generated heat with the left over in the workpiece and the tool, which leads to cutting tool softening and a sizable thermal stress. Therefore, tool cutting edge wears, increase surface roughness on the workpiece. These negative responses on both the tool and workpiece resulted in the need for cutting fluids to minimize heat and lower the chances of defect on both the workpiece and the tool, thereby reducing the catastrophic effect of high temperature level.

The machining characteristics of stainless steel varies depending on the adopted alloying elements. For instance, the compositions of AISI 304 alloy steel is different from other carbon steel series with respect to the properties and features it exhibit. The BSSA (British Stainless Steel Association) describes stainless steel as an iron alloy with 10.5% minimum chromium. There is an oxide thin layer produce by this chromium on the steel surface called 'passive layer', which hinders the surface from progressive corrosion (Patnaik *et al.,* 2020). Therefore, increasing resistance to corrosion is as a result of increased amount of chromium. The impact of varying properties like nickel and molybdenum help increase corrosion resistance and formability enhancement. This comes from some amount of other elements in stainless steel, like carbon, manganese and silicon to varying degrees. Currently, stainless steel are of five various forms:

(a) Stainless steel that are austenitic (b) Stainless steel that are ferritic (c) stainless steel that are duplex (austenitic with ferritic) (d) Stainless steel that are martensitic and (d) Stainless steel that are Precipitation by Hardening (HP).

In recent times, there are various applications amongst several others that requires the use of stainless steel. There is a lot of difficulty in machining austenitic stainless steels. Several steps have been taken to better the machinability of these steels. One of the common features with stainless steels is corrosion resistance. The tendency to develop high built-up edge, high deformation hardening and low heat conduction makes austenitic steel machinability difficult compared to other alloy steel. Therefore, austenitic grade AISI 304 can be largely deep drawn (AZOM, 2019). This characteristic have made AISI 304 a leading grade steel in food processing industries.

The compositions of AISI 304 alloy steel shows the unique properties and features it exhibit. The common and versatile used steel among all of the stainless steel is the AISI 304 and 304L alloy steel (NAS, 2016). They exhibit excellent low temperature characteristics and react well to hardening by cold working. They also exhibit high ductility, forming, excellent drawing and spinning characteristics (ASM, 2016). They are well known to be non-magnetic. However, with low machinability, they can be a bit magnetic when cold worked, and minimal susceptible to intergranular corrosion (ASM, 2016). The ability of a material to be easily machined is termed machinability. The machinability of materials vary from one to another. The carbon content of a material determines the level of its machinability (Anzalone, 2011).

1.1.1 Tool wear

Tool wear occurs when there is gradual failure of the cutting tool as a result of consistent usage. Therefore, tool life is determined by the amount of machining process the tool is involved. In machining processes, tool life is one of the metrics for measuring performance of a tool (Nithyanandhan *et al.,* 2014). The tool wear mechanisms reveals the most dominant type of wear such as abrasion, rake or crater which is sometime caused by high forces, fatique, and impact by chips formation. Factors such as the tool materials, the workpiece materials, the cutting conditions, the cutting operation and the lubricating or cooling systems

play effective roles on tool wear mechanism. Therefore, tool wear mechanisms is the major focus of this study. The need to avoid poor dimensional accuracy and quality of finished product in the machining industry is the main reason for tool wear monitoring (Avinash *etal.*, 2019). Tool wear monitoring involves machine vision development system which is for direct measurement of carbide cutting tool inserts flank wear. The images from the captured carbide inserts are processed with the images from the tool wear zone.

1.1.2 Surface roughness

Surface roughness plays a useful role to determine interaction between object and the environment (ISO, 2020). Surface roughness is a key indicator of the impact of a mechanical part, knowing irregularities may form sites of nucleation for cracks or corrosion on the surface. Surface roughness requires mathematical analysis of the relative roughness of a surface profile by employing one numerical parameter, Ra. The device for measuring surface roughness is surface roughness tester (SRT) or profilometer.This measurement tool determines the workpiece surface finish. Surface finish is an important technical requirement of the customer during machining process. (Nithyanandhan *et al.*, 2014). Therefore, the turning of AISI 304 alloy steel in this study, is for the purpose of evaluating and optimizing surface roughness and tool wear by employing response surface methodology with analysis of variance (ANOVA) using cutting fluids, and tungsten carbide tool on a traditional lathe.

1.1.3 AISI 304 alloy steel

Surface roughness tester is employed to ascertain the surface integrity of the AISI 304 alloy steel. The commonly used grade is the alloy steel which is mostly used in food and chemical processing industries. The alloy steel is also employed in beverage and dairy industries, used as heat exchangers and chemicals that are mild. Presently, stainless steels are a household name involve in everyone's life and greatly involve in wild range of industries

The 18% chromium and 8% nickel stainless steel is a classic that form the basic 300 series. Since the 300 series is the world most commonly used steel grade, it characteristics is responsible for its impact strength (toughness) at both higher and lower temperatures. The resistance to oxidation and corrosion is greatly improved by Nickel. The 'L' and 'H' types are the sub-grades of the 300 series grades. The extra corrosion resistance is aided by the 'L' type grade. The 'L' represents low carbon example 304L and 316L which is about 0.03% and is exclusively for welding. There is a minimum of 0.04% carbon and a maximum of 0.10% carbon in the 'H' grade which is always recommended when the material used, is at extreme temperatures. Though 304 grade is commonly used than 316, both grades 304 and 316 are used in various applications in stainless steel industries ranging from aircraft industries, household appliances, chemical processing industries, and in building nuclear processing plants etc. There are several grades of the 300 series that are commercially available, examples are 301, 302, 303, 304, 308, 309, 316, 304L, 316L, 317, 321 and 347 (http://spiusa.com).

1.1.4 Tungsten coated carbide insert

One of the characteristics that makes tungsten carbide exceptional is the resistance to galling at the surface (Anzalone, 2011). The work shows that tungsten carbide can exhibit minimal dry co-efficient of friction, improved wear resistance and withstand corrosion near noble metals level. The rigidity of tungsten carbide is doubled what is obtained with steel. This carbide possesses high resistance to deformation and deflection and also high impact resistant factor, heat, and oxidation resistance. The material for cutting hard and rigid materials is tungsten carbide, due to its high strength tool material. Tungsten carbide insert have a compressive strength that majority of forged or cast metals and alloys cannot resist. The hard alloy steel characteristics of the workpiece is the primary bases for the choice of this tool material. Generally, there are many types of tool materials that are used in the machining

industries, ranging from high carbon steel to ceramics and diamonds. Toughness and wear resistance are the characteristics of hardness and strength from cutting needed to produce quality and enduring parts that are economically viable. The experience of thermal deformation from machining operations on the workpiece and tool are a combine effect of friction-induced heat and plastic strain. This leads to rise in both surface roughness, tool wear and thermal error increase, resulting in increase in temperature during machining operation. Hence, the characteristics of the workpiece determines the variety of cutting tool materials that should be employed for the machining operation. In Summary, the need for suitable tool material that can reduce surface roughness, withstand the highest cutting force, high temperatures and wear resistance, has led to a continuous search in the machining industry (Anzalone, 2011).

1.1.5 Cutting fluids

The commonly used fluid during machining operation is known as cutting fluid. Most often, these fluids used for cutting are also refer to as coolant. A cutting fluid does many functions and cooling the tool and workpiece is just one out of the several functions (Club technical, 2019). Cutting fluids contribute to machining process because it acts as lubricant by reducing friction and thereby reducing the heat generated (Ademoh *et al.*, 2016). Also, the cutting fluid act as an effective coolant, because frictional heating cannot be completely eliminated and often, not even substantially reduced. Cutting fluid could act as an anti-weld agent by chip flushing to stop the tendency of the work material to weld the tool under heat and pressure (Ademoh *et al.*, 2016). Although, machining performance has effectively improved as a result of cutting fluid usage, traditional metal cutting fluids are becoming a devalued added cost to businesses in recent times in the machining industry (Singh & Gupta, 2006). There is a decrease in enterprise profit margins due to onerous regulatory and environmental burdens. Legislation of ISO14000 environmental series and lubricant industrial users are encouraged

to minimize, remove or replace metal cutting fluids from their form to a suitable substances that is environmentally friendly (Richard *et al.,* 2004) and (Singh & Gupta, 2006).

One of the commonly viewed and employed variable that is needed for high quality machining operation is the cutting fluid, because it prevent overheating of both workpiece and cutting tool, improves workpiece quality, and minimises cutting tool wear. Cutting tool transform raw material workpiece into desired workpiece during machining. Cutting parameters such as cutting speed, feed rate and depth of cut, are major factors that determine tool wear and tool life. The work of Kuram *et al.* (2013) shows that cutting fluid that is termed excellent must not be harmful and toxic to the operators' health, it must also be hazard-free, affordable and should be smoke-free or fog-free when in use. Kuram *et al.* (2013) also revealed that cutting fluids are seen as either mineral oil base or vegetable oil base. However, based on their chemical formulation, cutting fluids are classified under: straight oils (non-emulsifiable), soluble oils (emulsified oils or emulsions), synthetic oil (non-mineral oil but formulated from alkaline organic and inorganic compounds), and semi-synthetic oil (combination of the soluble oils and synthetic fluids).

Metal cutting process employs cutting oils with no dilution such as neat oil or straight cutting oil obtained from petroleum, animal or vegetable. Though these cutting oils have good lubrication, but they exhibit poor cooling properties with increased fire risk (Kuram *et al*., 2013). Sometimes hazardous substances in form of smoke or mist is experienced during machining by the machining operators. These authors observed that low temperature and low speed cutting operations limits the use of cutting oil. The characteristics of emulsified oils is oil droplets suspension in water. Therefore, the emulsion in water stability is improved by blending oil with emulsifier agents mostly anionic and soaps (Kuram *et al.,* 2013). A typical example of oil-in-water cutting fluids composition is as follows:

Base oil (mineral or vegetable) + emulsifier + injected additives

Injected additives
- Agents of neutralisation
- Inhibitors of rust and corrosion
- Additives for lubrication (anti-wear and EP additives)
- Biocides
- Inhibitors that foam

where EP = Extreme Pressure

The oil-in-water is dispersed with the introduction of emulsifiers in order to establish a stable oil-in-water emulsion. The amount of emulsifier increase, influences rise in pH, kinematic viscousity and thermal conductivity. The reduction in the amount of emulsifier influences the reduction in fire and flash points (Rao & Sirikant, 2007). The amount of critical property of soluble oils comes from emulsion stability that boast the highest. There must be sustenance without separation for minimum of six months of the cutting fluids concentrate (Kuram *et al.*, 2013). The presence of water in emulsion induces growth of bacteria, rust, losses of phosphorus, chlorine and sulphur based chemical additives known as EP (extreme pressure) additives, employed under extreme pressure conditions alone (Kuram *et al.*, 2013). Therefore, the means where extreme pressure additives form lubricant layer that are solid between cutting fluid and the metal surface is refer to as chemical reaction. The criteria for extreme pressure additives to be able to lower friction and wear significantly is good anti-weld properties and low shear strength (Kuram *et al.*, 2013).

Semi-synthetic fluids contain small amounts of oil and other additives like anti-oxidants and bioxide which enhance lubrication while providing better cooling property. One of the common characteristics possessed by these semi-synthetic fluids with soluble oil and synthetic cutting fluids, is less corrosion protection, lower lubricity and possible skin irritants. Synthetic or chemical fluids do not have oils; the content is a mixture of alkaline organic and

inorganic compounds, along with corrosion inhibition additives. Most times these oils offer high performance of cooling, quick ability to wet and low tension at the surface. These oils do not produce smoke or reject tramp oils. The chemical oxygen is at high level and possesses minimal lubricity needs. The advantages and disadvantages of the various cutting fluids are presented in Table 1.1.

Cutting fluids possess a lot of those liquids and gasses that are needed and are applied to the tool and the workpiece that is machined. A lot of quantities are employed every year to achieve a number of objectives. For example, cutting fluids prevent tool overheating, cool workpiece, reduce surface roughness, prevent corrosion of workpiece, aid satisfactory chip formation, prevent inaccurate final dimensions from machining results, flush away chip from the cutting zone and reduce power consumption. In conclusion, the right cutting fluid can reduce the number of unplanned stoppages and increase the life of both the tool and the cutting fluid (Richard, 2021).

1.1.5.1 Physicochemical properties of oils for cutting fluids

A study was carried out to evaluate the compositional quality of oils with the need to investigate the effect of using the same oil for repeated analysis. This study was based on the physiochemical properties of vegetable oils with respect to density, saponification value (SV), viscosity and iodine value (IV), boiling point, peroxide value (PV). The test analysis definitely changed the sensory properties and physiochemical nutrition of the oils. Oils and fat exhibit triacyglycerol and lipids naturally. The chemical composition includes saturated and unsaturated fatty acids and glycerides. The quantitative evaluation of heated oils requires employment of various analytical forms, such as ultra-visible spectrometry (UV), gas chromatography (GC), high performance liquid chromatography (HPLC) and Fourier transform infrared (FT-IR) spectroscopic techniques. The ease of sample handling gives the FT-IR, an advantage over the physical and chemical method. Also, FT-IR exhibits quickness,

minimal quantity of harmful solvents, signal to noise ratio improvement, scan time reduction and consistent high energy requirement. Therefore, all wavelengths are simultaneously recorded in this technique.

Table 1.1: Comparism of the different classes of lubricants (Kuram *et al.*, 2013)

Neat Oils	Emulsifiable Oils	Semi-chemicals	Chemicals
Advantages			
Satisfactory lubricity	Standard lubricity	Standard cooling	Satisfactory cooling
Satisfactory rust control	Standard cooling	Standard rust control	Satisfactory microbial control
		Standard microbial control	Non-flammable, non-smoking, good corrosion control
			Reduced misting and foaming problems
Disadvantages			
Minimal cooling	Problems of rust control	Foam easily	Poor lubricity
Fire hazard	Growth of bacteria	Water hardness affect stability	Other machine fluids cause contamination easily
Smoke or mist created	Evaporation losses	Other machine fluids cause contamination easily	Low speed Heavy Duty Cutting limitation

The formulation of a new generation of cutting fluids that delivers high performance machining and environmental friendliness could be realised with the use of vegetable oil base stock (Alves & Oliveira, 2008). Vegetable oils are generally extracted from plants and they are known to be triglyceride. Triglycerides are known to have lower densities compared to water, and may be solid (fats or butters) or liquid (oils) at normal room temperatures. Triglycerides which are also called Triacylglycerol (TAG) are made from glycerol molecules with three long chains fatty acids attached at the hydroxyl groups via ester linkages. These analysis shows that vegetable oil can prolong tool life, minimise surface roughness and improve the performance of cutting when compared to mineral oil (Kuram *et al.*, 2013; Woods, 2005).

1.1.5.2 Jatropha oil based cutting fluids

Cutting fluid that is jatropha oil-based is obtained from jatropha which is a genus in the spurge family that develop substances that are toxic to protect them against animals and other pests (BioPro, 2015). Jatropha shows a pattern of suitable fatty acid that is uniquely grown as a lone crop so as to stay off animal feed production competition and direct food competition (Winter *et al.,* 2012). The use of cutting fluids from jatropha oil-based are gradually gaining popularity in machining as a result of environmental and health impacts associated with the traditional mineral oil (Kazeem & Adesina, 2020). Jatropha oil based cutting fluid is employed as an anti-wear fluid and modifies friction as a result of their good interaction with the surfaces with which they are engaged (Joao *et al.,* 2019). This work seeks to characterise, evaluate and optimise unpopular vegetable oils like jatropha oil as machining cutting fluids. The effects of jatropha oil emulsion on tool wear and surface roughness in turning AISI 304 alloy steel using tungsten coated carbide insert were carried out in this work and compared with the traditional mineral oil. This study shows an evaluation of a jatropha oil-based cutting fluid during machining operation.

1.1.5.3 Neem oil based cutting fluids

Vegetable oils have proven in many instances to be a viable option for use as cutting fluid especially considering the added advantage of environmental degradation. The challenge is finding out whether neem seed oil can be used as cutting fluid. Nigeria is situated in tropical region of the world where temperature rarely drops to 8°C, hence, characterised and formulated Neem oil is suitable as coolants and can readily be poured (Ademoh *et al.*, 2016).

1.1.6 Response surface methodology

Response surface methodology (RSM) is a collection of mathematical and statistical techniques that are useful for modeling and analysis of problems in which a response of interest is influenced by several variables, and the objective is to optimize this response

(Montgomery, 1997). Once the problem is determined by the researcher including the experimentation dormain and the response, the RSM provides strategic experimental alternatives and viz-a-viz the requirement to evaluate them. The main advantage is that this adapted experimental task to the problem under study is achieved before the experiment is carried out. There is a three-dimensional space response surface which are flat planes or, interwoven plane in the interactions case obtained from the modelled two-level factorial designs (Sarabia & Ortiz, 2009). It is also reported that the two-level factorial designs are basically screening methods use to identify the important input variables in a typical project. In some situations, it can be satisfactory for the purpose of optimisation. However, there is often a significant curvature exhibited by response surfaces (Sarabia & Ortiz, 2009).

A lot of achievements have been made in terms of science and technology, with respect to high demand on machining activities in the manufacturing industry, and are directed most times on the machine shops practice (Rajesh, 2014). The difficulties in most production industries is the inability to minimise production cost, improve quality of product and increase production rate. One of the most specified customers' requirements in machining of parts is surface quality (Molńar, 2011; Uppal, 2013). Thus, the need for high precision parts means that, machined products should reach the minimal possible surface roughness. Various parameters such as cutting speed, feed rate and depth of cut determines a satisfactory surface quality during machining (Makadia & Nanavati, 2013). This means that factors that influence tool wear and surface quality in machining are cutting parameters, tools and workpiece material properties, and cutting conditions (Molńar, 2011; Uppal, 2013). In turning operation among other metal cutting processes, tool wear and surface roughness depend mainly on cutting speed, depth of cut and rate of feed (Makadia & Nanavati, 2013). Others are cutting fluid and its application, cutting force, cutting temperature, machine vibrations, mechanical properties of workpiece, some other properties of the workpiece material, and tool nose

radius. Some challenges faced by a lot of metal cutting industry are minimal tool wear and quality surface finish which is a criteria in order to achieve optimum operating conditions for the machine tool. However, these challenges are beginning to be handled by both researchers and machinists from the industry.

1.2 Statement of the problem

A lot of progress have been made in the machining industry in developing quality finished steel products using mineral cutting fluids. However, the environmental challenges pose by these mineral based cutting fluids including the non-biodegradable and non-recyclable types have raised serious concerns in the research community and prompted the renewal of research in this area and with focus on replacing the mineral-based cutting fluids with environmentally friendly cutting fluids. Another dimension of the challenge in the use of environmentally friendly cutting fluid in machining processes is that most of these oils are edible, and often leads to competition between consumption and its application for machining processes. It has been established by several researchers including Kazeem & Adesina, (2020), Lawal *et al.*, (2014), Alves & Olivera, (2008), that these environmentally friendly cutting fluids compete favourably with mineral-based cutting fluids. Therefore, this research focuses on the use of non-edible oils to formulate cutting fluids and its effect on machining characteristics when turning AISI 304 alloy steel with tungsten coated carbide cutting tool.

1.3 Aim and Objectives of the Study

The aim of this research is to evaluate and optimise surface roughness and tool wear during turning of AISI 304 alloy steel, using formulated cutting fluids. The specific objectives are to:

i. Determine the physicochemical properties of the two vegetable oils
ii. Formulate and characterise emulsion cutting fluids developed from vegetable oils

iii. Determine the contribution of cutting speed, feed and depth of cut as individual factors on the responses under different turning conditions.

iv. Determine the optimal conditions using the Grey Relational Analysis (GRA).

1.4 Justification of the Study

The importance of this study is to minimise both tool wear and surface roughness by evaluating and optimising the effects of cutting fluids on tool wear and surface roughness during turning operation. These was done by developing the two bio-degradable, non-harmful formulated cutting fluids from two plants seeds that are grown in Nigeria. The two vegetable cutting fluids were characterised and the fatty acid composition were analysed to ascertain the performance of each of these vegetable cutting fluids. Therefore, an effective approach for the optimization of turning parameters based on the Response Surface Methodology (RSM) was used, and the results from both responses were obtained. The wet cutting condition using two non-edible cutting fluids (jatropha curcas (jatropha) and azadirachta indica (neem) oils) was used and compared with mineral based cutting fluid, in order to determine the tool wear and surface roughness.

1.5 Scope of the Study

This study focuses on the tool wear and surface roughness measurement on AISI 304 alloy steel in a turning process using optimal parameters. RSM via minitab was designed and employed because it is usual friendly, precise and create allowances for each of the input parameters. The three parameters that is cutting speed, feed rate and depth of cut were investigated using the formulated cutting fluids (jatropha and neem) and compared with mineral oils. This study was limited to evaluating and optimising two responses (tool wear and surface roughness) using the characterised and formulated cutting fluids. The optimal

parameters were obtained using the grey relational analysis (GRA) which shows the combined optimal factors from the individual responses.

Chapter 2 present the various literature reviewed, for both surface roughness and tool wear, which helped to establish the research gap from the various work of the authors reviewed. The research gap sum up the basics for this thesis work and the findings made.

CHAPTER TWO

2.0 LITERATURE REVIEW

2.1 Tool wear and surface roughness in turning operation

The gradual failure of cutting tool as a result of continual operation is referred as tool wear. Therefore, one or more of the following wear modes may occur during operation: (a) flank (b) notch (c) crater (d) edge rounding (e) edge chipping (f) edge cracking and (g) catastrophic failure. Cutting tools are subjected to an extremely severe rubbing process. They are in metal-to-metal contact between the chip and work piece, under conditions of very high stress at high temperature. The situation is further worsened due to the existence of extreme stress and temperature gradients near the surface of the tool. During machining, cutting tools remove material from the component to achieve the required shape, dimension and minimal surface roughness. However, wear occurs during the cutting action, and it will ultimately result in the failure of the cutting tool. When the tool wear reaches a certain extent, the tool or the tool active edge has to be replaced to guarantee the desired cutting action. The common wear operations are mostly crater and flank wears.

Rake face wear and or Crater wears: The chip flows across the rake face, resulting in severe friction between the chip and rake face, and leaves a scar on the rake face which is usually parallel to the major cutting edge. The crater wear can increase the working rake angle and reduce the cutting force, but it will also weaken the strength of the cutting edge. There are

certain parameters used to measure the crater wear. The crater depth KT is the most commonly used parameter in evaluating the rake face

Flank wear (Clearance surface): Wear on the flank (relief) face is called flank wear and results in the formation of a wear land. Wear land formation is not always uniform along the major and minor cutting edges of the tool. Flank wear most commonly results from abrasive wear of the cutting edge against the machined surface. Flank wear can be monitored in production by examining the tool or by tracking the change in size of the tool or machined part. Flank wear can be measured by using the average and maximum wear land size *VB* and VB_{max}. The schematic diagram for machining process adopted for this work is as shown in Figure 2.1 (Amouzgar *et al.,* 2018).

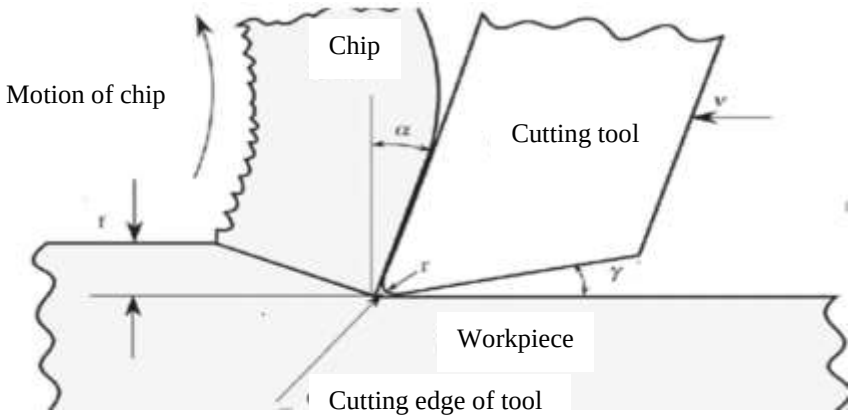

Figure 2.1: Schematic Diagram of Turning Operation (Amouzgar *et al.,* 2018)

where α is rake angle, ϒ is clearance angle, *r* is Nose radius, f is feed, and *v* is speed.

This ability to consider individual contribution will provide good surface finish on work material (Guide, 2015). Recent studies have also shown that crater wear promotes low cutting speed due to cycle of adhesion of work material and its removal. Also, the surface roughness of workpiece can be known with the aid of a mathematical or statistical model using cutting variables (Lin & Chang, 1998). Therefore, the growing need to minimise tool wear and surface roughness necessitate the application of machining operation such as turning.

Turning is a machining operation that removes metal from the outer diameter of a rotating cylindrical workpiece (Khandey, 2009). Turning operation causes the reduction of the diameter of the workpiece, normally, to a required dimension, and smooth finish on the metal is achieved. Most times, the workpiece will be turned so that adjacent sections have varying diameters. The machining operation that produces cylindrical parts is turning. The work of Yang and Tarng (1998), used turning operation to design the optimisation of cutting parameters for turning operations based on the Taguchi method as shown in Figure 2.2. Thus,

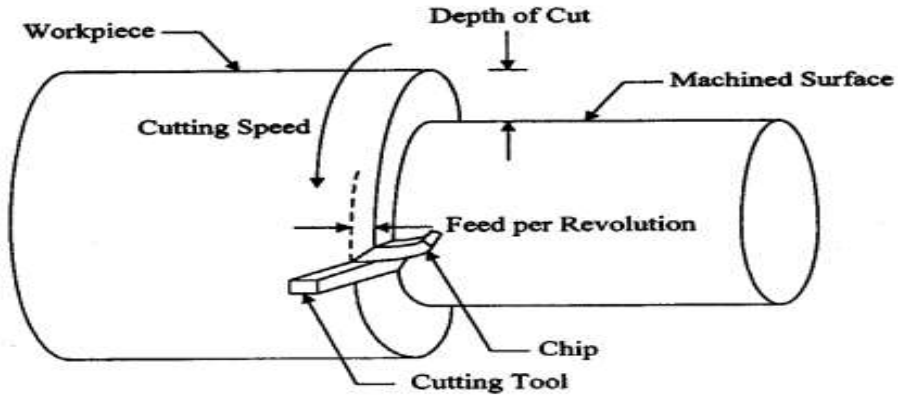

proper selection of the cutting parameters, are often accomplished using mathematical models, based on statistical regression techniques or neural computing (Chua *et al*., 1993). One of mathematical models that is normally employed to ascertain the desired cutting parameters is the Taguchi method. Therefore, to achieve the desired finished products, the experimentally designed methods need to be employed.

Figure 2.2: Basic Turning Operation (Yang and Tarng, 1998)

Aside turning, another widely used material removal process in the manufacturing industry is drilling. Material removal process that requires responses such as wear and cutting force must consider the design objectives along with the cutting tool (Yan & Jiang, 2013); Alot of design objectives have been employed in recent times that involves modelling and optimization

(Tandon, 2008; Hsieh, 2008). Nevertheless, numeric approximation and controversial precision could undoubtedly be depended upon (Hsieh, 2008; Wu *et al.*, 2010). In recent works, a lot of researchers and machine manufacturers attract the parallel kinematic machine due to flexibility with high structural rigidity, high accuracy and high speed which gives an edge (Wang & Tang, 2003). Etory *et al.* (2014), carried out appreciable and significant work on drilling operation by conducting milling experiments with 6mm space diameter solid carbide tools at different feed rate, radial depth of cut and contact angle on AISI P20 workpiece. Kadivar *et al.* (2014) investigated the effect of ultrasonic vibration on drilling force, reduction of burr size and surface roughness with two vibration systems. Though, recent experimental studies used PVD and CVD coated carbide inserts under dry milling in order to assess the machinability of steel, some other studies used cemented carbide inserts on surface roughness, tool wear and vibration of workpiece in boring operation (Rao & Kalyankar, 2014). Therefore, the need for surface roughness on friction and wear behaviours during test was carried out on brass sliding against steel using a wear model (Hanief & Wani, 2015).

Micro-milling is also one of the micro-mechanical machining processes (Emel & Babur, 2013). A lot of work have been carried out to design and fabricate tools for micro-milling, which uses tools that are miniature obtained from macro-tools (Fleischer *et al.*, 2008; Cheng *et al.*, 2011). Machining performance optimisation requires Taguchi method in micro-machining and grey relational analysis (Krishnamoorthy *et al*., 2012). Micro-milling, micro-drilling, micro-turning and micro-grinding are all micro-mechanical machining that has become front burners and areas of attraction of late, due to its ability in making structures of two dimension and a third dimension (21/2 D), and microstructures that are real three dimensional (3D) (Shelton and Shin, 2010). However, setbacks such as tool life uncertainty (Rahman *et al*., 2001), burr formation (Mian *et al.*, 2010), reality of chatter (Mascardelli *et*

al., 2013), error of tool alignment (Jun *et al.,* 2007), tool interfaces that is high friction due to workpiece rubbing (Marcon *et al*., 2010), and poor quality surface (Schaller *et al*., 1999), limit performance.

Tool wear monitoring has been discovered to be a hard process in micro-milling and steps have been taken in recent times to address the difficulty (Zhu *et al.,* 2009). Complex 2D and 3D shapes manufacturing is achievable from advance variety of engineering materials which produce micro-milling and micro-components that were successfully machined using micro-milling operation. Afazov *et al.* (2010), Ramesh *et al*. (2012), noted that for surface roughness Ra, when it comes to feed per tooth which holds significant factor, there was consistency in the results of micro-milling when compared with macro-machining. However, as a result of the uncertainty in tool life, it is always a difficult situation when micro-milling hardened steel (Ding *et al.,* 2011; Bissacco *et al.,* 2008). Hence, any contrast between a new and a used tool resulting from built-up edge (BUE) is termed as "wear" (Tansel *et al*., 1998).

Aside milling, basic challenges often exist in grinding materials like forces from large grinding (Yu *et al.,* 2016; Guo *et al.,* 2011; An *et al.,* 2015), temperatures from high grinding (Shen *et al.,* 2014), and deep tool wear which is due to thermal conductivity, excellent heat stability, and high-temperature plasticity (Huddedar *et al*., 2012; Yao *et al*., 2013). The behaviour of wear of abrasive tools often makes symbolic effects on the quality of machined surface and the life of the tool (Zhang *et al*., 2011; Yu *et al.,* 2015; Yu *et al*., 2014). This is caused by the grinding behavioural effects of material removal which is often produced by several wear of the abrasive tools. In recent times, landmark achievement and growth have been reached in single grain grinding method with increasing research work made on grain wear behaviour applying method of single grain grinding (Rasim *et al.,* 2015; Tian *et al.,* 2015; Wu *et al.,* 2016). Grinding forces and wear resistance of abrasive grains from grinding mechanism are deeply influenced by shape of grain and angle of rake (Malkin *et al.,* 2008).

Sharif *et al.* (2016), presented good feedback with respect to cutting forces, specific energy, temperature and surface finish. The outcome of variables related to air delivery mechanism is not reported yet. However, some authors reported work on the gains in terms of productivity (Damera and Pasam, 2008). Overtime, many alternatives to cooling techniques like nanofluid minimum quantity lubrication, biodegradable coolants, cryogenic cooling and minimum quantity lubrication have been carried out (Mao *et al*., 2014). Recently, other options that have been embraced is the use of solid powder as lubricant (Tsai and Jian, 2012; Prabhu, 2015).

2.1.1 Cutting fluids for machining operations

The high demand for qualitative workpiece product in various machining industries have made cutting fluids very essential element in the metal-work industry (Muniz, *et al.*, 2008). The function of lubricating, cooling, cleaning, protecting (anti-rust), improving surface quality among others, has made metal cutting fluid, a highly essential additive in metal cutting process (Yu *et al.*, 2010). Therefore, cutting fluids play a major role in the productivity of machining operations, prevent the cutting tool and machinery from overheating and also improve tool life and workpiece quality (Kuram *et al.*, 2013). Though it is sometimes loosely called lubricants or coolants, cutting fluids are liquids and gases used on the tool and workpiece to help achieve better machining operations (Jain & Chitale, 2010; Jain, 2009).

The need to dissipate heat, lubricate the cutting zone (tool- workpiece and chip interface) to lower friction and carry away chips from cutting zone necessitates the introduction of cutting fluids (Lawal *et al.*, 2014; Anzalone, 2011). This is in line with several vegetable oil-based

cutting fluids which have been used to carry out other machining operation in recent times. Various experimental design method have also been developed and employed along with regression analysis (RA) to predict values of tool wear, surface roughness and other responses using these vegetable oil-based cutting fluids. The application of cutting fluids has helped to determine the lowest point of the determined response values (Kuram *et al.*, 2010). Summarily, these aforementioned authors observed that vegetable cutting fluids were more effective on the reduction of tool wear, surface roughness and other related responses than the commercially available cutting fluids.

The major task facing metal-based industry is increasing the productivity and the quality of machined parts. Therefore, the need to focus and monitor all aspects of the machining processes is very important in order to achieve reliable results from the responses considered (Suhail *et al.*, 2011). The author discovered that tool wear and surface finish were key factor in determining the quality of machined parts. The condition and relation within production have changed significantly as a result of improvement and development of new technologies and the introduction of numerically controlled machine tools (Bajic & Majce, 2006). The production of desired quality workpiece is the goal of machining operations (Bajić *et al.*, 2012; Uppal, 2013). The achievement of high quality machine parts, with minimal tool wear, quality surface finish, workpiece dimensional accuracy, high production rate, minimal machining cost and increase in the performance of the products with reduced environmental impact are the challenges and the major focus of modern machining industries (Thamizhmaanii and Hassan, 2006).

The use of higher cutting speed and feed rates had been shown to achieve higher productivity during machining process (Molnar, 2011; Uppal *et al.*, 2013). High temperature generated at the workpiece-chip-tool interface is as a result of the increase in the cutting speed and the feed rates. The tribological characteristics of the workpiece-tool-chip system during

machining process have been improved, often with the use of cutting fluids (Lawal *et al.*, 2014).

A variety of cutting fluids are widely available nowadays. These cutting fluids are categorize into:

i. Cutting, neat or straight oils,
ii. Soluble oil (emulsified oils, emulsions),
iii. Synthetic (chemical) fluids,
iv. Semi-synthetic (semi-chemical) fluids, and
v. Gases.

Though cutting fluids have been shown to improve machining operations, it has also been linked to a lot environmental and health hazards (skin damage, respiratory difficulty and body contamination) which neccessited proper evaluation of the risks (Alves & Oliveira, 2008; Kuram *et al.*, 2013). Mineral-based oil form a significant portion of cutting fluids employed as lubricants. These mineral oil-based cutting fluids have caused adverse effects on the environment and the health of machine shop workers (Kuram *et al.*, 2013). These mineral oil-based, can also damage soil and water resources, causing adverse environmental effect. Health problems such as skin and respiratory challenges may be experienced by machine operators as the negative effects of cutting fluids on shop floors (Alves & Oliveira, 2008). These hazardous effects is the reason for the application of near-dry cutting application called minimum quantity lubrication.

Minimum quantity lubrication (MQL): a near-dry cutting application and use of biodegradable vegetable oil-based cutting fluids have been employed as a substitute for conventional mineral oil based cutting fluid in order to reduce the adverse environmental and health effects associated with this cutting fluid (Kuram *et al.*, 2013). The introduction of

vegetable oils as base stock, have improved quality performance in machining along with good environmental compatibility.

Nowadays, the industries have intensified the search for the appropriate cutting fluid that will suit every machining operation. A lot of limited successes have been experienced in machining processes due to direct dry cutting, cryogenic applications and the use of fluid of different properties. The formulation of vegetable oil-based cutting fluids is to combat the adverse health and environmental issues related with mineral-based cutting fluid. These formulated vegetable oil-based stock otherwise known as vegetable oil-based cutting fluids are sourced from vegetable seeds such as coconut, sunflower, canola, cotton, soya, neem and jatropha, among others (Alves & Oliveira, 2008). The effects of these vegetable oil-based cutting fluids in machining operations have been proven from recent work. Alves & Oliveira (2008), revealed that there is no adverse effect to the health of workers or to the environment from these recently developed vegetable oil cutting fluids, and are also biodegradable.

2.1.1.1 Fixed oil-based cutting fluids

Extracts from plants and animal fats are referred to as fixed oils. Oleochemistry results show that the use of vegetable oils and fats allows the development of competitive products, which are friendly to both the consumer and the environment (Hill, 2000). Plants and animals raw materials (tallow, lard) are the sources of oleochemical oils and fats; the most important ones are the vegetable raw materials such as soybeans, palm, rape seed and sunflower oils, owing to the amount involved (Hill, 2000). Research on green chemistry fats and oils also known as oleochemical raw materials shows that there is tremendous increase of approximately 3% yearly in the production of oil and fats from plants and animals (Hill, 2000). It is extimated that this trend will be sustained in the medium and long terms. Alternatives to the conventional mineral oil products is why these oils and fats are used as surfactants in

cosmetic formulation, plastic additives or components for composites or polymers and fatty acid-based esters in lubrication sector. The application of vegetable oil products as lubricants in the form of hydraulic oils chain-saw oil and gearbox oils is gaining ground (Hill, 2000). The long term potential of biodegradable lubricants in Europe is estimated to be 10 - 20% of the total market ($5 – 10 \times 10^5$ tonnes per year), while in 1997, 40,000 tonnes of biodegradable lubricants which is about 4.5% of the total market, were sold in Germany (Hill, 2000).

The use of plant seeds in the formulation of cutting fluids for machining operations is now the order of the day in the machining industries. These vegetable seed oil cutting fluids have demonstrated better performance when compared to mineral oil-based cutting fluids. These plant seed oil-based cutting fluids have noticeably produce better machining responses due to their biodegradability and non-toxic properties. Jatropha curcas and neem oil in recent time, are beginning to be a house hold name in Nigeria, owing to the abundance of rich content they both possess. Production of biodiesel oil seeds from jatropha curcas, sourced in Nigeria have been investigated (Aransiola *et al.*, 2012). Studies on the use of Jatropha curcas plant revealed that it has oil yield of 47.5% and 49.1% compared to oil yield of 39.7% from neem (Akintayo, 2004; Martin *et al.*, 2010). Jatropha curcas and neem oils are two plant seeds that meet the criteria for use as base stock in the production of vegetable oils for the formulation of cutting fluids in Nigeria. The oil content of these two plant seeds are shown to be higher than cotton seed (36%) and soybean (20%), with Jatropha curcas seed oil content higher than palm kernel (40%) and peanut (49%) (Agiang *et al.*, 2010; Ayinde *et al.*, 2012).

Aransiola *et al.*, (2012) in their work presents the fatty acid composition analysis from typical vegetable oils. These authors work shown in Table 2.1, shows the saturated, monosaturated and polysaturated compositions of the vegetable oils.

Table 2.1: Fatty acid compositions of typical vegetable oils (Aransiola *et al.*, 2012)

Fatty Acid	Jatropha seed oil	Neem seed oil
Myristic 14:0	0.1	-
Palmitic 16:0	14.2	18.1
Palmitoliec 16:1	0.7	-
Margaric 17:0	0.1	-
Stearic 18:0	7	18.1
Oleic 18:1	44.7	44.5
Linoleic 18:2	32.8	18.3
Linolenic 18:3	0.2	0.2
Arachidic 20:0	0.2	0.8
Saturated	21.6	37
Monounsaturated	45.4	44.5
Polyunsaturated	33	18.5

The work of Aransiola *et al.* (2012) work went further to present the physiochemical properties analysis from typical vegetable oils. The authors work in Table 2.2 shows the individual physicochemical properties of the vegetable oils.

Table 2.2 Physicochemical properties of typical vegetable oils Aransiola *et al.*, (2012)

Properties	Neem seed Oil	Jatropha seed Oil
Acid Value (mgKOH/g)	32.538	35.8
Iodine Value	81.28	-
Viscosity (cSt)	30^{o}C 43.75	room temp 41.4
Saponification	199.86	193
Physical state at room temperature	Liquid (Golden yellow)	Liquid (Golden yellow)
Cloud point (^{o}C)	13	10
Pour point (^{o}C)	7.0	2
Density at room temperature (Kg/m^{3})	918.2	895

2.1.1.2 Jatropha seed oil

Jatropha curcas is a typical plant of the genus *Euphorbiaceae*. The plant grows under various climatic conditions and is able to survive in arid regions with poor and stony soils, not suitable for food cultivation (Becker & Makkar 2008; Heller, 1996). During the last two decades the interest in its exploitation increased since jatropha seeds are rich in nonedible oil which can be processed to biodiesel (Juan *et al.,* 2011; Nazir *et al.,* 2009). However, in order to ensure the sustainability of Jatropha cultivation there is an urgent need for additional processing routes taking into consideration the by-product from oil extraction, namely, the jatropha meal. The meal offers a protein content of up to 40% (Becker & Makkar, 2008).

Shivani *et al*. (2011), investigated the extraction and analysis of Jatropha curcas seed oil. Jatropha curcas is a versatile shrub with several applications and many economic potentials for its seed oil, which can be turned into biodiesel (an alternative to petro-diesel). It aims to turn around energy challenges and also to minimise environmental changes. The fact that the oil of Jatropha curcas is not readily edible makes its usage very attractive and devoid of competition from other edible vegetable oils.

The present study deals with oil extraction by various methods and its physico-chemical analysis. Figure 2.3 shows the Jatropha seeds optimized using organic solvents to get the jatropha seed oil. The effects of parameters on the oil extraction namely type of organic solvents and different techniques were also considered to optimize the processing conditions for achieving maximum oil yield with the acid value and antioxidant property of the oil were also investigated. The maximum oil yield was obtained by using Soxhlet extraction method and hexane as a solvent.

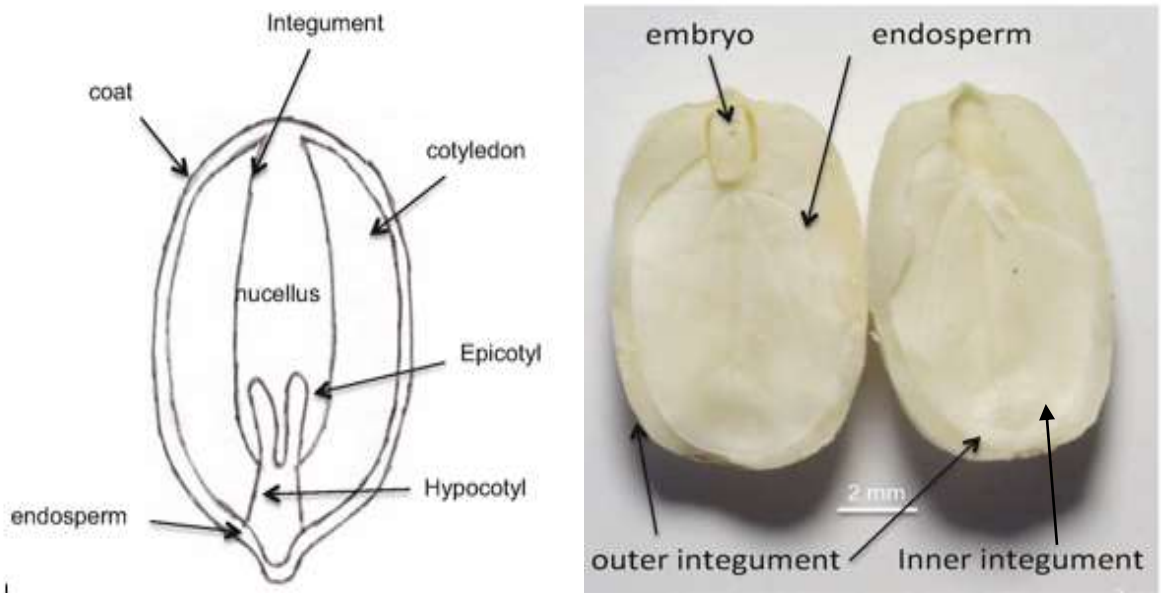

Figure 2.3: Jatropha Curcas Seed (Source: Huerta-Ocampo & Barba de la Rosa, 2019)

2.1.1.3 Neem seed oil

Neem seed oil also known as azadirachta indica oil originates from India as one of the richest sources of secondary metabolites in nature and grows as a tree found in the temperate woodlands of southern West Africa (Gossé *et al.,* 2007). Traditionally, the products of the tree (leaves, bark and seed) are used for medicinal purposes. The ripe seeds of neem could be available in the month of June. The fruit and the shell removed (endocarp) can be opened to collect the seed, then sun-dried and ground for extraction (Gossé *et al.,* 2007). Apart from medicinal purposes, it is rich in skin and hair treatment. Earlier studies have found the presence of fatty acids and oily substance in the extract of the neem seed (Robbers *et al.,* 1996; Wodarz & Nowak, 1999). Neem seed oil is a good anti-corrosion agent, and is often used as a value-added additive in the formulation of cutting fluid (Shamar *et al.,* 2009). The fatty acid composition is important in determining the stability of the properties of the oil (Shamar *et al.,* 2009). The dry neem seed with it chemical chain $C_{35}H_{44}O_{16}$ is shown in Figure 2.4.

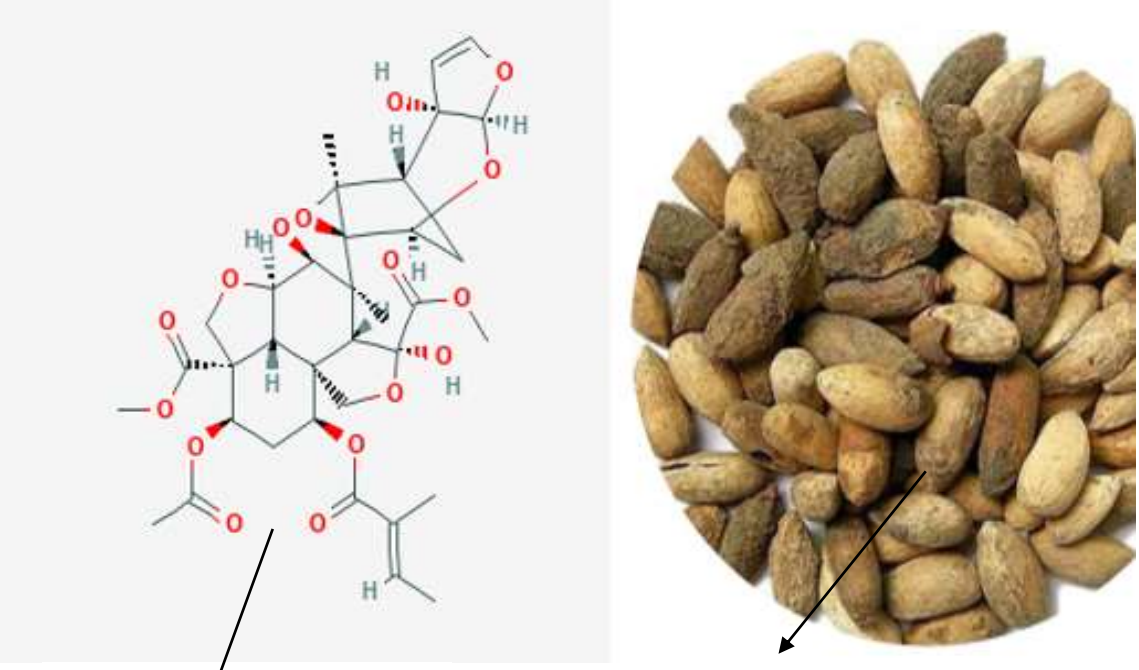

Figure 2.4: Dry Neem Seed with its chemical chain (Source: CAS Common Chemistry, 2021)

2.1.2 Properties of vegetable oil suitable for based cutting fluids

Kuram *et al.* (2013), revealed that vegetable oils consist of triacylglycerides (triglycerides) which are glycerol molecules with three long chain fatty acids attached at the hydroxyl group via ester linkages. Desirable properties of lubricants are provided by the triglycerides structure of vegetable oils. High strength lubricant films which interact strongly with metallic surfaces and reduce both friction and wear are provided by the long, polar fatty acid chains. Thermal and oxidation stability of these oils are limited, despite vegetable oils have a higher viscosity index (Abdalla & Patel, 2006). Kuram *et al.* (2013) also discovered that vegetable oils out-perform other oils, for the following reasons:

i. Vegetable oils machining temperature increases due to a high natural viscosity. At high temperature the viscosity of vegetable oil drops more slowly than that of mineral oils.

ii. Vegetable oil molecules are quite homogenous in size, but mineral oil molecules vary in size. Consequently, the properties of mineral oils such as viscosity and boiling temperature are more susceptible to variation (Krahenbuhl, 2002).

iii. Vegetable oils have good properties for lubrication. The vegetable oil molecules make possible the highly lubricating properties of vegetable oils, as well as the chemical structure of the oil itself. Dense homogenous alignment of vegetable oils molecules create a thick, strong and durable film layer of lubricant, which gives the oil greater capacity to absorb pressure in contrast to mineral oil.

iv. Vegetable oils reduce smoke formation and fire hazard because it possesses a higher flash point (Krahenbuhl, 2002; Wood, 2005). The cutting fluid is used in high temperature conditions because it possesses higher flash point value.

v. Vegetable oil results in less loss from vaporization and misting because it possesses higher boiling point and greater molecular weight (Khan & Dhar, 2006).

Biresaw and Mittal (2014), presented a summary of the comparison of bio-based oils with petroleum oils in Table 2.3.

Table 2.3: Bio-based Oil Typical Characteristics as compared to Petroleum Oil (Biresaw & Mittal, 2014)

Property	**Method**	**Unit**	**Petroleum Oil**	**Bio-based Oil**
Lubricity	ASTM D6079		Low	High
Oxidative Stability	OSI Time	Hour	300	50

Index (OSI)	110^0C			
Viscosity Index			100	200
Hydraulic Stability	ASTM D2624		High	High
Conductivity	ASTM D2624	Ohm	Low	High
Saturation	ASTM D1959	$g(I_2)/100g(oil)$	Saturated	Un-saturated
Flash Point	ASTM D93	^{0}C	93	232
Pour Point	IP 35	^{0}C	-37	-37

2.1.3 Typical process of cutting fluid formulations

The composition of oil-in-water cutting fluids can be characterised as the addition of water to base-oil and emulsifier. Other components which may also be added to the fluid are: solution improvers, biocide/fungicides, corrosion and rust inhibitors, neutralising agents, agents to improve stability in hard waters and foam inhibitors (Alves & Oliveira, 2008). Alves & Oliveira (2008), presented the formulation processes of cutting fluid as follows:

(a) Additives selection: important check and balances should be done in selecting components that are not challenging or hazardous to health or the environment. Juneja *et al.* (2003), listed some of the additives and their function in Table 2.4.

(b) Mixing: add the base oil to water and stir for 2 min. Then other substances (additives) are added and stirred to mixture consistency for 15 min. A test mixture must repose for 24 hrs without oil/water separation. If the emulsion is not stable, the amount of emulsifier needs to be adjusted.

(c) Cutting emulsion verification: the chemical and physical properties of the cutting fluid need to be checked such as: pH, viscosity, corrosion and biodegradability which may necessitate adjustment of formulation.

Tables 2.4: Cutting fluid additives and their functions

Additive	Function
Mineral oils and other hydrocarbon	Base oil
Polyglocoether (for water soluble oils)	Emulsifier
Aliphatic amines (for water soluble oils)	Neutralizing oil
Aliphatic amines in neutralized form	Neutralizing agent
Sulphonates	Corrosion protection and extreme pressure addidictive (EPA)
Fatty acid amides	Lubricating Improvement
Sulphur/ Phosphorous Compound	Extreme Pressure addictives
Aldehyde derivatives (for water based coolants)	Biocides

Source: Juneja *et al.*, (2003)

Alves & Oliveira, (2008) presented the processes required to determine the corrosion grade of the cutting fluid among other cutting fluid formulation processes. These processes are corrosion test, pH level test and viscosity test.

i. Corrosion

Corrosion test is for the purpose of measuring corrosion grade of the cutting fluid.. Some grams of cast iron chips, initially washed in acetone and dried, were placed on a piece of filter paper in a petri-dish. The chips were evenly spaced around the filter paper, prevented from contacting one another and humidified in 2 ml of the test cutting fluid. The chips were left in the covered petri dish for 2 hrs. At the end of 2 hrs, the iron chips were discarded and the filter papers were rinsed in acetone. The cutting fluid corrosion grade is measured by observing the number of spots that appeared in the filter paper surface. The aim of this analysis is to determine the anti-corrosive characteristics of emulsion cutting fluids.

ii. pH level

Most cutting fluids have a pH value within the range of 9 (Richard, 2021).

iii. Viscosity

A ball viscometer aid to determine the viscosity of the cutting fluid using

$$\eta = t(\rho 1 - \rho 2)k \quad 2.1$$

Where η = the dynamic viscosity (MP_aS), t = fall time between the two marks of tube (s), ρ_1 = the ball density (g/cm^3), ρ_2 = the fluid density (g/cm^3) and K is the ball constant ($0.13MP_acm^3$)/g. The Table 2.5 shows the corrosion grade identification with the corresponding mean and filter paper surface.

Table 2.5: Corrosion Grade Identification

Corrosion Grade	Mean	Filter paper surface
0	No corrosion	Spots free
1	Vestiges of corrosion	Maximum of three spots
2	Minimal corrosion	Below 1% paper area with spots
3	Medium corrosion	Between 1 and 5% paper area with spots
4	Much corrosion	Above 5% paper area with spots

Source: Alves & Oliveira (2008).

iv. Biodegradability

Ready Biodegradability: The 301B CO_2 Evolution Test adopted in 1992, can be used to investigate the new emulsion biodegradability. A system of aeration of continue flux, so as to filter the air, various flashes with Sodium hydroxyl were employed in this test. The test is conducted in the dark, around 20 – 25 ^oC and within 28 days. CO_2 evolution that was

absorbed by $Ba(OH)_2$ solution during test period is what is used to evaluate the cutting fluid's biodegradability. Titration with HCl determines the CO_2 evolution.

2.1.4 Tool wear mechanisms

There are five primary causes of wear. Thus, tool wear mechanisms are categorised into five parts and can happen when two or more of these parts are combined or even as a single part. The reason for wear do not often occur in the same form nor even constantly affect wear at equal degree under same condition of cutting (Nee, 1998).

1. Abrasive wear is a form of mechanical action that happens on the cutting tool surface, dislodge sections or sometimes in the workpiece cut, chip or groove.

2. Diffusion between work and tool material happens as a result of tool section reaching a temperature at critical point, and a composition change occurs between the surface of the chip and the tool. This form of change in composition is due to an increase in temperature, where torn away section from the tool is followed by a strengthened bond between chip and section.

3. A chemical reaction is experienced at an increased temperature between the workpiece and the tool. Hence, due to the temperature and pressure at the cutting process, a weakened tiny section which forms smaller particles within, produces an existing bond between the workpiece and the tool, due to the reaction of the workpiece material. Whenever strength is developed by the bond, the tool weakened particles are done away with chip or remain with the workpiece.

4. Plastic deformation is often experienced by a very high pressure incurred on the cutting edge and which results to edge depression or edge bulging. There is an increase in the tool temperature and pressure when the tool deformation increases, leading to the gradual disappearing of the edge.

5. Asperities welding between the workpiece and the tool happens at a minimal temperature, compared to the chemical reaction and the diffusion. After removal of the work-hardened chip, there is a joining between these asperities and the workpiece. The asperities are been removed from the tool just as the workpiece is separated from the chip, due to high pressure in the cutting process.

However, a lot of researches been done on tool wear uses finite element analysis on tool wear prediction. Some other research works employed predictive mapping techniques in analysing tool wear. Feed force and the tangential force are the first force ratio employed and the second is radial force using neural network model obtained from a force ratio and a dynamometer readings which are used for flank wear prediction during turning of S45C workpiece and uncoated carbide cutting tools (Lee & Lee, 1999). Though, tool wear is common and normal, however, it does not cause a threat to tool performance until there is serious degradation in the cutting edge, which causes failure due to a very high feed rate, or a very low spindle speed. When tool temperature is at the highest in orthogonal cutting, this form of occurrence is experienced. Though, it is at a height equalling the cutting depth that crater wear occurs.

2.2 Turning Operation

Pralhad & Vivek (2018), predicted surface roughness and cutting force under MQL turning of AISI 4340 with nano fluid, by using response surface methodology. A cylindrical bar of AISI 4340 workpiece material was used, having BHN 217, 100mm length and 24mm diameter. CCMT-090308 tungsten carbide insert was used as cutting tool. Mitutoyo made surface roughness tester (SJ-201P) with a cut-off value of 0.8mm was employed to measure the turned workpiece. Kistler Dynamometer, a charge amplifier and PC software were employed to measure the cutting forces. Cutting speed, feed rate, depth of cut and tool nose radius were the cutting parameters considered for the machining operation. The experimental design was

full factorial design matrix with RSM employed for experimental analysis. CNC lathe was used to conduct MQL machining trials with nano fluid. The authors were able to develop a surface roughness and cutting force predictor mathematical model, in relation to cutting speed, feed, depth of cut and tool nose radius for alloy steel (AISI 4340) material, under MQL mode with nano fluid. Prediction error related to validation experiments showed that surface roughness average error was below ±11% for maximum error mathematical prediction, while cutting force average error was below ±5%. Also, cutting force (F_z) and surface roughness (R_a) predicted values yielded suitable fit with quadratic model from ANOVA results, and the confirmation experiments conducted.

Zheng *et al.* (2018), studied the effects of cutting parameters on wear behaviour of coated tool and surface roughness in high-speed turning of 300M. The HRC47 hardness workpiece material used was a 300M (40CrNi2SiMoVA) of low alloy medium carbon martensitic high-strength steel, 110 mm diameter and 300 mm long. The tool was a coated cemented carbide with high content of cobalt matrix. The tool insert and the tool holder were SNMG120408FN and MSSNR2020K12 respectively. The turning operation was conducted using a CNC lathe (Model CKD6136i, Dalian Machine Tools Group, China), with max spindle speed of 6000 rev/min. The experiment was carried out under dry condition, with a (Model USB200) digital tool microscope. VBave = 0.3 mm was the average wear width of the flank face requirement for tool failure. Cutting force and temperature were measured, using a thermal tracking instrument (Model TH5104R, NEC, Japan). Surface roughness tester (Model CS-3200 was used to detect the machine surface roughness (*Ra*). The machining operation conclusively yielded 130N-240N as the resultant cutting force, which in the initial cutting stage was not very large. Axial force *Fz*, is the maximum component obtained. Cutting speed, *vc* = 300–500 m/min, feed, *f* = 0.10–0.20 mm/rev, and depth of cut, *ap* = 0.15, 0.25 mm affected the cutting force. Also at the initial stage, the cutting temperature was within the range of 300–500 °C.V*c* is the most important factor leading effect on the cutting temperature, while *ap* is the

least effect factor. Peeling off and micro-chipping were some of the damages characteristics experienced at the rake face at *Vc* = 600 m/min. The main wear mechanisms of the coated tool are the oxidation wear, diffusion wear, adhesive wear and abrasive wear. Surface roughness, *Ra* is majorly influenced by the feed, *f*, and *Ra* is likely to rise with increase in the average flank wear. Also, increase in cutting parameters resulted in accelerated tool flank wear. Therefore, optimization of cutting parameters, prediction of tool life and machined surface roughness, depended on the positive role from the results of the work.

Korkut *et al.* (2004), determined the optimum cutting parameters during machining of AISI 304 austenitic stainless steel (ASS). The machining test were performed by single point turning of AISI 304 ASS with dimensions 200 mm long and 30 mm in diameter. The experiments were conducted using CNC Johnford TC-35 lathe, with cemented carbide as cutting tool. A continuous variable spindle speed of up to 3500 m/min, with a maximum power of 20kW was obtained during the machining operation. The result obtained showed the flank wear (V_B) curve in the machining of the workpiece (AISI 304 ASS) at a cutting speed of 120,150 and 180m/min. The results also showed the cutting parameters readings as 0.24mm/rev feed rate, and 2.5 mm depth of cut.

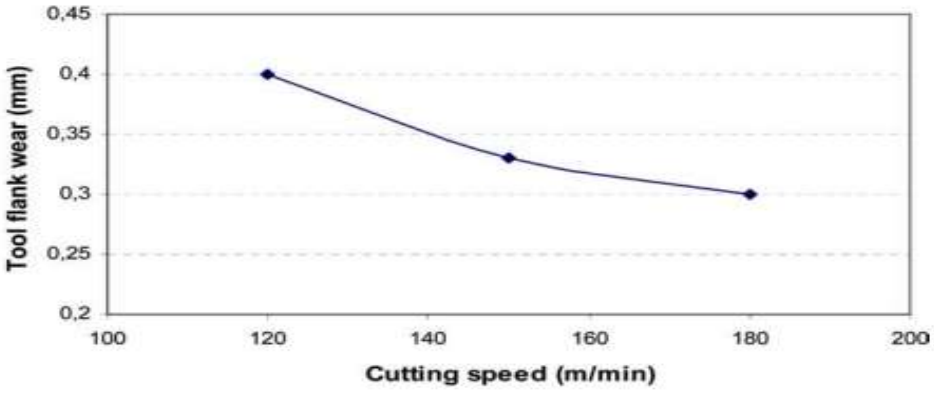

Figure 2.5: Flank wear when machining AISI 304 ASS (Korkut *et al.*, 2004)

Figure 2.5 shows that tool wear increases with increase in cutting speed. The author further showed that tool wear started to increase at 210 m/min cutting speed when more test were carried out.

Lawal *et al.* (2012), conducted a comprehensive review on the application of vegetable oil-based metalworking fluids (MWFs) in machining ferrous metals. The cause of heat and friction were removed when vegetable oil-based MWFs were employed, which made provision for lubrication between chips of both interfaces. The work further discussed the machinability of several ferrous metals with vegetable oil-based MWFs as fluids for cutting. The authors pointed out that research and development (R & D), and environmental impact, are the factors and challenges faced when using MWFs in machining. The work was concluded that MWFs inclusion in machining, showed better performance. Coconut oil showed better performance compared to mineral oil, in terms cutting parameters (90 m/min cutting speed, 1 mm depth of cut, and 0.35 mm/rev feed rate). The surface roughness values obtained were 4.5 µm and 5.5 µm for coconut and mineral oils respectively.

Xavior & Adithan (2009), determined the influence of cutting fluids on tool wear and surface roughness during turning of AISI 304 austenitic stainless steel, with carbide cutting tool, using different cutting fluids (coconut oil, emulsion and neat cutting oil-immiscible with water). The Taguchi design of experiment (DOE) $L_{27}(3)^4$ orthogonal array was employed for the work, with cutting speed, feed rate, depth of cut and cutting fluids as variable input parameters. The results of machining operation obtained showed that coconut oil had the highest effect on surface roughness and tool (1.91, 2.06, and 2.11µm and 0.045, 0.055, 0.071 mm) followed by cutting oil (2.25, 2.50 and 2.43 µm, and 0.098, 0.095 and 0.104 mm). Soluble oil had the lowest effect of (2.68, 2.92, and 2.92 µm, and 0.076, 0.094 and 0.10 mm), with cutting parameters (0.5 mm constant depth of cut, 0.2, 0.25, and 0.28 mm/rev feed rate, and 38.95, 61.35 and 97.38 m/min cutting speed). The observation from the authors' showed

that feed rate contributed 61.54% to surface roughness, while cutting speed had 46.49% contribution to tool wear. Coconut oil proved to have better effect than the conventional mineral oil in terms of improving surface finish and reducing tool wear.

Singh and Kumar (2004), studied tool wear optimisation in turning operation by Taguchi method. The machining test were performed using turning operation on an En24 alloy steel rods, with dimension 500 mm long and 90 mm diameter. The experiment was conducted on an H-22 centre lathe of H.M.T., using TiC coated carbide inserts cutting tool under dry cutting condition. The process parameters were cutting tool, workpiece and cutting parameters (cutting speed, depth of cut, feed), dry cutting and wet cutting. The flank wear width and the crater wear depth required machining time of 4 minutes to measure, using large tool maker's microscope and light section microscope, respectively. The S/N ratio were computed for each of the 27 trials and were reported. The authors findings of TiC coated carbide inserts for minimum tool wear were cutting speed 2 (250 m/min.), depth of cut 1 (0.70 mm) and feed 1 (0.14 mm/rev). Each parameter percentage contribution to the tool wear variation was obtained, that is, flank wear width (cutting speed=35.12, depth of cut=24.38, feed=10.49), crater wear depth (cutting speed=84.27, depth of cut=5.97, feed=2.48). The results also showed that cutting speed and depth of cut interaction were significant in ANOVA, with the crater wear depth characteristics which affected the average response value. Finally, the authors obtained an optimum tool wear predicted range of 0.143 < flank wear depth < 0.201 and 0.166 < crater wear depth < 0.322.

Lawal *et al.* (2013), investigated vegetable and mineral oil-in-water emulsion cutting fluids, in turning AISI 4340 steel with coated carbide tools. The turning process was carried out using Colchester VS Master 3250 (165 ×1,270 mm) gap bed centre lathe, powered at 7.5 kW, with a TiN coated tungsten carbide tool insert, using 3,250 rpm spindle speed on a round bar, AISI 4340 alloy steel with a diameter of 90 mm and a length of 360 mm for sustaining

cylindrical turning length ratio, and achieve the require stiffness of workpiece/cutting force/chuck. The metal machining industry have accepted and applied hardened HB 270-310 AISI 4340 alloy steel, which has become popular in industrial sector for manufacturing of shafts, gears, and aircraft landing gear. Cutting speed, feed rate and depth of cut are the three cutting parameters considered for the experimentation with DOE via Taguchi method specified L_{27} (3^4) orthogonal array, as the basic experimental set up employed plus four input parameters with three assumed levels each. Tool insert configuration and machine rating determine parameter selection. In each experimental run, a fresh cutting tool insert was used for a fixed cutting time of 15 min. Flank wear was observed and measured after each turning for 15 min, using an optical microscope. Signal to noise ratio (S/N) for the optimal cutting parameters for the cutting force were: 160 m/min of cutting speed (level 1), 0.18 mm/rev of feed (level 1), 1.75 mm of depth of cut (level 2), and 2.97 mm^2/s palm kernel oil based cutting fluid (level 3). The significant factors that affected flank wear obtained from ANOVA is 85.36% cutting speed; 4.81% feed rate; followed by 2.5% depth of cut, and 1.8% cutting fluid. For high machining of stainless steel, there is extremely high temperature on cutting tools in the cutting zone, resulting in rapid tool wear. The experimental work employed cooling during the machining process, so as to limit heat. Also, employing regression analysis with Minitab 14, mathematical model for cutting speed, feed rate, depth of cut and cutting fluids can be obtained. The experimental results obtained from this work indicated that flank wear when turning AISI 4340 steel with coated carbide tools, can be improved with the use of the developed novel vegetable oil-in-water emulsion cutting fluids formulations.

Mishra and Gangele (2012), applied Taguchi method in the optimization of tool flank wear width in turning operation of AISI 1045 steel. The machining test was carried out on an engine lathe of HMT, employing tungsten carbide inserts in dry condition. The cutting parameters were speed, feed and cutting depth. The workpiece was AISI 1045 steel rod of

dimension 80mm diameter and 400mm length. For each trial condition tungsten carbide positive rake triangular inserts for all the three edges were used. This was in line with the trial condition specified by orthogonal array 27 cutting edges of carbide inserts using 4 min. as machining time. Magnifying glass of 10X magnification was employed to measure the tool flank wear width. The tool flank wear width were prominently affected by three machining parameters (cutting speed, feed rate and depth of cut). ANOVA was employed to obtain percentage contribution of each machining parameters. The authors obtained average confirmation run of the three confirmation runs conducted at 88.33 µm surface roughness selected optimal settings for the turning process parameters. The work found Taguchi method suitable for tool flank wear width optimisation. Minimum tool wear for the machining operation were found to be cutting speed at level 1(110m/min), feed rate at level 1 (0.15mm/rev) and depth of cut at level 1 (0.10mm). Percentage contribution of Machining parameters to tool wear characteristics contribution were cutting speed 47.45%, feed rate 25.75%, and depth of cut 16.52%. Tool flank wear width reduction of 23.85% was obtained during working from the experimental work.

Das *et al.* (2012), optimized cutting parameters on tool wear and workpiece surface temperature in turning of AISI D2 steel. The machining test was carried out on a CNC lathe (JOBBER XL, ACE India), having 3500 rpm maximum spindle speed, and 16 kW maximum power in dry conditions. The facial hole-drilled workpiece supported at the tailstock was an AISI D2 steel in round bar form (selected due to manufacturing tools field application), with a dimension of 50 mm diameter and length of 120 mm. A non-chip breaker geometry coated carbide inserts cutting tool of ISO designation CNMG 120408 (800 diamond shaped inset) was employed for the experiment, using Taguchi orthogonal array design, a three level, L_9 (3^4) orthogonal array which helped in reducing the number of experiments was achieved.

The temperature range of -30^{o}C to 550^{o}C was used to machine samples which were measured, using infrared thermometer. Cutting speed, depth of cut and feed were the cutting parameters. A Minitab 15 software package was used to analyse tool wear and workpiece surface temperature, which yielded an error contribution of 0.91% and 2.8% for tool wear and workpiece surface temperature respectively. The authors result showed that cutting speed increase is equal to tool wear continuous increase, whereas feed rate increase was equal to tool wear decrease. Though, depth of cut increase was equal to tool wear increase to about 0.75 mm. Thus, 0.75 mm depth of cut yielded maximum tool wear, and a minimum tool wear of 0.5 mm. The low value results and at the main effects plot were at the same levels for workpiece surface temperature, i.e., cutting speed of 150 m/min, depth of cut of 0.5 mm and feed of 0.25 mm/rev. This means that on the cutting tools, less tool wear is a product of lower surface temperature. Hence, 41.17% and 34.45% were the cutting speed and depth of cut contribution respectively, for workpiece surface temperature with feed providing 21.58% of the total variation. The tool wear predicted optimal range was $0.21 \leq \mu TW \leq 0.31$ and temperature for workpiece was $37.51 \leq \mu T \leq 43.21$. Also, 60.85% depth of cut and 33.24% cutting speed were the percentage contribution in tool wear variation which was more when compared to 5.70% feed contribution. Multiple regression equation was employed to relate cutting parameters (cutting speed, depth of cut, feed) and performance measure (tool wear and workpiece surface temperature).

Senthil and Senthilkumaar (2014), analysed flank wear and chip morphology when machining super duplex stainless steel in a gas cooled environment. The workpiece, SAF 2507 super duplex stainless steel was used as test specimen. The dimensions of the cylindrical bar used for the turning tests were 65mm diameter and 450mm length, using a plain rigid-turned lathe machine, by employing uncoated cemented carbide cutting tool inserts (CNMG120408-QM, grade H13A), attached rigidly to a tool holder (PCLNR25M12).

Cutting temperature and contact stress interactions existing between workpiece and cutting tool strongly influenced flank wear. A gas coolant environment was formed using liquid CO_2. The cooled gas machining was compared with the wet and dry machining. Flank wear was measured after a total of 18 conducted experiments, using tool makers' microscope. The authors employed the same tool characteristics and cutting conditions on the three cooling methods. The chips removed were together gathered and evaluated with the different cutting conditions in the course of the experimental process.

The machining parameters optimised values were predicted, employing Minitab 15 software and response surface methodology. Predicted and experimental values were compared, using the confirmation test conducted. The scanning electron microscope (Joel Model 6390), was used in the analysis of the optimised values of both the flank wear and the chips produced. The authors' conclusions showed that gas cooled machining produced reduction in flank wear. Super duplex stainless steel optimised values of machining parameters during turning conditions of dry, wet and gas cooled machining were (i) cutting speed = 120 m/min, feed rate = 0.06 mm/rev and depth of cut = 0.65 mm, (ii) cutting speed = 116.36 m/min, feed rate = 0.06 mm/rev and depth of cut = 0.71 mm, and (iii) cutting speed = 100 m/min, feed rate = 0.06 mm/rev and depth of cut = 0.62 mm respectively. Also, a considerably reduction in the temperature and acting force during the turning operation, in the case of gas cooled machining environment. Finally, the challenge of disposing traditional cutting fluid is not encountered by employing CO_2 liquid. Gas cooled machining was discovered to be an excellent option (even economically in terms of cost) to the traditional dry and wet machining.

Lan (2010), studied tool wear optimization for general CNC turning, using fuzzy deduction. The machining tests were conducted on an ECOCA-3807 CNC machine, using S45C workpiece with a dimension of (Ø 45mm × 250mm), and a Mitsubishi NX2525 cutting tool

insert in order to obtain S/N ratio, using Taguchi experiment to achieve the defuzification tool wear result by turning operation with three various levels (low, medium and high), based on optimised finish turning of the L_9 (3^4) orthogonal array. The four turning parameters (A-speed, B-cutting depth, C-feed rate and D-tool nose run off), were considered for the work. The effect of process parameters even at optimal levels was obtained using statistical analysis of variance (ANOVA).

Fadare *et al.* (2009), modelled tool wear parameters in high-pressure coolant assisted turning of titanium alloy Ti-6Al-4V, using Artificial Neural Networks. An 11 kW CNC Lathe with 18-1800 rpm speed range was used to conduct the machining trials, at 1411 Nm of torque. The workpiece was a Ti-6Al-4V (IMI 318) alloy bar with a dimension of 600mm×300mm (diameter by length). The cutting tools used were coded T1 and T2 uncoated carbide inserts, and coded T3 double TiAlN/TiN, PVD coated carbide inserts, with CNMG 120412 as the carbide inserts design. Using magnification of 25x on a toolmaker microscopy, wear of tool was measured for every machining trials. Design for the neural network was carried out on a MATLAB® Neural Network Toolbox. The results obtained were dependent on the correlation coefficient between the predicted and the experimented, in which 0.996 and 0.999 were values obtained for both tool life and tool wear respectively, using the entire data set. The sum validation reach for the network prediction capability was in between the following order, that is, tool life < wear rate. The model peak network produced 20 neurons (covered layer trained) multilayer neural network with joint algorithm (Livenberg-Marquard), and regularisation (Bayesian). The authors concluded that for both conventional and high pressure cooling, cutting speed increase results inspeed of decreased tool life. At lower 80 m/min speed a 2-fold increase in the life of tool was obtained, at 70 bar coolant pressure when conventional cooling was compared. At higher speed of 110 m/min, about 110 and 203 bar were obtained for both 4-fold and 5-fold respectively.

Avila and Abrao (2001), investigated the performance of three types of cutting fluids namely: *X* fluid = emulsion without mineral oil, *Y* fluid = emulsion synthetic, and *Z* fluid= emulsion with mineral oil. The authors also carried out dry cutting with continuous turning of hardened AISI 4340 steel (49HRC) using alumina inserts (Al_2O_3 + TiC). Chips for both rough and finish machining were evaluated including tool life, surface finish and tool wear measurement. Different cutting speeds (V_c) of 50 to 100 m/min, for a depth of cut (a_p) of 2.0 mm, and feed rate (*f*) of 0.15 mm/rev were carried out under rough machining test. Cutting speed (V_c) of 200 to 400 m/min, for a depth of cut of 0.5 mm and feed of 0.05 mm/rev were achieved during the finish machining setting. A tool life criterion of average flank wear VB_B = 0.3 mm were conducted, according to ISO 3685 standard, and the tests were interrupted after 60 min, when the criterion had not been met. It was observed that cutting fluid '*A'* provided the longest tool life during rough turning, with feed of 0.15 mm/rev and depth of cut of 2.0 mm. This was followed by dry cutting and fluid *B,* while the emulsion containing mineral oil (fluid *C*) showed the worst result. When finish turning with feed of 0.05 mm/rev and depth of cut of 0.5 mm, the same condition was observed, VB_B = 0.2 mm as tool life criterion. The presence of grease in its composition may have attributed to the superior performance of fluid *A* which is accountable for increased lubricating action, especially for heavy cutting operations. The best tool life results were as a result of the effect of reduction in the concentration of fluid *A* from 5 to 3% during finish turning. The authors observed that the lowest surface roughness values were: R_a = 1.7 µm (dry cutting), R_a = 1.73 µm (fluid *A*), R_a = 1.89 µm (fluid B) and R_a = 2.14 µm (fluid *C*), during rough turning at V_c = 50 m/min, a_p =2.0 m and *f* = 0.15 mm/rev. The best surface finish was obtained with fluid *C,* as the cutting speed was increased to 75 and 100 m/min. Irrespective of cutting speed and the measured average surface roughness (R_a) value, the drop in concentration of fluid *A* from 5 to 3%, as turning tests finished, did not represent any considerable change on surface roughness. The conclusions of the authors were that the use of a cutting fluid based on an emulsion with no

mineral oil presented an outcome of a longer tool life, not similar to dry cutting. The drop in the cutting fluid concentration of emulsion with no mineral oil from 5 to 3% presented an outcome of lower tool life, especially at 300 m/min cutting speed.

Krishna *et al.* (2010), investigated nanoboric acid suspensions performance in SAE-40 and coconut oil during turning of AISI 1040 steel, with cemented carbide (SNMG 120408) as cutting tool. The differences in cutting tool temperatures, the surface roughness of the machined surface with cutting speed and average tool flank wear were studied using lubricating oil containing nanosolid lubricant suspensions. The conducted experiments were under the following conditions: cutting speed (60, 80 and 100 m/min), depth of cut (1.0 mm), feed (0.14, 0.16, 0.2 mm/rev). Lubrication with solid lubricants of boric acid of particle size of 50 nm, lubricating oil SAE-40 and coconut oil with flow rate of 10 ml/min were used. The embedded thermocouple put at the tool insert bottom in the tool holder measured the temperature. The authors reported that the cutting tool temperature measurement presented evidence of the cooling action of the lubricant with nanosolid lubricant suspensions. It was also observed that irrespective of the lubricant, cutting temperature increased with cutting speed, and was less with coconut oil, compared to SAE-40 for identical cutting conditions. Furthermore, at all the lubricant conditions, cutting temperature increased with increase in feed. Tool flank wear was measured at various cutting speeds and at different lubricating conditions. Speed and feed increase, gradually increased flank wear. The reduction in flank wear was due to the joint effect of solid lubricant and vegetable oil with suspended particles of 0.5% nanoboric acid in coconut oil, compared to other left over conditions. The authors also reported that all the lubricating conditions, that increased with increase in feed was due to surface roughness initially reduced, and then increased with increase in cutting speed. The report equally observed that coconut oil reduced surface roughness compared to SAE-40 oil, and within the coconut oil lubricants, nanoboric acid suspensions of 0.5% gave better results. They concluded that, base oil in comparison with cutting temperatures, tool flank wear and

surface roughness decreased significantly with nano lubricants as a result of boric acid lubricating action, and that in all the cases, in comparison to SAE-40 based lubricant, coconut oil, nano particle suspensions showed better performance. This was as a result of the better lubricating properties of the base oil.

Ramanujam *et al.* (2014), modelled and optimised cutting parameters in dry turning of Inconel 718 bar of dimension 35mm and 600mm in a 7.5kW, and 1600rpm medium duty lathe, using coated carbide inserts tool. Dry turning Taguchi's L_9 orthogonal array was the experimental designed used. This included independent variables, response variable selection and the variables interaction. Table 2.6 gave the relative levels and the parameters selected for the experimentation. Signal-to-Noise (S/N) ratio, and the factor level settings which maximized the S/N ratio to quality characteristics optimisation were designed. The trials of experiment and their relative S/N ratio values, the cutting force (Fz) and surface roughness (Ra) values were measured. Based on the experiments and responses obtained along with ANOVA, the results from the cutting parameter optimization for Ra, Rt, Rz and Fz were $A_{2,}$ $B_{1,}$ $C_{2,}$ with 50m/min cutting speed, 0.103 mm/rev feed, and 0.4 mm depth of cut, respectively. The major important parameter was feed rate generating 91.8%, 77.8% and 88.8% highest contribution percentage, next was depth of cut with 3.72%, 19.13% and 9.77%. The least effective on surface roughness was cutting speed. The important parameters for cutting force (Fz) with 56.69% and 38.46% was seen to be feed rate and depth of cut as shown in Table 2.6. Also, cutting force and depth of cut showed high significant responses by the developed model; hence, the regression equation developed have high determination coefficient (R^2) for both cutting force and surface roughness, which explained 91.8%, 91.2%, 94.3%, 88.2% of outcome. Therefore, due to the friction and thermal softening at cutting speed from 30m/min to 70m/min, the common tool wear mechanisms were abrasion, edge chipping and oxidation.

Table 2.6: Process Parameter and their levels (Ramanujam *et al.,* 2014)

Process parameters	Unit	Level 1	Level 2	Level 3
Cutting Speed (A)	m/min	30	50	70
Feed rate (B)	m/rev	0.103	0.206	0.294
Depth of cut (C)	Mm	0.2	0.3	0.4

Ciftci (2006), investigated the machining characteristics of austenitic stainless steels (AISI 304 and AISI 316), employing coated carbide tools of multi-layer chemical vapour deposition (CVD). Four various cutting speeds with a constant depth of cut and feed rate were carried out using turning operation. The impact of cutting speed, workpiece grade and cutting tool coating layer were conducted on machined surface roughness and cutting forces. Hence, surface finish values decreased with increasing cutting speed.

Thakre *et al.* (2019) researched on the measurements of tool wear parameters using machine vision system. Turning operations were conducted on a CNC turning machine (Seimens control; DX200, Jyothi Company) using carbide inserts (TNMG-16- 04-04-QM J13 A) for the machining of internal diameter. The digital camera (SONY Cyber-shot DSC-HX400 V) was used for capturing the image of worn out tool inserts. LED was used for illumination purpose of tool insert and calibration square. Image processing toolbox of the MATLAB software was used for the image processing. The worn out carbide tool inserts (SEMT 1304 PETR-M TT8020, TagueTec) were used for conducting the experiments in this work. The algorithm is used to calculate three tool wear parameters, i.e., average tool wear width, tool wear area, and wear perimeter. The measurements of an average tool wear width, with the present vision system are found to be in close agreement with that of the digital microscope. The average absolute error in measuring average tool wear width for all the twelve inserts was found to be 3.08%. Average wear width, wear area, and wear perimeter were seen increasing with the machining time.

Pawar *et al.* (2016) optimized reviewed parameters in CNC Turning Operation. The work piece materials used for the optimization of CNC turning process parameters were Al/SiC-MMC, Aluminum rod, Glass fiber reinforced plastics (GFRP), cylindrical bar of AISI 1080 steel, Ti-6Al- 4V alloy, AISI 1040 carbon steel, S45C, semi-crystalline thermoplastic polyethylene (PE), EN 24 medium alloy steel, Al 6063 with 10% silicon carbide metal matrix composites, AISI 52100 steel, Red mud-based aluminum metal matrix composites, 6061 aluminum, Inconel 718, Martensitic stainless steel (SS40) steel. The cutting tools used for the optimization of CNC turning process parameters were T max- U positive rhombic insert (uncoated tungsten carbide of WC), CERMET cutting tool, HSS single point cutting tool, CNMG 120408-883 inserts, cemented carbide (K20), CNMG 120408-883 inserts, Mitsubishi NX2525 insert, C type negative, multilayer coated inserts CNMG 120404, inserts VCGX16 04 04-AL (H10), Ti-N coated tungsten carbide inserts, Mixed ceramic (AL2 O3+TiC) inserts, Coated carbide tool inserts M30,Ti-Al-N- coated tungsten carbide. The review showed that the performance parameters like surface roughness, tool wear rate, flank wear, crater wear, tool life, cutting time, total cost, power consumption and vibration and material removal rate depend on independent process parameter.

Kirby *et al.* (2006) conducted experiment on aluminium rod utilizing CNC lathe and determined the optimal turning operation parameters for surface finish under varying conditions by utilizing the Taguchi's method. This method was applied utilizing a concrete set of control (spindle speed, victual rate, depth of cut and implement nasal perceiver radius) and noise parameters (implement number and temperature range) and a replication variable of surface roughness. It was found that the control factor has varying effects on the responsible variable, with aliment rate and implement nasal perceiver radius having the highest effects on the other hand, the noise factor does not have any conspicuous effect. The utilization of the

Taguchi's Parameter Design Techniques was thus considered prosperous as an efficient method to optimize surface roughness in turning operation.

Homami *et al.* (2013), conducted experiment on commercial Inconel 718 nickel-predicated super alloy utilizing CNC lathe with Ti-Al-N-coated tungsten carbide cutting implement prepared by PVD with the optimization of turning process parameter (cutting velocity, aliment rate, nasal discerner radius, approach angle, depth of cut) for two dependent variables such as implement wear and surface roughness utilizing design of experiment for full factorial design, statistical analysis for experimental result analysis, artificial neural network (ANN) for system modeling and determinately genetic algorithm (GA) for optimization. The applied keenly intellective techniques results show that victual rate, nasal discerner radius and approach angle have a paramount effect on the flank wear and the surface roughness, but the cutting velocity has a paramount effect on the flank wear alone.

Senthikumar *et al.* (2012) performed machining experiment (turning and facing) on Inconel 718 utilizing CNC lathe with K 10 type uncoated carbide inserts. The effect of control variables (cutting speed, victual and depth of cut) on multi-replication variable (flank wear, surface roughness) led to utilizing ANN and analysis of variance (ANOVA) techniques. The result of this experimental study shows that alignment has the most consequential factor on surface roughness in facing operation and low cutting speed, medium depth of cut, and low victual are the optimum machining parameter for the turning operation.

Zang *et al.* (2007) evaluated the turning operation on 6061 aluminum on a CNC lathe. A full factorial design is utilized in the experimental design. An In-Process Surface Roughness Adaptive Control (ISRAC) system was developed for turning operations. ANN was employed to establish two sub-systems: the neural network-predicted, in-process surface roughness prognostication (INNSRP) sub-system and the neural network-predicated, in-

process adaptive parameter control (INNAPC) sub-system. The two sub-systems surface

S/N	Author(s)	Machining Operation	Machining Response(s)	Workpiece	Cutting Tool	Cutting Types	Gap left

roughness and acclimated victual rate utilizing cutting parameters (aliment rate, spindle speed and depth of cut), and vibration signal detected by an accelerometer sensor. The result shows the vibration signal detected by the accelerometer employed in the proposed system was a good designator of surface roughness. Victual rate is the most consequential factor impacting the surface quality of turned products.

The summary of the researches on turning process in this work is presented in Table 2.7; which highlight the Authors, machining operations carried out, the responses considered, the input parameters, the cutting environment considered and left over research gaps for exploration.

Table 2.7: Summary of researches on turning process

1.	Pralhad and Vivek (2018)	Turning	surface roughness and cutting force	AISI 4340	Tungsten carbide insert	Nano fluid	Tool wear
2.	Zhenga *et al.* (2018)	Turning	Tool wear and Surface roughness	300M (40CrNi2SiMoVA) low alloy medium carbon	Coated cemented carbide	Dry	Test with AISI 304 alloy steel
3.	Korkut *et al.,* (2004)	Turning	Flank wear and surface roughness value Tool wear optimisation	AISI 304 ASS	coated cemented carbide	Dry	Test under wet condition
4.	Singh and Kumar (2005)	Turning	Tool wear optimisation	En24 alloy steel	TiC coated carbide inserts	Dry	Test under dry condition
5.	Lawal *et al*. (2014)	Turning	Investigated emulsion cutting fluids	AISI 4340	Coated carbide	Dry and Wet (Vegetable and Mineral oil-in-water)	Optimisation using 304
6.	Mishra and Gangele (2012)	Turning	Optimization of tool flank wear width	AISI 1045 steel	Tungsten Carbide inserts	Dry	Cutting under wet condition
7.	Das *et al.* (2012)	Turning	Optimized cutting parameters on tool wear and workpiece surface temperature	AISI D2 steel	Coated carbide inserts	Dry	Cutting under wet condition

Summary of researches on turning process continue…

8.	Senthil Kumar and Senthilkumaar (2014)	Turning	Flank wear and chip morphology	SAF 2507 SS (super duplex)	Uncoated cemented carbide inserts	Dry and Wet (Liquid CO_2)	Surface roughness
9.	Lan (2010)		Surface		Mitsubishi	Dry	Tool

		Turning	roughness optimization	S45C	NX2525 inserts		wear
10.	Fadare *et al.*, (2009)	Turning	Modelled Tool Wear Parameters	Ti-6Al-4V (IMI 318) alloy bar	Coded T1 and T2 uncoated carbide inserts and coded T3 double TiAlN/TN	Dry and Wet (coolant pressure)	Surface roughness
11.	Avila and Abrao (2001)	Turning	Cutting fluids performance	AISI 4340 steel (49HRC)	Alumina inserts (Al_2O_3 + TiC)	Dry and Wet (emulsion, synthetic and mineral oil)	Surface roughness and Tool wear
12.	Krishna *et al.*, (2010)	Turning	Investigated nanoboric acid	AISI 1040 steel	Cemented carbide (SNMG 120408)	Dry and Wet (coconut oil and SAE-40)	Surface roughness and Tool wear
13.	Ramanujam *et al.*, (2014)	Turning	Modelled and optimised cutting parameters	Inconel 718 bar	Coated carbide inserts	Dry	Surface roughness and Tool wear
14.	Ciftci (2006)	Turning	Surface roughness and cutting forces	AISI 304 and AISI 316	Coated Carbide tool	Dry	Tool wear
15.	Thakre *et. al* (2019)	Turning	Tool wear parameters	AISI 1045	Carbide tool insert	Dry	Surface roughness
16.	Pawar *et.al* (2016)	Turning	Parameters optimization	AISI, Inconel and SS series	Rhobic, cermet, HSS, Carbide inserts	Dry and Wet	Surface roughness and Tool wear

Summary of researches on turning process continue…

17.	Kirby E. Daniel *et al*. (2006)	Turning	Surface finish optimization	AISI 410		Dry	Tool wear
18.	Homami *et al.*	Turning	wear and surface	Inconel 718	Ti-Al-N-coated	Dry	Wet condition

	(2013)		roughness	nickel-predicated super alloy	tungsten carbide		
19.	Senthi kumar J.S. (2012)	Turning and facing	flank wear, surface roughness	Inconel 718	uncoated carbide inserts	Dry	Wet condition
20.	Zang J.Z. (2007)	Turning	Surface roughness	6061 aluminum	Carbide insert	Dry	Wet condition

Chapter 3 presents the various materials, equipments and methods employed to carry out the step by step analysis of the formulated cutting fluids, the design of experiment and equipment set-up for carrying out the measurement of the individual responses.

CHAPTER THREE

3.0 MATERIALS AND METHODS

3.1 Materials

The materials used to carry out the evaluation and optimisation of the turning operation are base oil, additives, workpiece, cutting tool and machine tool components.

3.1.1 Base-oil

Base-oils are known to be used to manufacture products like lubricating greases, motor oil and metal processing fluids. The different compositions and properties in the oil is as a result of the different products.

3.1.1.1 Jatropha curcas seed oil

The jatropha curcas seed oil (JSO) (i.e. oil extracted from Jatropha curcas seeds) used in this work, was from AgriEnergy Nigeria. The packaging was carried out commercially at the Technology Incubation Centre (TIC) complex, Kano state, Nigeria.

3.1.1.2 Neem seed oil

Neem seed oil (NSO) used for this work was sourced from indigenous local market in Katsina, Katsina state.

3.1.1.3 Mineral soluble oil

Mineral soluble oil (MSO) was sourced from Agarawu market in Lagos highland, Lagos state. The MSO act as control base oil during this work.

3.1.2 Required components for cutting fluids formulation

The components required for the formulation of the cutting fluids are additives. These additives are required to improve the performance of the cutting fluids. The formulated cutting fluids for this work employed oil additives which helped in achieving the significant effect parameters needed to achieve the optimum imput parameters for the turning operation.

3.1.2.1 Oil additives

Oil additives are chemical compounds that are used to improve the performance of lubricant of base oil. One of the very important constituents in the formulation of cutting fluids is

additives. They confer special substances and features on cutting fluids. They contribute to the fluid performance, as well as better machined parts, tooling and equipment. With regard to the lubricating and cleaning mechanisms, additives in cutting fluid enhance good wettability and permeability, and hence, can lubricate the cutting edge of the tool to decrease the cutting load, cool the cutting edge to keep it sturdy, and clean the surface of the cutting edge to keep it sharp. The additives considered, in this work, in the formulation of the cutting fluid mulsion are emulsifier, antioxidant, anti-corrosion, and biocide. These addtives were used for the purpose of developing an environmentally friendly vegetable oil-based cutting fluids.

(i) Anti-corrosion agent

Metals corrosion control is of great importance in terms of technical, economic, environmental, and aesthetical gain (Rani & Basu, 2011). One of the options of protecting metals and alloys against corrosion is the use of inhibitors. The other options commonly used are barrier coatings, hot-dip galvanization, alloyed steel (stainless), cathodic protection and EONcoat (EONCOAT, 2016). What prompted the search for green corrosion inhibitors is because of the environmental toxicity of organic corrosion inhibitors. Green corrosion inhibitors are biodegradable, do not contain heavy metals or toxic compounds like COOH, NH_2, NO_2 or CHO (Rani & Basu, 2011). Therefore green corrosion inhibitors enjoys several advantages over the organic counterpart. Banana plant juice was used as anti-corrosion. The pseudo-stem which produces the plant juice is a part of the banana plant that looks like a trunk, which consists of a soft central core and tightly wrapped up to 25 leaf sheaths (Subagyo & Achmad, 2018). The major uses of banana pseudo-stem fibre are in making specialized and high-quality sanitary products such as baby pampers, textiles, ropes and papers such as banknotes. The extraction process was carried out as soon as the pseudo-stem's leaves are cut. The common method in practice is a combination of water retting and

scraping. The first step, called tuxing, is separating the fiber bundles from the remaining parts. Tuxing can be done either manually or mechanically using machine (Pappu *et al.,* 2015). The leaves are stripped from the cut pseudo-stems. Afterward, a knife is put at the butt end between the outer and middle layers of the leaf shaft, and then the outer part is held firmly and pulled out. The plant juice used was sourced locally at Minna, Nigeria.

(ii) Anti-oxidant agent

The content of the anti-oxidant is a mixture of equal concentration of 0.5M Zinc Chloride + peroxide + calcium carbonate solution. The Chemical Engineering laboratory of Federal University of Technology, Minna, Nigeria was where the anti-oxidant was prepared.

(iii) Biocide

The content of the biocide was a mixture of equal concentration of 0.5M hypocholride + phenolic solution + tris (hydroxymethyl) nitro methane. The Chemical Engineering laboratory of Federal University of Technology, Minna, Nigeria was where the biocide was prepared.

(iv) Emulsifier

A mixture of 0.5M sodium lauryl sulphate + sodium tripolyphospate + sulphonic acid + calcium carbonate in 5 litres of water contained in the emulsifier, was used in this study. The Chemical Engineering laboratory of Federal University of Technology, Minna, Nigeria was where the preparation of the emulsifier took place.

3.1.3 Workpiece material

The workpiece material for this study is an austenitic chromium-nickel stainless steel categorised as AISI 304 as shown in Plate I. Stainless steel types 1.4301 is also known as grades 304. AISI 304 can also be referred to as 18/8 which is derived from the nominal

composition of type 304, being 18% chromium and 8% nickel. Stainless steel type 304 is a part of a family of stainless steel alloys (301, 302, 303, 304, 316, and 347).

Plate I: AISI 304 alloy steel workpiece (25mm diameter and 500mm length)

Type 304 is the most versatile and widely used stainless steel (AZoM 2019)**.** The general chemical composition of this work material are presented in Tables 3.1.

3.1.3.1 Chemical composition of AISI 304 alloy steel

The chemical composition of stainless steel is the chemical element deposits within the steel. 304 alloy steel has 9 visible elements in percentage just like other 304 series in Table 3.1.

Table 3.1: Chemical composition for 304 stainless steel alloys

%	304	304L	304H
C	0.0 - 0.07	0.0 - 0.03	0.04-0.08
Mn	0.0 - 2.0	0.0-2.00	0.0-2.0
Si	0.0 - 1.00	0.0-1.00	0.0-1.0
P	0.0 - 0.05	0	0.0-0.04
S	0.0 - 0.03	0.0-0.02	0.0-0.02
Cr	17.50-19.50	17.50-19.50	17.00-19.00
Ni	8.00 - 10.50	8.00-10.50	8.00-11.00
Fe	Balance	Balance	Balance
N	0.0-0.11	0.0-0.11	0.0-0.10

Source: *AZoM.com* (2019)

3.1.4 Cutting tool

The cutting tool employed for this work is RP8025 CNMG120404-PM 3688-288L 10PCS tungsten carbide insert per pack. One important machining component that determines and makes machining possible and achievable is cutting tool.

Plate II: Tungsten coated carbide insert

Two packs of the tungsten coated carbide insert was used for the turning operation. Each pack contains 10 pieces of the insert as shown in Plate III. Plate II shows one of the insert in the pack used for the turning operation. The finishing outlook of each of the insert varies from one cutting fluid to the other and from different selected input parameters employed.

Plate III: Insert packs

Table 3.2: Physical properties of cutting tool

Properties	Values
Chemical formula	WC
Molar mass	195.85 $g.mol^{-1}$
Appearance	Grey-black lustrous solid
Density	15.6 g/cm^3
Melting Point	2,785-2,830°C (5,045-5,126°F; 3,0583,103K)
Boiling point	6,000°C (10,830°F; 6,270K) at 760 mmHg
Solubility in Water	Insoluble
Solubility	Soluble in HNO_3, HF
Magnetic susceptibility (X)	1.10^{-5} cm^3/mol
Thermal conductivity;	110 W/(m.K);
Thermal expansion coefficient;	5.5 $\mu m.m^{-1}.K^{-1}$
Vickers number	2600
Young modulus	530-700 GPa
Bulk modulus	630-655 GPa
Shear modulus	274 GPa
Ultimate tensile strength	344 MPa
Ultimate compression	2.7 GPa
Poisson's ratio	0.31

Source: *AZoM.com* (2019)

3.2 Machine tools and equipment

3.2.1 Lathe

A MEUSER M00L conventional centre lathe as shown in Figure 3.1 was used for this research and is located at Air Force Institute of Technology (AFIT) workshop in Kaduna, Nigeria. The machine configuration are as follows:

Model Number	M00L Lathe 37475
Manufacturer	Meuser ETM GmbH, Gruendau 63584, Germany
Controls	Electric buttons
Bed size	1.2m
Crosslide Travel	12”
Bed width	80”
Spindle mount	D1.6
Current	7.5Amps
Voltage	380 – 440V
Speed (motor)	8/10 hp
Spindle speed	28 – 1250rpm

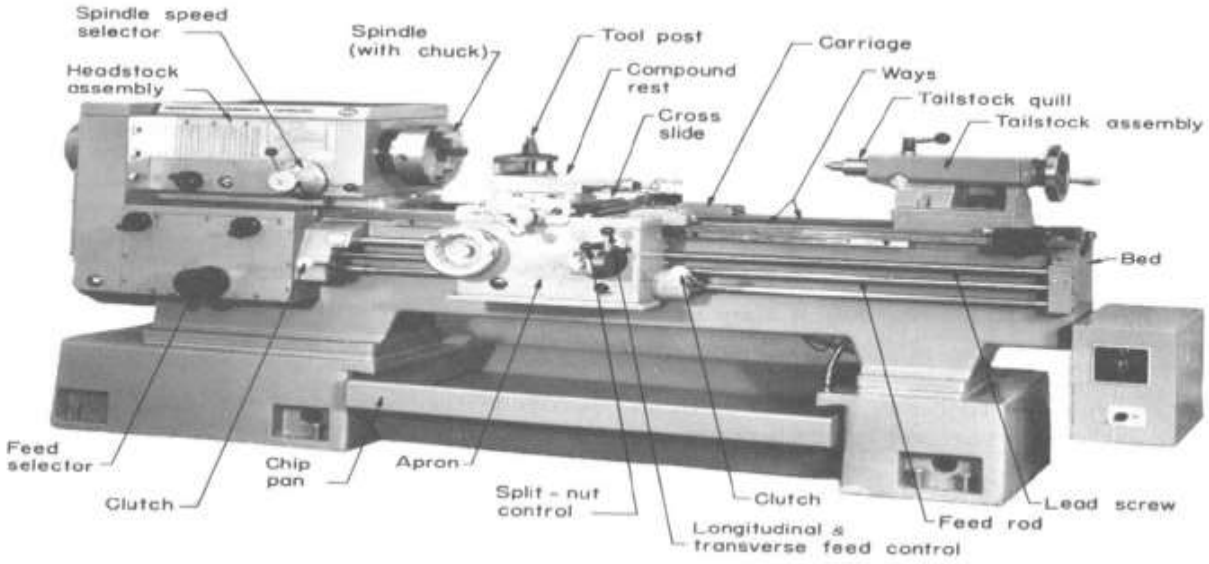

Figure 3.1: AFIT Workshop meuser lathe for orthogonal turning process (Source: AFIT files)

3.2.2 Cutting tools holder

The cutting tool holder as shown in Figure 3.2 is a right hand cutting tool insert (indexable) holder made by Associated Production Tool Ltd.

Model -MTJNR 2020 K16.

Brand -Canela.

Cut -93^{o} Right Hand Cutting 20x20mm with Shank width of 25mm and 125mm long.

Figure 3.2: MTJNR 2020 K16 Cutting tool insert holder

3.2.3 Measuring devices

i. Dino-Lite version 2017Q2 IDCP BV designed and produced in Taiwan is a Dino-Lite digital tool wear microscope. The DinoCapture software as shown in Figure 3.3 is designed to give the best possible digital microscopy experience by the inventors of the handheld digital microscope. The DinoCapture software runs on computers with a Windows XP, Windows Vista or Windows 7/8/10 operating system.

ii. Digital Separate Surface Roughness Tester: Model SRT-6210S with ±10% accuracy and not more than 6% fluctuation display value. This surface roughness tester as shown in Figure 3.4 was manufactured by GuangZhou Landtek Instruments Company, Ltd, China.The Retort stand in Figure 3.4 is for firm holding of the Dino-Lite to ensure effective operation of the Dino-Lite for accurate result findings.

iii. Casio Stop Watch model G-Shock, water absorbing, shock and water resistant made by Casio, Thailand.

Dinolite digital Measuring device

Retort stand

Laptop

Coated carbide insert

Figure 3.3: Set up component of digital microscope tool wear measuring device

Figure 3.4: Digital surface roughness tester

3.3 Experimental methods

3.3.1 Determination of physicochemical properties

The physicochemical properties of the jatropha curcas seed and neem seed oils were determined at the laboratory of the department of Water Resources, Aquaculture and Fisheries Technology (WAFT), School of Agriculture and Agricultural Technology (SAAT), Federal University of Technology, Minna, Niger State, while the determination of fatty acid composition was conducted at the American University of Nigeria, Yola. The following parameters were determined:

(i) pH value, (ii) Acid V mgKOH/g, (iii) Specific Gravity, (iv) Viscosity @40^{0}C, (v) Flash

point, and (vi) Pour Point Fatty acid composition (FAC).

The standard method used in determining the physicochemical properties of the vegetable oils is presented in Table 3.3.

Table 3.3: Physiochemical properties of vegetable oils

Property	Method	Description
Specific gravity	$\frac{weight\ of\ oil}{weight\ of\ equal\ vol\ of\ water}$	The weight of oil was compared to the weight of equal volume of distilled water to determine t specific gravity of the extracted oil by using specific gravity bottle.
Free fatty acid		Free Fatty Acid (FFA) = $\frac{Acid\ value}{2}$
Viscocity@ 40^{o}C	ASTM D445 and ISO 3104	Equation used was: $\frac{\eta}{dt} = A - Bt^2$
Acid value	Acid value mg/KOH/g	= $\frac{Titre\ value\ x\ 0.1\ M\ KOH\ x\ 56.10}{weight\ of\ sample\ (g)}$
Peroxity Value	ASTM DD5348	The muffle furnance was used to heat the oil Till weight remain constant
Flash Point	ASTM D93	The flash point tester was used to determine the fla point of the various sample
Saponification value	ASTM D558	
pH value		The pH values of the vegetable oils were determir using the pH meter.
Iodine value		AOAC (2006) was used to evaluate the Iodine
Density @ 15^{o}C	ASTM D4052	Specific Gravity (SG) = $\frac{Weight\ of\ Xml\ of\ oil\ x\ 0.1\ x\ 12}{Weight\ of\ Xml\ of\ Water}$ = $\frac{B-A}{C-A}$

3.3.2 Gas Chromatography and Mass Spectrometer

A mass spectrometer (GC-MS) instrument GC-MS-QP2010 Shimadzu system, from Japan was used to analyse the Fatty Acid Composition (FAC), which was conducted using a gas chromatograph interface at the American University in Yola, Nigeria. The machine set-up used is as follows: column over temperature of 70.0°C, injection temperature of 250.0°C, column flow was 1.80mL/min with total flow of 40.8mL/min at linear velocity of 49.2cm/sec and pressure of 116.9kpa. The FAC analysis results for both vegetable oils (jatropha seed oil and neem seed oil) are presented in chapter 4.

3.3.3 Formulation of jatropha curcas and neem seeds oils

The cutting fluid formulation was based on percentages of oil and additives to water in the ratio 1: 9. The preparation approach was primarily on the method adopted by Lawal *et al.,* (2012), Onuoha *et al.,* (2016), and Muniz *et al.,* (2008). The work of these aforementioned authors centred also on emulsion cutting fluids. A controlled condition for addition of the additives to the oil was done in the procedure to the formulation of the vegetable oil. For each mixture, a time of 12 min. was observed at ambient temperature using a locally made mechanical stirrer. Different additives were added to the jatropha seed and neem seed oils, including emulsifier, antioxidant, anti-corrosive and biocide in different percentages, and mixed thoroughly with a mechanical stirrer. Water was added to a percentage volume of 90, thus making the emulsion ratios of 1:9 of base oil (jatropha seed oil or neem seed oil) and water. Three readings of viscosity and pH value were measured. The percentage ratio of additives in the work of Onuoha *et al.* (2016), was adopted for the formulation, as follows:- 9.35% emulsifier, 0.97% biocide, 10.61% anticorrosive agent, 0.64% antioxidant. The purpose for adopting the percentage ratio used by Onuoha *et al.* (2016), was based on the excellent output obtain in terms of stability, pH, corrosion level and viscosity during the formulation. The formulation involved the mixture of oil and additives and stirred before the balance for the required volume was

made from water. The flow chart of the formulation is shown in Figure 3.5.

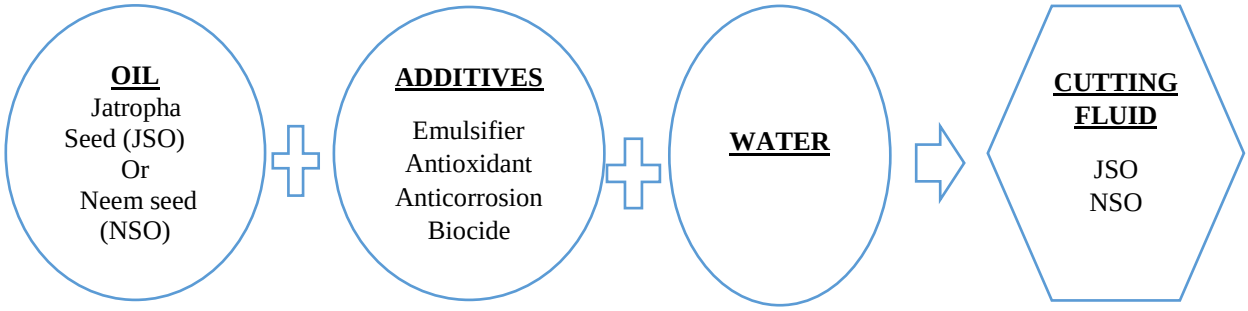

Figure 3.5: Vegetable oil-based cutting fluids formulation

The experimental locations for the formulated oils is the Mechanical Engineering Department and the Water and Fisheries Technology Laboratories of the Federal University of Technology, Minna. The materials for the formulations were:

i. Additives (emulsifier, antioxidant, anti-corrosion and biocide)

ii. Jatropha seed oil and Neem seed oil

while, the following equipments were also used:

i. Bakers, mini and medium test tubes

ii. Distilled water

iii. Filter paper

iv. Bowls and dishes

v. Local made Mechanical stirrer (Figure 3.6)

vi. Drilling machine (Figure 3.6)

vii. Stop watch.

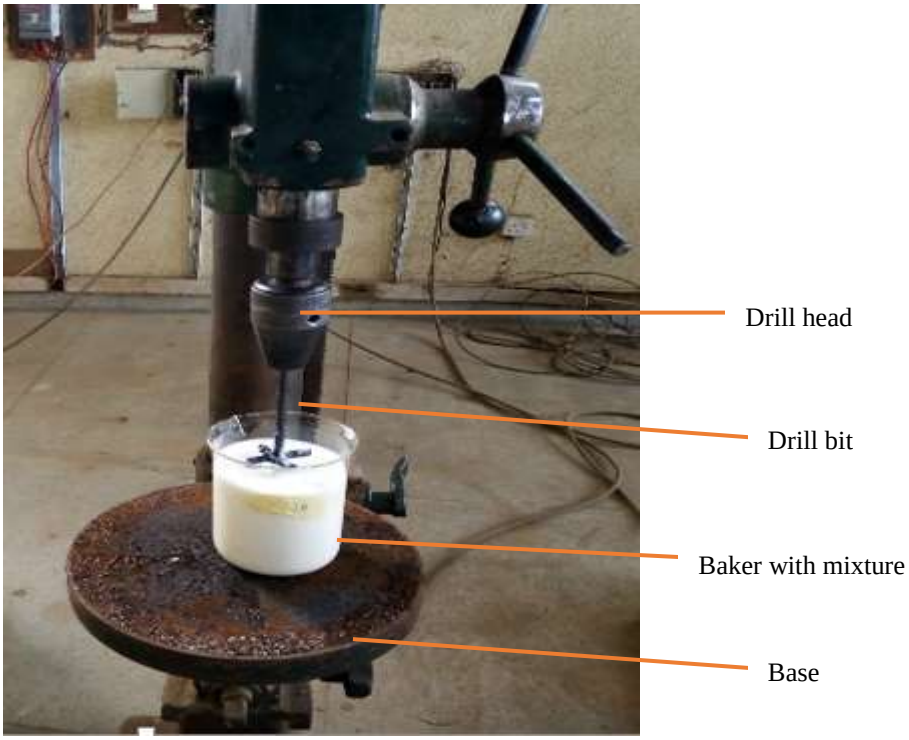

Figure 3.6: stirring oil-in-water mixture

The following calculation was used to obtain the appropriate volume of each component in preparation of one litre of cutting fluid. Mixing the soluble oil (concentrate) with water at the ratio of 1:9 was applied in the formulation of mineral-based cutting fluid.

3.3.4 Experimented formula samples

Sample	Emulsifier	Anti-corrosion	Anti-oxidant	Bioxide
A	8.31%	2.93%	0.95%	0.99%
B	11.81%	3.67%	0.76%	0.64%
C	9.35%	10.61%	0.64%	0.94%

3.3.5 Characterisation and evaluation of formulated cutting fluids

(a) pH value test

The pH value of the six samples were analysed in the laboratory of the Water Resources and Fishery Technology, Federal University of Technology, Minna. Research has shown that acceptable pH values is between 8 and 11. The pH values obtained are shown in chapter 4,

using model pHS-25 pH meter. The pH value signifies the general state of acidity or alkalinity of the fluid. One of the hazards and challenges to human operators which also lead to disposal problem is cutting fluid with very high or very low pH value. Acidic medium instead of alkaline medium is the channel to which microbial contamination of cutting fluid takes place. Thus, better resistance of the fluid to microbial attack is promoted by a higher pH value (Rao *et al*., 2007). A pH value of between 9 and 11 should be considered (Alves and Oliveira, 2008). A low acidic pH value is known to reduce the corrosion protection of the workpiece and machined parts, and therefore reduces stability. Thus, there is the tendency by the cutting fluid to degrease the skin and remove the natural protection of the skin if the cutting fluid pH is too high (strong alkaline), resulting in hazard to both the operators and users. The pH value reaction on worker's health is presented in Figure 3.7.

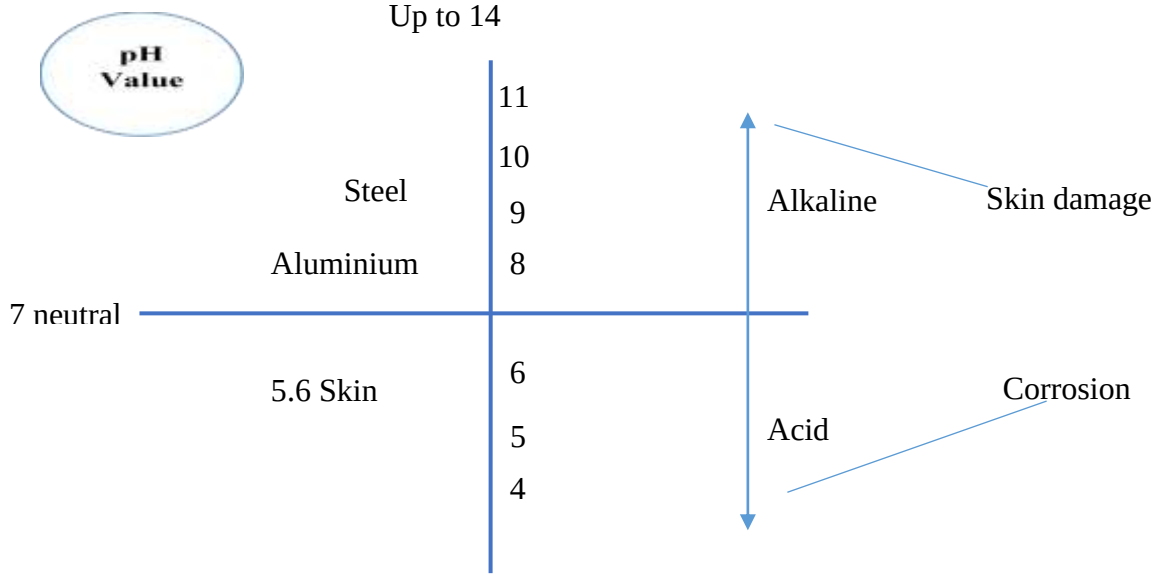

Figure 3.7: pH Value reaction on Worker's Health and Materials (Source: www.theworks-works.com)

The pH values of the cutting fluids were measured using pH meter in the Chemical Laboratory of the Federal University of Technology, Minna, Niger State, Nigeria. A standard solution was employed in the calibration of the pH meter. Distilled water was used to clean the electrode of the pH meter before taking each reading.

(b) Viscosity test

The viscosity value of the six samples were analysed in the laboratory, of the Water Resources and Fishery Technology Federal University of Technology, Minna using ASTM D445 standard. Each of the six samples was subjected to three tests and an average value was taken. The model pHS-25 pH meter was employed to obtain the average viscosity values. It relies on the ratio of shear stress to the rate of shear during flow. One of the deciding parameters to evaluate the performance of a cutting fluid as a lubricant is kinematic viscosity. A rise in kinematic viscosity means a rise in the lubricating property of the cutting fluid (Rao *et. al.*, 2007).

(c) Corrosion level test

The formulated cutting fluids corrosion level was determined using the ASTM D4627 cast iron chips on filter paper, and the method adopted by Alves and Oliveira (2008). Corrosion tests was used to study the release of the non-required components into the oil that was prepared as cutting fluid. The ASTM standard practice procedure employed in this work is for corrosion testing of the oil been prepared as cutting fluid. The product from the corrosion test were removed from reacted specimen prior to weighing in the ASTM procedure. However, this test was carried out to evaluate the number of corrosion spots on a test filter paper, from the formulated vegetable cutting fluids corrosive action(s). The experiment was carried out by measuring 2g of cast iron chips on a filter paper. The particular 2ml vegetable oil cutting fluid collected was stirred and gradually poured on the iron chips in a baker, and then shaken for 2 mins to mix the chips and fluid. The fluid was decanted and chips placed on a filter paper for 2 hrs. Thereafter, the iron chips were removed and the filter paper carefully rinsed out with tap water. Corrosion assessment was carried out, based on the corrosion inhibiting ability of the emulsion cutting fluids formulated. The G&G electronic scale was employed for accurately measuring 2.0mg of iron chips and mixed with a portion of each of the six sampled formulated

cutting fluid. It was observed that incidences of corrosion were very minimal on both NSO and JSO test, which varied for the six samples formulated. This is in line with the pH values of all the samples, which is significantly above acidic level where the filter paper used in the corrosion test for one of the sample tested. Negligible spots were observed on the filter paper after the experiment.

(d) Stability test

For purpose of stability the formulated cutting fluids were evaluated using a visual transparency within a period of 72hrs at room temperature (25^{o}C) as to separation of water and oil in a graduated 1000 ml test tubes.

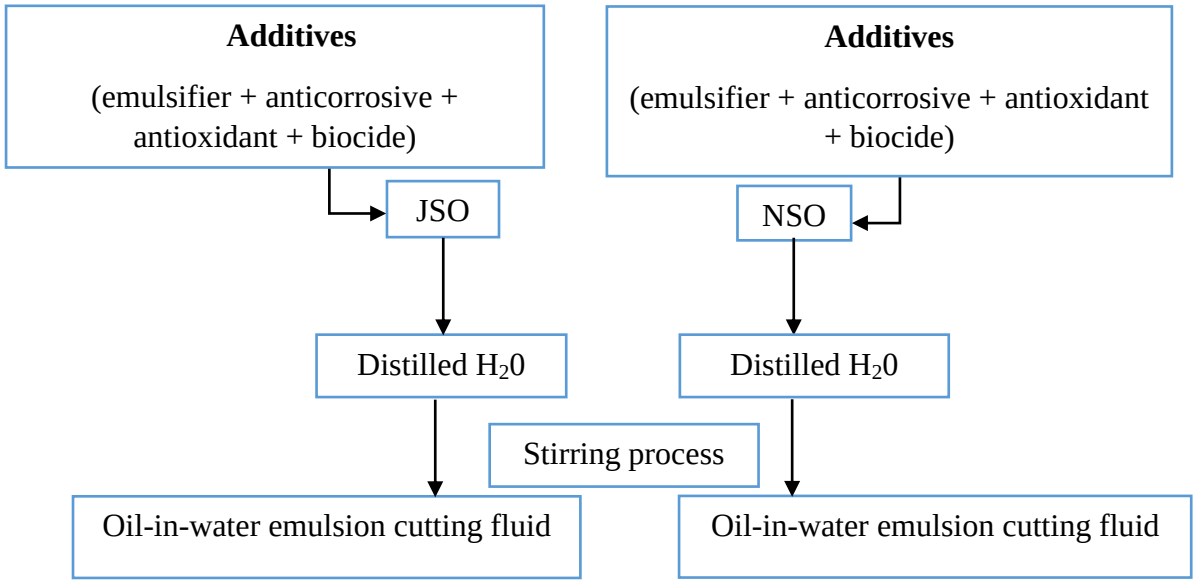

Figure 3.8: Schematic diagram of the oil in water mixture

The stability test for the cutting fluid formulation was carried out by adopting three formula samples and picking the sample that gave optimum and reliable result from the three. Thus, each of JSO and NSO were subjected to the three adopted formulae which gave a total of six samples under observation and test. The vegetable oil-in-water emulsion cutting fluids stability was evaluated after experimentation, based on visual transparency within a period of 72 hours at room temperature (25^{o}C) as to phase separation in a graduated 100 ml test tubes. The stability

test was carried out for the optimized samples of vegetable oils cutting fluids. The adopted formulae and the reported individual samples stability analysis results based on percentage by volume of water that separated from the mixture, are presented in chapter 4.

3.4 Design of experiment

The process of planning experiments so that appropriate data can be analysed by statistical methods is termed Design of Experiment (DOE) which makes for valid and objective conclusions (Masounave *et al.*, 1997). One-factor-at-a-time (OFAT) experimental approach which is seen as time consuming and cost ineffective is widely replaced nowadays with experimental design methods such as factorial design, Taguchi design and response surface methodology (RSM) (Das *et al.*, 2013). The effects of machinery parameters such as cutting speed, feed rate, depth of cut, tool nose and others, have employed design of experiment in order to determine such response as surface roughness, cutting temperature (Makadia and Nanavati, 2013). For purpose of performing trend analysis of cutting force and material removal rate, full factorial method has been successfully tested in metal cutting involving turning and milling processes with respect to various combinations of design variables of feed rate, depth of cut and cutting speed (Tamrakar *et al.*, 2015). Also, for the purpose of improving experimental process analyses, experimental design is a critically important tool in the scientific and engineering world. Experimental design methods are basically important in engineering design activities, where new products are developed and existing ones improved. The process of planning the experiment so that appropriate data will be collected and analysed using statistical methods, resulting in valid and objective conclusions is known as statistical DOE. Any experiment has two paths: the experimental design and the statistical analysis of data. The pre-experimental planning activities for this study includes the recognition and statement of the problem, which is the cutting fluids performance evaluation (jatropha seed oil, neem seed oil and mineral oil based cutting fluids) during the turning of AISI 304 stainless steel. Other pre-

experimental activities include:

i. Selection of the response variable: tool wear, workpiece surface roughness, and type of chip formation; and

ii. Choice of factors levels and range.

In this experimental study design, the machining parameters such as cutting speed, feed rate and depth of cut are of key importance as input factors. Also, the three cutting fluids being investigated and evaluated had effect on the tool wear and surface roughness of the workpiece and therefore are also input factors considered. Hence, the experimental design factors are: 1, cutting speed (A) 2, feed rate (B) 3, depth of cut (C) 4, types of cutting fluids (D). In this study are jatropha seed oil and neem seed oil-based cutting fluids, and commercially available mineral oil-based cutting fluids. Two experimentation levels are chosen as low (-1) and high (+1) with three different oil based cutting fluids of 20 runs each, and a total of 60 runs.

3.4.1 Response surface methodology (RSM)

Response Surface Methodology (RSM) is a statistical technique for measuring and exploring the relationship between several explanatory variables and one or more response variables. RSM originated from a seminar paper presented by Box and Wilson (1951). The linear effects is the screening model that we used for the first order situation which involves a single cross product factor, and represents the linear x linear interaction component.

$$\gamma = \beta_0 + \beta_1 x_1 + \beta_2 x_2 + \cdots + \beta_{12} x_1 x_2 + \Sigma \quad (3.1)$$

The steepest ascent model ignore cross products which gives an indication of the curvature of the response surface that is fitted as:

$$\gamma = \beta_0 + \beta_1 x_1 + \beta_2 x_2 + \Sigma \quad (3.2)$$

A close thought somewhere near the 'top of the hill' will fit a second order model. This includes in addition the two second-order quadratic terms.

$$\gamma = \beta_0 + \beta_1 x_1 + \beta_2 x_2 + \beta_{12} x_1 x_2 + \beta_{11} x_1 2 + \beta_{22} x_2 2 + \Sigma \quad (3.3)$$

where $\beta's$ are the unknown parameters and the x's are the line spaces. The globally accepted techniques to predict the responses in hard turning problems is response surface methodology (RSM) (Sahoo & Sahoo, 2013; Keblouti *et al.,* 2017). RSM (uncoded unit) at 95% confidence level help to develop regression models for responses with supposed orthogonal array data set (Sahoo & Sahoo, 2013; Nouioua *et al.,* 2017). In addition, the predicted model, its factors, the interaction of those factors and curvature are said to be noteworthy if the p value in ANOVA table is lower than 0.05. Thus, this confirms the worthiness of the predicted model, its factors, the interaction of those factors and curvature.

The chosen DOE method is the RSM for the following reasons:

I. It is the most user friendly and effective tool which leads to more accurate and powerful test by reducing error variance;
II. It provides better precision which can be obtained in estimating the overall main factor effects; and
III. Interaction between different responses can be properly identified and explored without confounding the effects.

Tables 3.4 and 3.5 showed some DOE methods with the criteria for selection. There are three factors in the present study which was tested at two levels thereby leading to a 2^3 factorial design. A total of 20 runs each (2^3) of experiments was performed for the three different oil-based cutting fluids as shown in Table 3.4.

Table 3.4: Cutting parameters and levels

Factor	**Unit**	**Level 1 Low (-1)**	**Level 2 High (+1)**	**Types of cutting fluid mm^2/s**
Cutting speed (A)	m/min	-1	+1	JSO

Feed rate (B)	mm/rev	-1	+1	NSO
Depth of cut (C)	mm	-1	+1	MBO

The data obtained for all the experimental runs was analysed statistically using the Minitab 17 statistical software. Second degree polynomial statistical software approximated by equation 3.3, for RSM analysis is to be used. It is often known that RSM work with variable models which are coded models where $\beta's$ are the unknown parameters and x's are the line spaces, such as expressed earlier on page 71.

The techniques that is globally accepted for predicting the responses in hard turning problems is RSM (Keblouti *et al.*, 2017).

Table 3.5: Machining variables (factors) and their levels

Factor	**Unit**	**Level 1 Low (-1)**	**Level 2 cutting High (+1)**	**Types of fluids mm^2/s**
Cutting Speed	rev/min	630	1000	JSO
Feed Rate	mm/rev	0.65	1.0	NSO
Depth of Cut	mm	0.3	1.0	MSO

The RSM experiment of two-levels-three-factors 2^3 array matrix was employed. The minimum values of the three input parameters of cutting speed, feed rate and depth of cut which served as a control was used for a single dry cut made. The experimental runs were conducted with the four input parameters of cutting speed, feed rate, depth of cut and cutting fluid type as shown in

Table 3.6, using RSM which gave a total of $2^3 = 20$ runs (8 cubic points, 6 axial points and 6 centre points). For each experiment, a fixed length of 350mm and new cutting edge of the cutting tool insert was used for each cutting fluid. The conventional wet method was employed for the cutting fluids application. These parameters were chosen during the actual experimentation with respect to the lathe configuration.

Table 3.6: Experimentation layout for L_{20} orthogonal array

Run Order	Cutting Speed	Feed Rate	Depth of Cut	Type of Cutting Fluid
1	-1	-1	-1	JSO
2	+1	-1	-1	NSO
3	-1	+1	-1	MBO
4	+1	+1	-1	NSO
5	-1	-1	+1	MBO
6	+1	-1	+1	MBO
7	-1	+1	+1	MBO
8	+1	+1	+1	MBO
9	+σ	0	0	JSO
10	- σ	0	0	MBO
11	0	+1.63	0	MBO
12	0	-1.63	0	NSO
13	0	0	+1.63	JSO
14	0	0	-1.63	MBO
15	0	0	0	JSO
16	0	0	0	NSO
17	0	0	0	JSO
18	0	0	0	NSO
19	0	0	0	NSO
20	0	0	0	JSO

3.5 Experimental method for orthogonal turning process

A 4-jaw MEUSER M00L conventional centre lathe made by Meuser ETM GmbH, Gruendau 63584, Germany, with variable spindle speed of 30 - 400 rpm and 5Hp rated power was where all turning experiments were conducted. A squared tungsten carbide tool inserts TNMG 1604 by Canela Tools, mounted on a right hand tool model MTJNR 2020 K16 was used with a new cutting edge for each experiment. The experimental evaluation of tool wear and surface roughness were conducted on the workpiece of 25mm diameter and 500mm length, to achieve a ratio of diameter to length of 1:20, which ensures rigidity and eliminates flexing during the turning operation. Ambient temperature condition was used to carry out the turning operations. During turning, each experimental specimen was mounted on the lathe, and a thin outer surface of each experimental specimen was machined off before the start of the experiments.

3.6 Surface roughness measurement

Each machined portion of the workpiece was measured three times for each run with the average reading recorded, using Surface Roughness Tester model STR-6210S, at three locations on the circumference of the round bar workpiece, and the average of these readings recorded for each experiment are as shown in Figure 4.11. Digital Separate Surface Roughness Tester: Model SRT-6210S with ± 10% accuracy and not more than 6% fluctuation display value.

3.7 Tool wear measurement

Tool wear monitoring is very vital in machining industry as it may result in loss of dimensional accuracy and quality of finished product (Thakre *et al.,* 2019). This work included the measurement of tool wear using Dinolite digital tool wear microscope as a measuring device. The system consists of a digital camera to capture the tool wear image, a good light source to illuminate the tool, a retort stand to stabilise the dinolite and a computer for image processing. Inline automatic calibration is a new method of a pixel, which is employed in the work. The

carbide inserts captured images are processed, and the segmented tool wear zone was obtained by image processing. The vision system extracts tool wear parameters such as average tool wear width, tool wear area, and tool wear perimeter. The results of the average tool wear width obtained from the vision system were experimentally validated with those obtained from the dinolite digital microscope as presented in chapter 4. The tool wear reading was measured three times for each run and the average recorded. The average error found for measurements of all used carbide inserts was recorded. The images of the wear zone showed the severe abrasion marks and damage to the cutting edge for higher machining time. The study indicated that the efficient and reliable dinolite digital system can be employed to measure the tool wear parameters.

Chapter 4 presents the results from the oils characterisation, the formulated oils (jatropha oil-based cutting fluid, (JBCF), neem oil-based cutting fluid (NBCF) and mineral oil-based cutting fluid MBCF) as shown in the first ten tables in chapter 4, and the adopted formula for the formulated oils was employed in the machining experimental design and operation to which evaluation and optimisation of the machining process was achieved.

CHAPTER FOUR

4.0 RESULTS AND DISCUSSION

4.1 Physiochemical Properties of Oils

The physiochemical properties of the jatropha and neem oils, were carried out in the Department of Water Resources and Fisheries Technology, Federal University of Technology, Minna. The test analysis carried out highlighted the physical and chemical characteristics of these oils. Table 4.1 shows the physiochemical properties of the oils.

Table 4.1: Physiochemical properties of jatropha seed oil (JSO) and neem seed oil (NSO)

Physiochemical Properties	JSO Sample	NSO Sample
pH value	6.35	5.28
Acid Value mgKOH/g	4.86	5.80
Specific Gravity	0.907	0.919
Viscosity @40^0C	21.30	25.10
Flash Point	260	238
Pour Point	-1	4
Peroxity Value	6.20	8.6

4.1.1 Gas Chromatography Mass Spectrometer (GC-MS) Analysis

The fatty acid composition results for the two oils samples indicated that jatropha seed oil (JSO) has an approximately 21.6% saturated fat with the main contributors being 14.2% palmitic acid, 7% stearic acid and 0.4% other acids. On the other hand, 78.4% of JSO is unsaturated fat with 44.7% oleic acid (mono-unsaturated) and 32.8% linoleic acid (poly-unsaturated). Neem seed oil (NSO) has approximately 37.0% saturated fat with the main contributor being 18.1% palmitic acid and 18.1% stearic acid, while about 63.0% is unsaturated with 44.5% oleic acid (mono-unsaturated) and 18.3% linoleic acid (poly-unsaturated) are major

contributors. The fatty acid composition or profile for one of the two samples of oils is shown in Figure 4.1 showing the mass spectrum for JSO analysis.

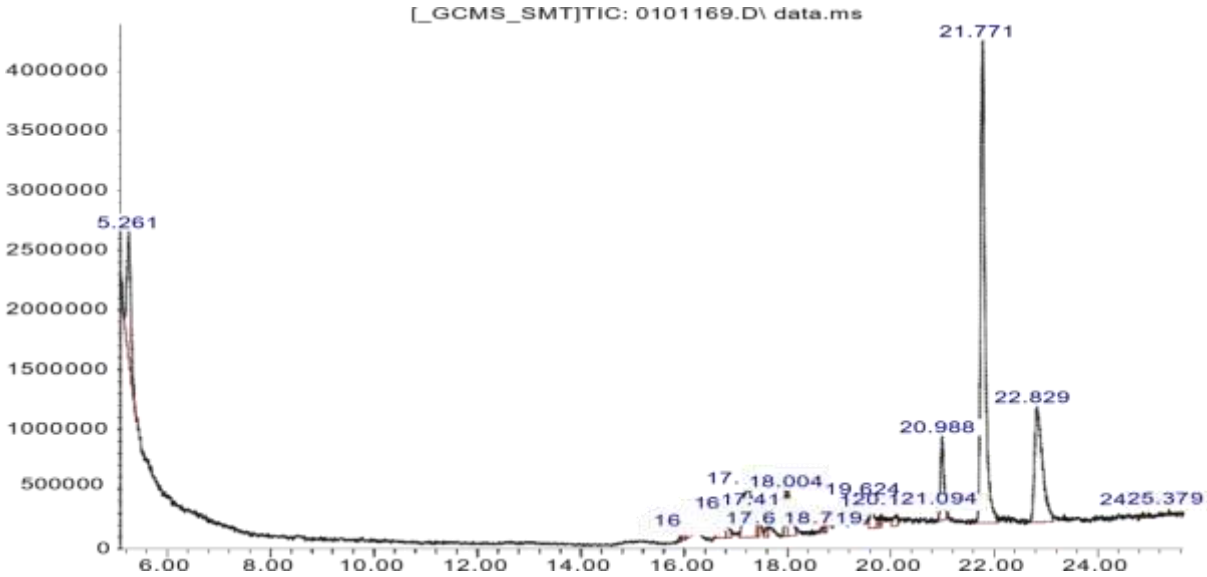

Figure 4.1: Gas Chromatography and Mass Spectrum (GCMS) Test Analysis for JBCF

The results obtained in Figure 4.1 and Table 4.2 are in agreement with existing literature such as the findings in the works of Aransiola *et.al* (2012), Akbar *et al., (*2009) and Martín *et al.,* (2010).

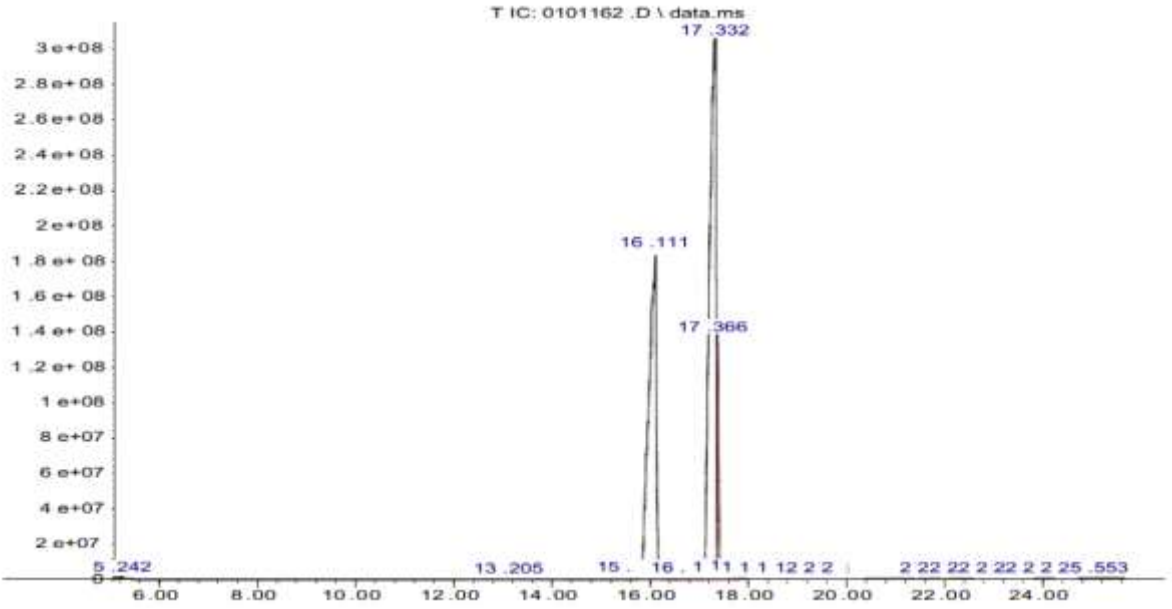

Figure 4.2: Gas Chromatography and Mass Spectrum (GCMS) Test Analysis for NBCF

Table 4.2: Fatty acid composition of jatropha and neem oils

Type of acid		Symbol	Fraction (%)	
Common Name	Formula		JSO	NSO
Palmitoliec acid	$(CH_3(CH_2)_{10}COOH)$	C16:1*	0.7	-
Myristic acid	$(CH_3(CH_2)_{12}COOH)$	C14:0*****	0.1	-
Palmitic acid	$(CH_3(CH_2)_{14}COOH)$	C16:0*****	14.2	18.1
Stearic acid	$(CH_3(CH_2)_{16}COOH)$	C18:0*****	7	18.1
Oleic acid	$(CH_3(CH_2)_7CH=CH(CH_2)_7COOH)$	C18:1******	44.7	44.5
Linoleic acid	$(CH_3(CH_2)_4CH=CHCH_2CH=CH(CH_2)_7COOH)$	C18:2******	32.8	18.3
Linolenic acid	$CH_3CH_2CH=CHCH_2=CHCH_2=CH(CH_2)_7CO_2H$	C18:2*****	0.2	0.2
Arachidic acid	$(CH_3(CH_2)_{16}(CH_2)_2COOH)$	C20:0*	0.2	0.8
Margaric acid	$(CH_3(CH_2)_{14}CH_2COOH)$	C17:0*	0.1	-
Total saturated acids			21.6	37.0
Total unsaturated acids			78.4	63.0
Ratio of saturated / unsaturated			1:3	2:3

***** saturated acids ****** unsaturated acids

Table 4.2 shows the analytical common names, the formulae and the percentage fraction of the two vegetable oil profile. pH is a measure of a fluid acidity or alkalinity. The choice and quantity of additives influence on the pH value of formulated cutting fluids. A limited alkalinity of 8.3 to 11 is the required value that should be maintained for a cutting fluid (Alves and de Aliveira, 2008). The values of jatropha sample ‘C’ (JC, 8.70) and neem sample ‘C’ (NC, 8.84) in Table 4.3 were higher and was adopted in this work. JA, JB and JC conote jatropha samples A, B and C, and NA, NB and NC conote neem samples A, B and C.

Table 4.3: pH values for the samples

pH Test Evaluation	
Samples	Values
JA	8.36
JB	8.40
JC	8.70
NA	8.67
NB	8.44
NC	8.84

The ability of a fluid to resist flow is known as viscosity. An acceptable cutting fluid should have moderate viscosity which enable pumping from the sump through hoses and pipes into the cutting zone to permeate the tool-chip interface for cooling to remove the heat generated and for lubrication to reduce friction and heat. JB, JC, NB and NC value in Table 4.4 gave an appreciable value which is consistent with the work of (Diamante & Lan, 2014).

Table 4.4: Viscosity values for the samples

Samples	$\frac{x+y+z}{3}$=K	$\frac{K}{30mm}$ mm^2/s
JA	14.3	0.47
JB	15.7	0.52
JC	15.7	0.52
NA	13.3	0.44
NB	16.7	0.56
NC	15.0	0.50

The three different formulated samples of pH and viscosity for both JSO and NSO were compared with JC and NC been the most suitable formulation by Onouah *et al.*, (2016) and was adopted as shown in Table 4.5.

Table 4.5 Viscosity and pH value of formulated emulsion cutting fluids

Cutting fluid	Optimized pH value	Validated pH value	Viscosity (40^oC) mm^2/s
Jatropha seed oil	8.70	8.70	0.52
Neem seed oil	8.84	8.84	0.50

The varying samples of the different formulae used in the three experiments carried out are shown in Table 4.6 with sample C whose values for pH, stability, viscosity and stability were consistent with existing aforementioned literatures and thus adopted in the preparation of the vegetable oil cutting fluids.

Table 4.6: Cutting fluid formulation formula samples

Sample	Emulsifier	Anti-Corrosion	Anti-Oxidant	Biocide
A	8.31%	2.93%	0.95%	0.99%
B	11.81%	3.67%	0.76%	0.64%
C	9.35%	10.61%	0.64%	0.94%

Table 4.7: Stability test measurement for Jatropha seed oil samples

Start Time (AM/PM)	Duration (Hrs)	JA		JB		JC	
2:30PM	0	Oil	Water	Oil	Water	Oil	Water
5:30PM	3	9	91	11	89	7	93
8:30PM	6	9	91	10	90	7	93
11:30PM	9	6	94	7	93	8	92
2:30AM	12	5.5	94.5	7	93	7.5	92.5
5:30AM	**15**	5.5	94.5	7	93	**7**	**93**
8:30AM	18	5.5	94.5	7	93	7	93
11:30AM	**21**	**5**	**95**	**6.5**	**93.5**	7	93
2:30PM	24	5	95	6.5	93.5	7	93
5:30PM	27	5	95	6.5	93.5	7	93
8:30PM	30	5	95	6.5	93.5	7	93
11:30PM	33	5	95	6.5	93.5	7	93
2:30AM	36	5	95	6.5	93.5	7	93
5:30AM	39	5	95	6.5	93.5	7	93
8:30AM	42	5	95	6.5	93.5	7	93
11:30AM	45	5	95	6.5	93.5	7	93
2:30PM	48	5	95	6.5	93.5	7	93
5:30PM	51	5	95	6.5	93.5	7	93
8:30PM	54	5	95	6.5	93.5	7	93
11:30PM	57	5	95	6.5	93.5	7	93
2:30AM	60	5	95	6.5	93.5	7	93
5:30AM	63	5	95	6.5	93.5	7	93
8:30AM	66	5	95	6.5	93.5	7	93
11:30AM	69	5	95	6.5	93.5	7	93
2:30PM	72	5	95	6.5	93.5	7	93

The mixture stirring time was 12 min/sample. The measuring tube maximum level was 100ml, the angle speed from the stirrer is 1400 rev/min, and the starting day/time was 1/2:30pm. These procedure was used for both stabilities (jatropha and neem) in Table 4.7 and 4.8 respectively.

Table 4.8: Neem seed oil stability test results

Start Time (AM/PM)	**Duration (Hrs)**	**NA**		**NB**		**NC**	
2:30PM	0	Oil	Water	Oil	Water	Oil	Water
5:30PM	3	13	87	13	87	8	92
8:30PM	6	13	87	13	87	8	92
11:30PM	**9**	12.5	87.5	12	88	8	92
2:30AM	12	12.5	87.5	12	88	8	92
5:30AM	15	12.5	87.5	12	88	8.8	91.5
8:30AM	18	12.5	87.5	12	88	8.8	91.5
11:30AM	21	12.5	87.5	12	88	8.8	91.5
2:30PM	**24**	12.5	87.5	12	88	8	92
5:30PM	27	12.5	87.5	12	88	8	92
8:30PM	30	12.5	87.5	12	88	8	92
11:30PM	**33**	13	87	12	88	8	92
2:30AM	36	13	87	12	88	8	92
5:30AM	39	13	87	12	88	8	92
8:30AM	42	13	87	12	88	8	92
11:30AM	45	13	87	12	88	8	92
2:30PM	48	13	87	12	88	8	92
5:30PM	51	13	87	12	88	8	92
8:30PM	54	13	87	12	88	8	92
11:30PM	57	13	87	12	88	8	92
2:30AM	60	13	87	12	88	8	92
5:30AM	63	13	87	12	88	8	92
8:30AM	66	13	87	12	88	8	92
11:30AM	69	13	87	12	88	8	92
2:30PM	72	13	87	12	88	8	92

All the samples passed stability test. However, JA (jatropha seed oil-based cutting fluid sample A) and NC (neem seed oil-based cutting fluid sample C) presented higher stability test conditions with stability value in Table 4.9.

Table 4.9: Optimum stability test condition

Sample	% vol of water
Jatropha Seed Oil cutting fluid	95
Neem Seed Oil	92

4.2 Analysis of the Vegetable Oil-based Cutting Fluids

The characteristics of the oil-in-water emulsion cutting fluids formulated are shown in Table 4.10. The results for pH value, viscosity, corrosion level, stability and colour of the formulated cutting fluids which involved 10% of oil with the additives and 90% of water by volume for the two samples of oils.

Table 4.10: Characteristics of oil-in-water emulsion cutting fluids

S/N	Property	JSO	NSO
1	pH value	8.36	8.67
2	Viscosity	0.52 mm^2/s	0.50 mm^2/s
3	Corrosion level	Resistant	Resistant
4	Stability	Stable	Stable
5	Colour	Milky	Deep yellowish

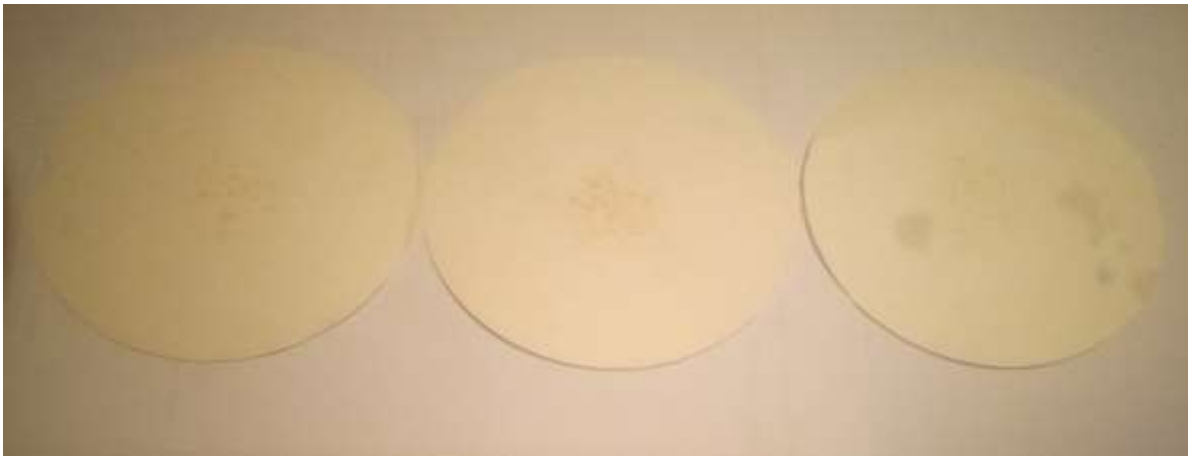

Plate IV: JSO formulated cutting fluids samples corrosion test

All the samples in Plate IV are the three jatropha samples (JA, JB and JC) which were put to test and all the samples passed the corrosion test.

Plate V: NSO formulated cutting fluids samples corrosion test

Plate V is the samples (NA, NB and NC) for the neem oil corrosion test. The corrosion test result for neem was reliable showing negligible corrosion that means neem oil can be employed as an additive for anti-corrosion test.

4.3 Workpiece material composition

The result of the characterisation of the workpiece material conducted via Optical Emission Spectrometer is presented in Table 4.11. The Midwal Engineering test laboratory was where the material composition results and certification of characterisation were obtained. Appendices C

and D shows the certificates for both composition and characterisation, respectively.

Table 4.11: AISI 304 alloy steel workpiece composition

Element	Fe	Cr	Ni	Mn	Si	Cu	Co	C	V	N
Composition (%)	70.7	18.04	8.33	1.36	0.41	0.33	0.19	0.09	0.07	0.04

The result obtained in Table 4.11 is similar with the expected composition of AISI 304 as reported by *AZoM.com* (2019) as presented in Table 3.1. This means the workpiece material used aligns with the intended investigation of AISI 304. The material composition test laboratory certificate is attached as Appendix D.

4.4 Turning Experimental Results

Response Surface Methodology was the basis for the DOE used for the turning of AISI 304 alloy steel. For each of the three cutting fluids (JBCF, NBCF and MBCF), 20 experimental runs were conducted which makes a total of 60 experimental runs carried out. Signal-to-noise ratio and procedure for ANOVA optimisation was used to analyse the experimental results with the aim of machining performance appraisal with respect to surface roughness and tool wear.

Characteristics of performance using S/N ratio are normally employed (Onuoha, 2016). The characteristcs are as follows:

$$\text{Larger-the-better, S/N} = -10\log\left[\frac{1}{n}\sum_{i=1}^{n} 1/y_i^2\right] \quad (4.1)$$

$$\text{Norminal-the-better, S/N} = 10\log\left[\frac{\bar{y}^2}{5^2}\right] \quad (4.2)$$

$$\text{Smaller-the-better, S/N} = 10\log\left[\frac{1}{n}\sum_{i=1}^{n} y_i^2\right] \quad (4.3)$$

where S/N is the signal-to-noise, S = standard deviation of the responses for the given factor level combination, n = number of responses for the given factor combination, and y_i = individual

responses. The design employed in this work is smaller-the-better equation.

The experimental design layout shown in Table 3.6 was employed to obtain the experimental process parameters and results shown in Table 4.12 for the three cutting fluids (JBCF, NBCF and MBCF).

Table 4.12: Experimental result for different cutting fluids

RO	V_c (rev/min)	FR (mm/rev)	DOC (mm)	JBCF R_a (μm)	Tw (mm)	NBCF R_a (μm)	Tw (mm)	MBCF R_a (μm)	Tw (mm)
1	630	0.65	0.30	0.89	0.23	0.61	0.09	2.63	0.13
2	1000	0.65	0.30	0.89	0.24	0.42	0.15	2.86	0.10
3	630	1.00	0.30	0.89	0.25	0.67	0.02	2.89	0.11
4	1000	1.00	0.30	0.85	0.15	0.44	0.51	2.62	0.12
5	630	0.65	1.00	0.94	0.31	0.53	0.18	3.39	0.62
6	1000	0.65	1.00	0.86	0.12	0.45	0.20	3.14	0.29
7	630	1.00	1.00	0.86	0.16	0.45	0.12	3.71	0.31
8	1000	1.00	1.00	1.38	0.29	0.46	0.16	4.77	1.02
9	500	0.82	0.65	0.64	0.11	0.47	0.26	2.42	0.07
10	1250	0.82	0.65	0.56	0.15	0.48	0.13	1.40	0.13
11	800	0.52	0.65	0.91	0.09	0.45	0.18	1.42	0.13
12	800	1.15	0.65	0.84	0.09	0.64	0.20	2.17	0.07
13	800	0.82	0.10	0.87	0.46	0.41	0.09	2.29	0.07
14	800	0.82	1.24	1.51	0.27	0.49	0.39	3.09	0.12
15	800	0.82	0.65	0.87	0.17	0.79	0.13	4.48	0.12
16	800	0.82	0.65	0.83	0.18	0.80	0.14	4.47	0.14
17	800	0.82	0.65	0.87	0.15	0.79	0.15	4.45	0.12
18	800	0.82	0.65	0.84	0.16	0.79	0.15	4.47	0.13
19	800	0.82	0.65	0.85	0.16	0.81	0.14	4.47	0.14

20	800	0.82	0.65	0.86	0.17	0.80	0.15	4.48	0.13

The experimental result of NBCF for both machining responses (surface roughness and tool wear) carried out, shows NBCF performed better than both JBCF and MBCF. The experimental results shows NBCF is a better lubricant and coolant compared to JBCF and MBCF respectively. However, JBCF performed better when compared to MBCF.

4.5 Analysis of the Signal to Noise Ratio for the Different Cutting Fluids

The characteristic equation for the S/N ratio for both surface roughness, Ra and tool wear (Tw), for the different cutting fluids (JBCF, NBCF and MBCF) is the smaller the better. The input parameters (cutting speed, (Vc), feed (f), and depth of cut (DoC), for the turning operation yielded the S/N ratio for the two determined responses as shown in Table 4.13.

Table 4.13: S/N ratio for different cutting fluids

				S/N ratio for JBCF		S/N ratio for NBCF		S/N ratio for MBCF	
	Vc	f	Doc	Ra	Tw	Ra	Tw	Ra	Tw
1	630	0.65	0.30	1.34	18.49	4.36	21.31	-9.82	18.70
2	1000	0.65	0.30	1.40	16.23	7.55	16.34	-7.69	22.82
3	630	1.00	0.30	3.82	19.18	3.43	32.57	-9.92	10.76
4	1000	1.00	0.30	-3.58	11.42	7.19	5.77	-9.24	19.06
5	630	0.65	1.00	1.56	20.41	5.55	14.98	-6.72	22.61
6	1000	0.65	1.00	1.32	15.69	6.87	13.94	-11.39	10.08
7	630	1.00	1.00	0.57	10.12	6.86	18.71	-10.62	4.13
8	1000	1.00	1.00	1.36	15.54	6.67	15.66	-13.02	18.51
9	500	0.82	0.65	1.20	15.33	6.51	11.72	-12.99	17.15
10	1250	0.82	0.65	1.57	15.00	6.45	17.46	-12.97	18.22
11	800	0.52	0.65	0.86	20.13	6.90	14.95	-3.03	17.78
12	800	1.15	0.65	0.93	12.63	3.94	13.78	-9.14	19.63
13	800	0.82	0.10	5.07	16.46	7.67	20.43	-2.94	17.58
14	800	0.82	1.24	1.07	12.52	6.09	8.23	-8.39	17.46
15	800	0.82	0.65	1.25	16.26	2.08	17.54	-13.01	17.79

16	800	0.82	0.65	1.48	15.80	1.92	17.46	-13.00	17.34
17	800	0.82	0.65	-2.79	10.76	2.07	14.95	-13.57	-0.14
18	800	0.82	0.65	1.41	16.18	2.02	13.78	-13.02	17.88
19	800	0.82	0.65	1.24	6.75	1.86	20.43	-7.22	23.10
20	800	0.82	0.65	0.99	12.01	1.89	8.23	-8.37	18.43

The performance evaluation of JBCF compared to NBCF and MBCF during turning operation with the same input parameters is consistent all through the 20 runs for each of the cutting fluids, as shown in Table 4.13. The S/N ratio for JBCF is better than those of NBCF and MBCF in terms of both surface roughness and tool wear.

4.6 Surface Roughness, Ra (μm)

4.6.1 Main effect plot for Surface roughness, Ra (μm)

4.6.1.1 Main effect plot for JBCF

The plot of the main effect of SN ratio as shown in Figure 4.3a was used for optimum value determination for each input parameters during turning process for the surface roughness. For surface roughness response, it is the smaller the better characteristics that was chosen as shown Equation (4.3). For the machining operation, the surface roughness optimal turning parameters are 1250 m/min of cutting speed (level 5), 1.15 mm/rev of feed (level 5), 0.65 mm depth of cut (level 3).

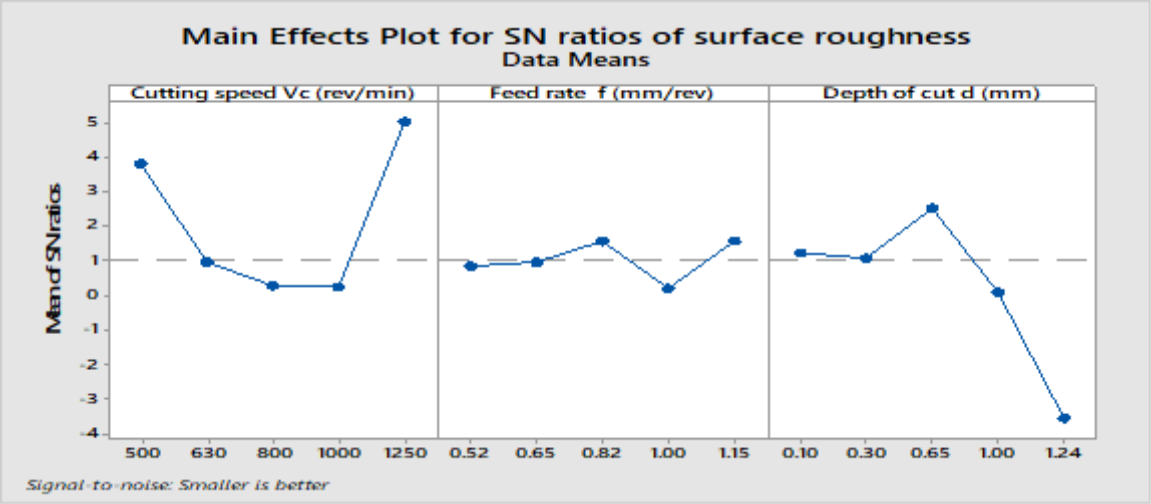

Figure 4.3a: Main effect plot of S/N ratio for surface roughness using JBCF

(a) JBCF

$$Surface\ roughness\ Ra\ (\mu m) = 2.30 + 0.0007Vc - 0.000002Vc \times Vc + 0.219Fr - 2.605DOC + 1.078DOC \times DOC + 0.00230Vc \times Fr + 0.000897Vc \times DOC + 0.964Fr \times DOC.$$

$$= 2.30 + 0.0007(1250) - 0.000002(1250) \times (1250) + 0.219(1.15) \times (1.15)\ 2.605(0.65) + 1.078(0.65) \times (0.65) + 0.00230(1250)\ (1.15) + 0.000897(1250) \times (0.65) + 0.964(1.15) \times (0.65)$$

$$= 0.9102$$

$$R - sq\ =\ 85.14\%\ \text{and}\ \ R - s(adj)\ \ =\ 71.76\%$$

4.6.1.2 Main effect plot for NBCF

The main effect plot from the SN ratio as shown in Figure 4.3b was employed for optimum value determination for each input parameters during turning process for the surface roughness. For surface roughness response, it is the smaller the better characteristics that was chosen. For the machining operation, the surface roughness optimal turning parameters are 1000 m/min of cutting speed (level 4), 0.52 mm/rev of feed (level 1), 0.10 mm depth of cut (level 1)

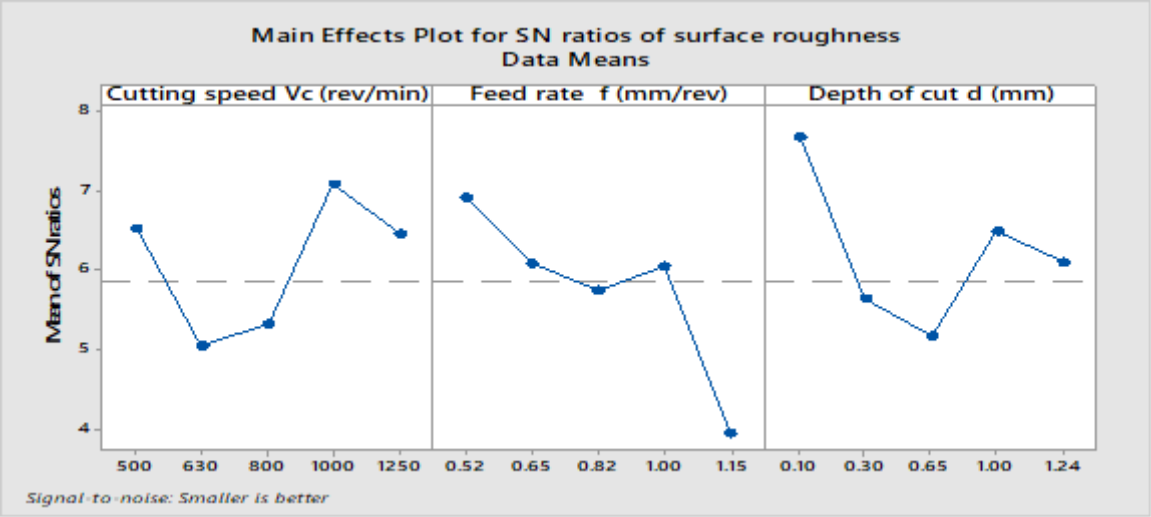

Figure 4.3b: Main effect plot of S/N ratio for surface roughness using NBCF

(b) NBCF

$$\text{Surface roughness Ra } (\mu m) = -2.534 + 0.00265\,Vc + 4.47\,Fr + 1.066\,DOC - 0.000002Vc \times Vc - 2.498\,Fr \times Fr - 1.031\,DOC \times DOC + 0.000023Vc \times Fr + 0.000656\,Vc \times DOC - 0.318\,Fr \times DOC$$

$$= -2.534 + 0.00265(1250) + 4.47\,(1.15) + 1.066(0.65) - 0.000002(1250) \times (1250) - 2.498\,(1.15)(1.15) + 0.231(0.65) \times (0.65) + 0.000023(1250) \times (1.15) + 0.000656(1250) \times (0.65) - 0.318 \times 1.15 \times (0.65)$$

$$= 0.7126$$

$$R - sq = 82.88\% \text{ and } R - sq(adj) = 67.46\%$$

4.6.1.3 Main effect plot for MBCF

The main effect plot from the SN ratio as shown in Figure 4.3c was employed for optimum value determination for each input parameters during turning process for the surface roughness. For surface roughness response, it is the smaller the better characteristics that was chosen. For the machining operation, the optimal turning parameters for surface roughness are 1250 m/min of cutting speed (level 5), 0.52 mm/rev of feed (level 1), 0.65 mm depth of cut (level 3).

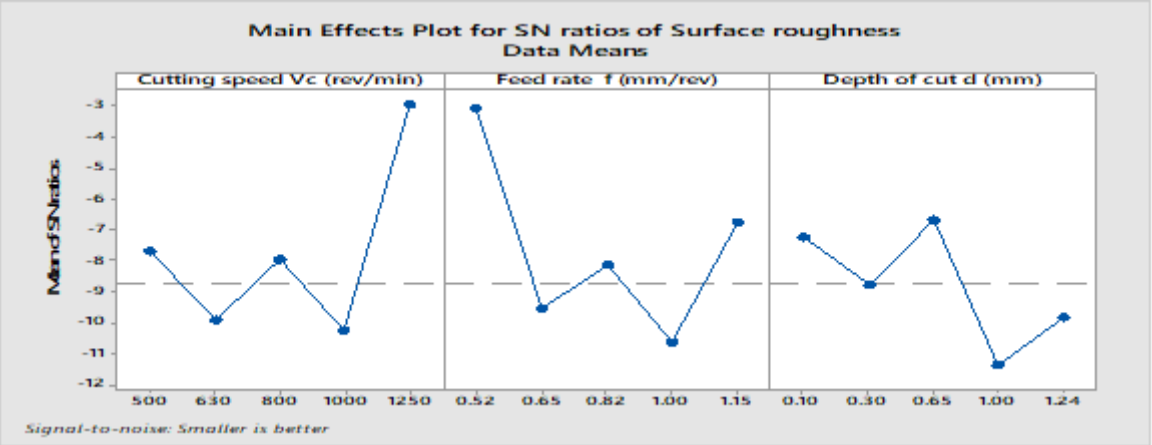

Figure 4.3c: Main effect plot of S/N ratio for surface roughness using MBCF

(c) MBCF

Surface roughness Ra (μm)

$$= 20.10 - 0.02227\,Vc + 33.59\,Fr - 1.47\,DOC - 0.000016Vc \times Vc - 22.52\,Fr \times Fr + 3.80\,DOC \times DOC - 0.00310\,Vc \times Fr + 0.00172\,Vc \times DOC + 3.96\,Fr \times DOC$$

$$= 20.10 - 0.02227(1250) + 33.59\,(1.15) - 1.47\,(0.65) - 0.000016\,(1250) - 22.52\,(1.15) \times (1.15) + 3.80\,(0.65) \times (0.65) - 0.00310\,(1250) \times (1.15) + 0.00172(1250) \times (0.65) + 3.96(1.15) \times (0.65)$$

$$= 1.2513$$

$$R - sq = 84.44\% \text{ and } R - sq(adj) = 70.43\%$$

The effectiveness of the formulated cutting fluids in the surface roughness reduction are placed in the resulting sequence; neem oil-based cutting fluid, jatropha oil-based cutting fluid and mineral oil-based cutting fluid. This sequence is expected considering the viscosity properties of the oils. The fatty acid composition of the oils is the reason for the behaviour of the different cutting fluids. The tool-workpiece interface is believed to form a thin wall film. There is a high proportion of saturated fatty acids in NSO which enhance the oil to release high strength lubricant films that relate strongly despite the little amount of oil in the formulation. This study observed that both vegetable oils shows lower tool wear and surface roughness when compared with the mineral oil-based cutting fluid which agrees with the work of Yan and Jiang (2013) on the performance of cutting fluid during machining operation in inproving surface quality and

extending tool life.

4.6.2 Analysis of variance

4.6.2.1 Analysis of variance for surface roughness under JBCF condition

The ANOVA statistics shown in Table 4.14 was used to study the significance of the input parameters on the surface roughness when cutting with JBCF. The significant effect of cutting speed, feed and depth of cut on the surface roughness during cutting with JBCF are as follows: cutting speed (CS) of (27.39%), feed rate (FR) of (6.16%) and depth of cut (DOC) of (62.73%). These results show that depth of cut has more significant impact on the surface roughness, followed by cutting speed. This indicated that depth of cut and cutting speed are more significant than feed on the surface roughness.

Table 4.14: ANOVA for surface roughness, Ra

Factor	DOF	SS	MS	F	P
CS (m/min)	4	0.22	0.06	12.90	27.39
FR (mm/rev)	4	0.05	0.01	2.89	6.16
DOC (mm)	4	0.51	0.13	29.54	62.73
Error	7	0.03	0.00		3.72
Total	19	0.81	0.04		100

Figure 4.4 shows the contour plots of the effect of depth of cut (mm) and cutting speed (m/min) on surface roughness, Ra (μm). It was observed that as cutting speed increase with decrease in depth of cut, the surface roughness decrease when JBCF is employed.

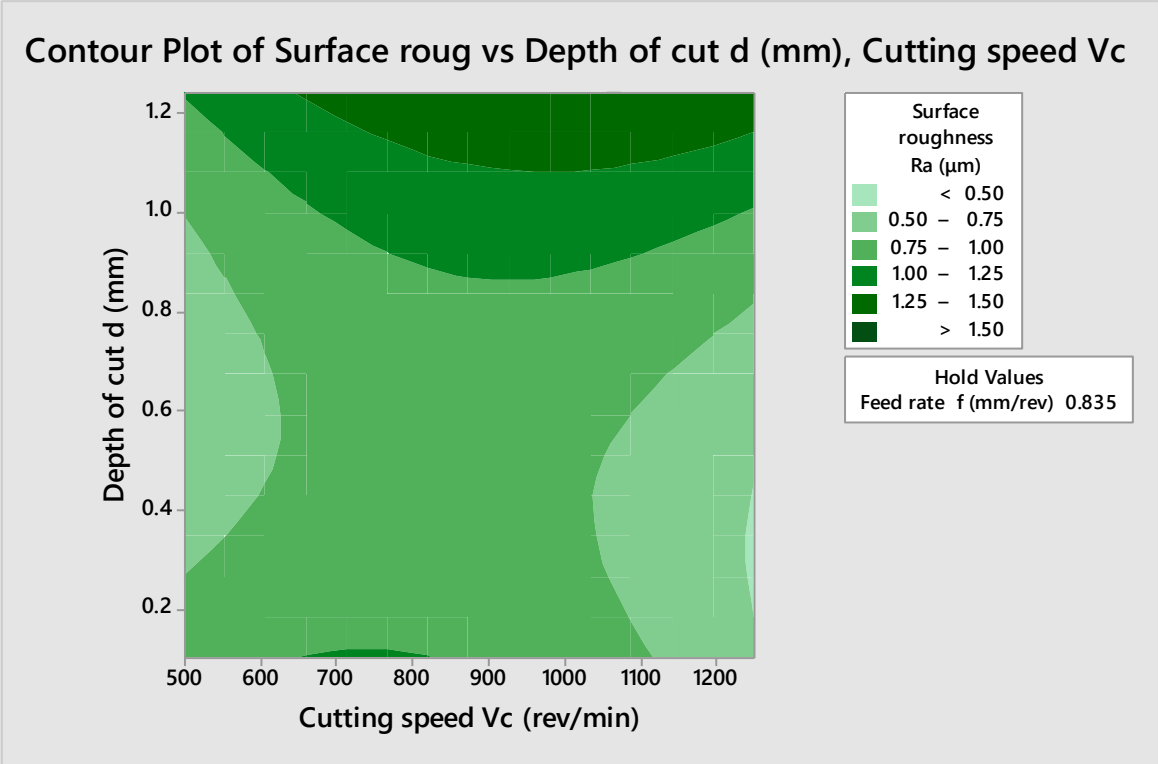

Figure 4.4: Contour plot for surface roughness with JBCF

The effect of cutting of speed and depth of cut on the surface roughness is shown using 3D surface plot in Figure 4.5. The flattened curve shape fit the design model. It is observed that as depth of cut increased with cutting speed, the surface roughness decreased and this follow similar trend with the contour plot.

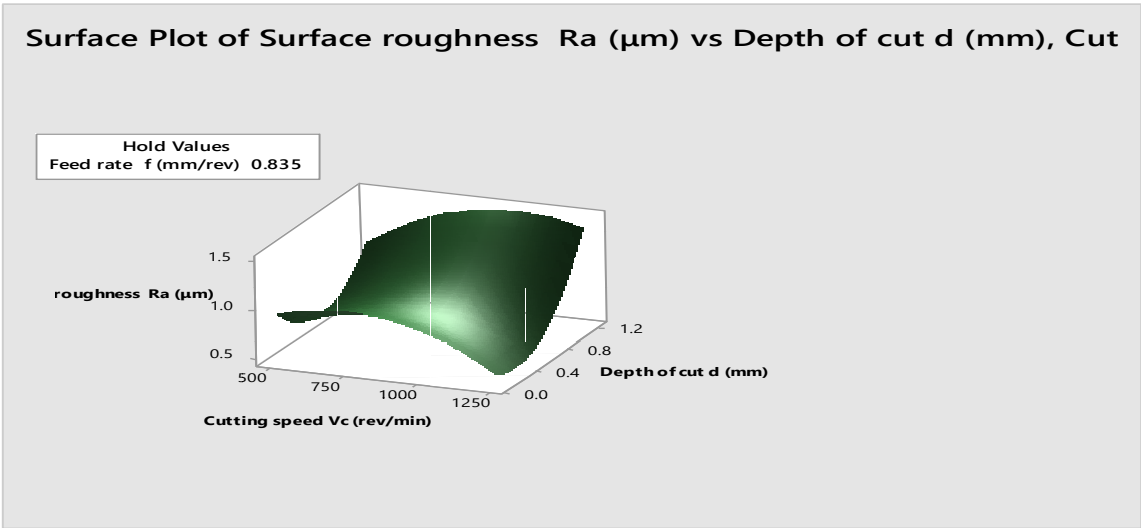

Figure 4.5: 3D surface graph for surface roughness with JBCF

4.6.2.2 Analysis of variance for surface roughness under MBCF conditions

The ANOVA statistics as shown in Table 4.15 was employed to study the significance of the input parameters on the surface roughness when cutting with NBCF. The significant effect of cutting speed, feed and depth of cut on the surface roughness during cutting with NBCF are as follows: cutting speed (CS) of (37.26%), feed rate (FR) of (24.78%) and depth of cut (DOC) of (36.74%). The results show that cutting speed has significant impact on the surface roughness, followed by depth of cut. Hence, cutting speed and depth of cut are more significant than feed rate on the surface roughness when NBCF is employed.

Table 4.15: ANOVA for surface roughness, Ra

Factor	**DOF**	**SS**	**MS**	**F**	**P**
CS (m/min)	4	0.17	0.04	53.55	37.26
FR (mm/rev)	4	0.11	0.03	35.61	24.78
DOC (mm)	4	0.17	0.04	52.81	36.74
Error	7	0.01	0.00		1.22
Total	19	0.46	0.02		100

Figure 4.6 shows the contour plots of the effect of cutting speed (m/min) and depth of cut (mm) on surface roughness, Ra (μm). It was observed that as cutting speed increase with decrease in depth of cut, the surface roughness increase when NBCF is employed.

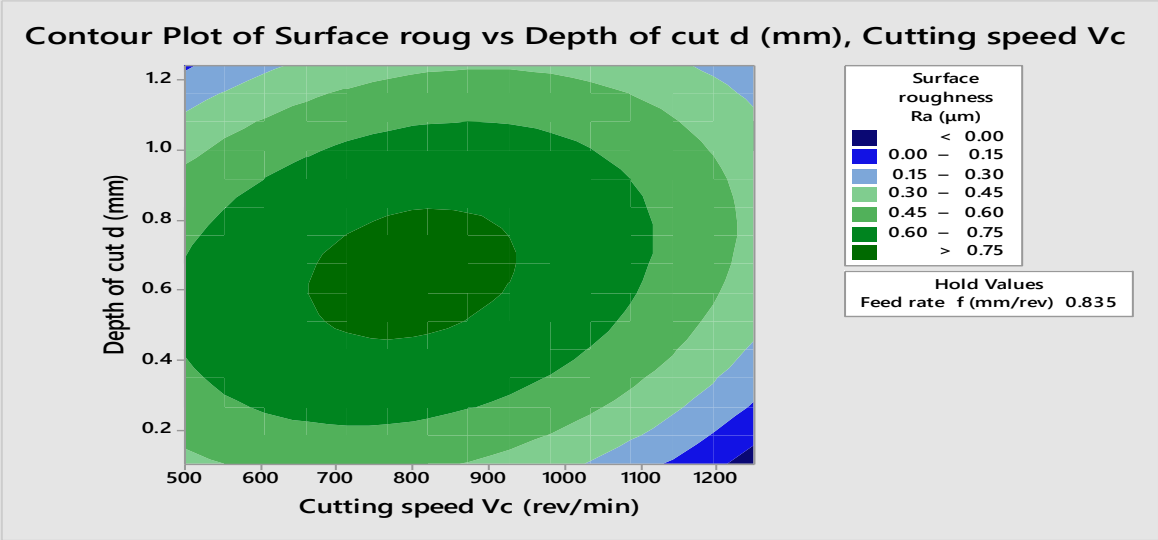

Figure 4.6: Contour plot for surface roughness with NBCF

The 3D surface plot in Figure 4.7 shows the effect of cutting speed and depth of cut on the surface roughness with a design model fitted flattened curve shape. It is observed that as cutting speed increased with depth of cut, the surface roughness increase, in agreement with the trend of the contour plot.

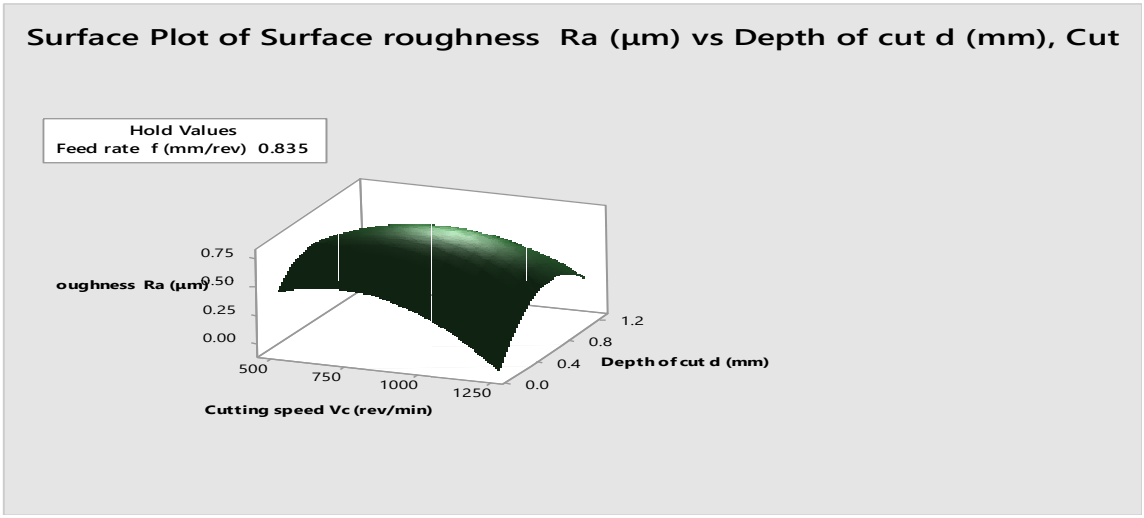

Figure 4.7 graph for surface roughness with NBCF

4.6.2.3 Analysis of variance for surface roughness under MBCF conditions

The ANOVA statistics with MBCF as shown in Table 4.16 was employed to study the significance of the input parameters on the surface roughness when cutting under MBCF environment. The significant effect of cutting speed, feed and depth of cut on the surface

roughness during cutting with MBCF are as follows: cutting speed (CS) of (33.69%), feed rate (FR) of (38.29%) and depth of cut (DOC) of (24.53%). These results show that feed rate has significant impact on the surface roughness, followed by cutting speed. This indicated that feed rate and cutting speed are more significant than depth of cut on the surface roughness when cutting with MBCF.

Table 4.16: ANOVA for surface roughness, Ra

Factor	**DOF**	**SS**	**MS**	**F**	**P**
CS (m/min)	4	7.43	1.86	16.88	33.69
FR (mm/rev)	4	8.44	2.11	19.18	38.29
DOC (mm)	4	5.41	1.35	12.29	24.53
Error	7	0.77	0.11		3.49
Total	19	22.04	1.16		100

Figure 4.8 shows the contour plots of the effect of feed rate (mm/rev) and cutting speed (m/min) on surface roughness, Ra (μm). It was observed that as feed rate increase with decrease in cutting speed, the surface roughness increase when MBCF is employed when compared to JBCF and NBCF.

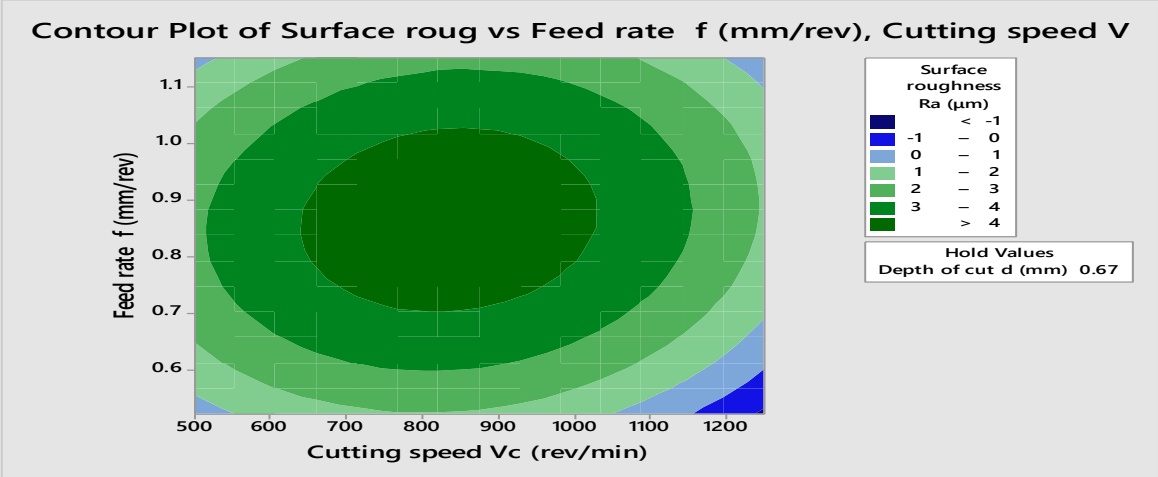

Figure 4.8: Contour plot for surface roughness with MBCF

The effect of cutting speed and depth of cut on the surface roughness is shown on 3D surface plot in Figure 4.9 with a design model fitted flattened curve shape. It is observed that as feed rate increased with cutting speed, the surface roughness increase in trend with the contour plot.

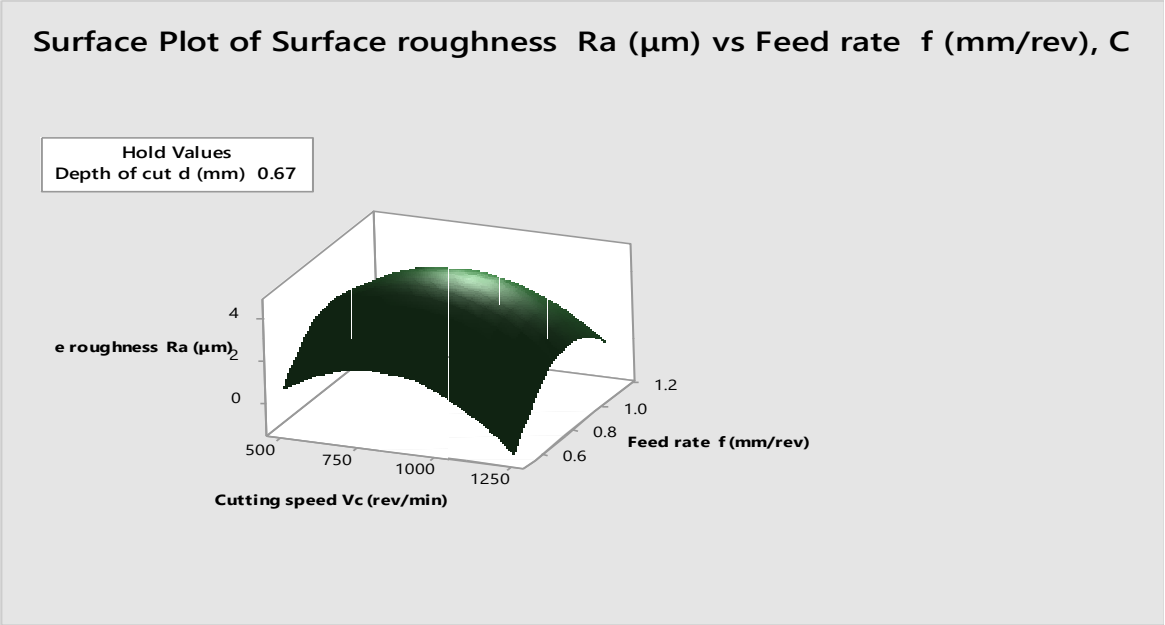

Figure 4.9: 3D surface graph for surface roughness with MBCF

4.7 Tool Wear, Tw (mm)

4.7.1 Main effect plot for tool wear, Tw (mm)

4.7.1.1 Main effect plot for JBCF

The main effect plot for SN ratio as shown in Figure 4.10a was employed for optimum value determination for each input parameters during turning process for the tool wear. For the tool wear response, it is the smaller the better characteristics that was chosen as shown in Equation (4.3). For the machining operation, the tool wear optimal turning parameters are 500 m/min of cutting speed (level 1), 1.15 mm/rev of feed (level 5), 0.65 mm of depth of cut (level 3).

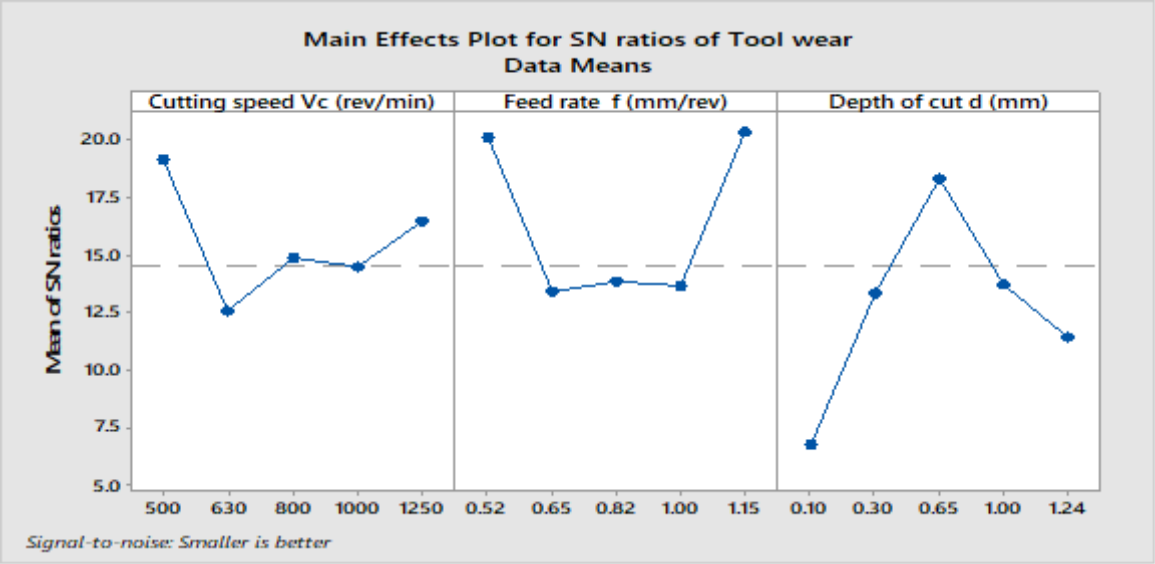

Figure 4.10a: Main effect plot of S/N ratio for tool wear using JBCF

(a) JBCF

$$\text{Tool wear Tw (mm)} = 0.708 - 0.000565\,\text{Vc} + 0.20\,\text{FR} - 1.115\,\text{DOC} - 0.000000\,\text{Vc} \times \text{Vc} - 0.608\,\text{FR} \times \text{FR} + 0.626\,\text{DOC} \times \text{DOC} + 0.000821\,\text{Vc} \times \text{FR} + 0.000084\,\text{Vc} \times \text{DOC} + 0.192\,\text{FR} \times \text{DOC}$$

$$= 0.708 - 0.000565\,(1250) + 0.20(1.15) - 1.115(0.65) - 0.000000\,(1250) \times (1250) - 0.608(1.15) \times (1.15) + 0.626(0.65) \times (0.65) + 0.000821 \times (1250) \times (1.15) + 0.000084(1250) \times (0.65) + 0.192(1.15) \times (0.65)$$

$$\text{R} - \text{sq} = 71.24\% \text{ and } \text{R} - \text{sq(adj)} = 56.35\%$$

4.7.1.2 Main effect plot for NBCF

The main effect plot for SN ratio as shown in Figure 4.10b was employed for optimum value determination for each input parameters during turning process for the surface roughness. For surface roughness response, it is the smaller the better characteristics that was chosen as shown in Equation (4.3). For the machining operation, the surface roughness optimal turning parameters are 630 m/min of cutting speed (level 2), 1.0 mm/rev of feed (level 4), 0.10 mm of depth of cut (level 1)

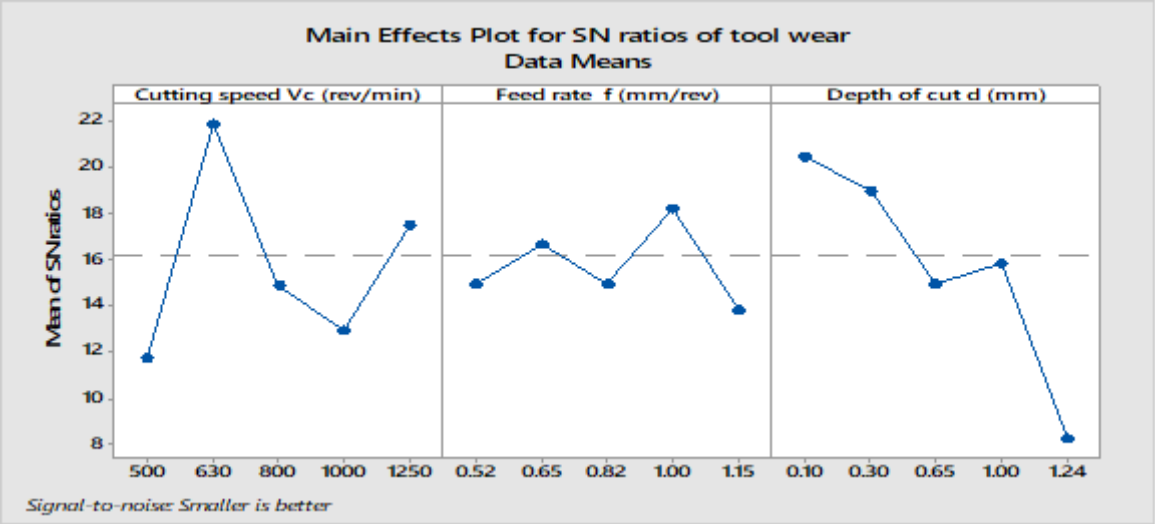

Figure 4.10b: Main effect plot of S/N ratio for tool wear using NBCF

(b) NBCF

Tool wear Tw (mm)

$$= 0.39 - 0.00060\,Vc - 1.24\,FR + 1.237\,DOC - 0.000000\,Vc \times Vc + 0.256\,FR \times FR + 0.244\,DOC \times DOC + 0.00180\,Vc \times FR - 0.000985\,Vc \times DOC - 0.831\,FR \times DOC + 0.102\,Fr \times DOC$$

$$= 0.39 - 0.00060(1250) - 1.24(1.15) + 1.237(0.65) + 0.000000(1250) \times (1250) + 0.256\,(1.15) \times (1.15) + 0.244(0.65) \times (0.65) + 0.00180(1250) \times (1.15) - 0.000985(1250) \times (0.65) - 0.831(1.15) \times (0.65) + 0.102(1.15) \times (0.65)$$

$R - sq = 63.75\%$ and $R - sq(adj) = 57.13\%$

4.7.1.3 Main effect plot with for MBCF

The main effect plot for SN ratio as shown in Figure 4.10c was employed for optimum value determination for each input parameters during turning process for the surface roughness. For surface roughness response, it is the smaller the better characteristics that was chosen as presented in Equation (4.3). For the machining operation, the surface roughness optimal turning parameters are 500 m/min of cutting speed (level 1), 1.15 mm/rev of feed (level 5), 0.10 mm of depth of cut (level 1).

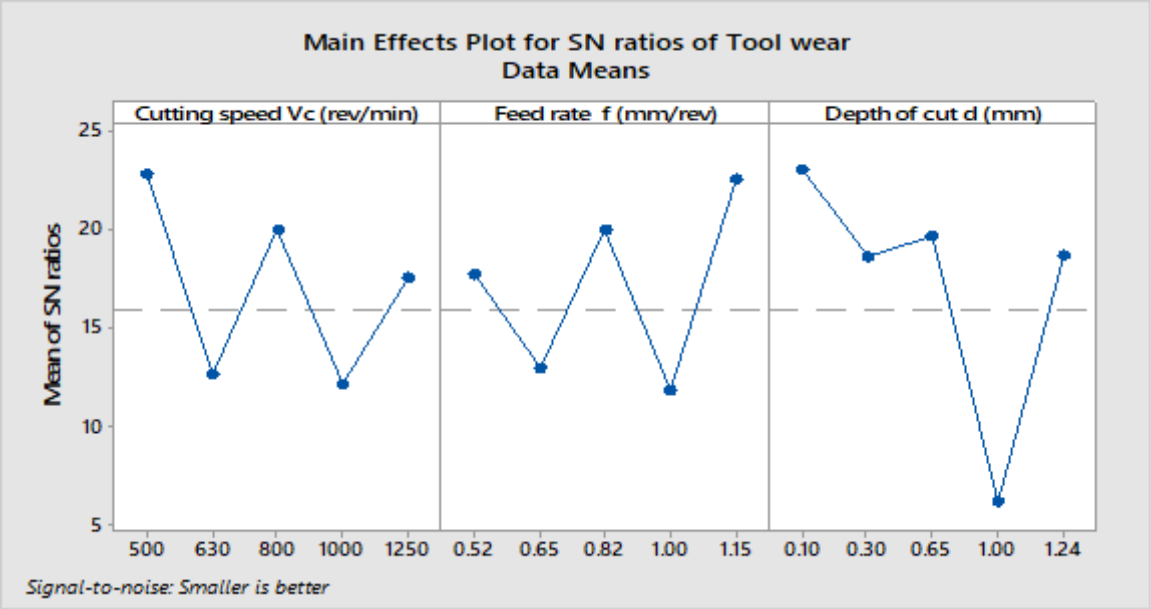

Figure 4.10c: Main effect plot of S/N ratio for tool wear using MBCF

(c) MBCF

Tool wear Tw (mm)

$$= 4.35 - 0.00437\,Vc - 5.35\,FR - 1.43\,DOC + 0.000000\,Vc \times Vc + 0.88\,FR \times FR + 0.288\,DOC \times DOC + 0.00423\,Vc \times FR + 0.00086\,Vc \times DOC + 0.91\,FR \times DOC$$

$$= 4.35 - 0.00437\,(1250) - 5.35(1.15) - 1.43(0.65) + 0.000000\,(1250) \times (1250) + 0.88(1.15) \times (1.15) + 0.288(0.65) \times (0.65) + 0.00423(1250) \times (1.15) + 0.00086(1250) \times (0.65) + 0.91(1.15) \times (0.65)$$

$$= 0.5506$$

$R - sq = 70.48\%$ and $R - sq(adj) = 55.92\%$

4.7.2 Analysis of variance

4.7.2.1 Analysis of variance for tool wear under JBCF conditions

The ANOVA statistics as shown in Table 4.17 was employed to study the significance of the input parameters on the tool wear when cutting with JBCF. The significant effect of cutting speed, feed and depth of cut on the tool wear during cutting with JBCF are as follows: cutting speed (CS) of (10.62%), feed rate (FR) of (15.29%) and depth of cut (DOC) of (70.83%). These results show that depth of cut has high impact on the tool wear, followed by feed rate. This indicatedthat depth of cut and feed rate are more significant than cutting speed on the tool wear using JBCF.

Table 4.17: ANOVA for tool wear, Tw (mm)

Factor	DOF	SS	MS	F	P
CS (m/min)	4	0.02	0.00	5.71	10.62
FR (mm/rev)	4	0.02	0.01	8.23	15.29
DOC (mm)	4	0.10	0.03	38.06	70.83
Error	7	0.00	0.00		3.26
Total	19	0.15	0.01		100

Figure 4.11 shows the contour plots of the effect of depth of cut (mm) and feed rate (mm/rev) on tool wear, Tw (mm). It was observed that as feed rate increase with decrease in depth of cut, the tool wear decrease when JBCF is employed.

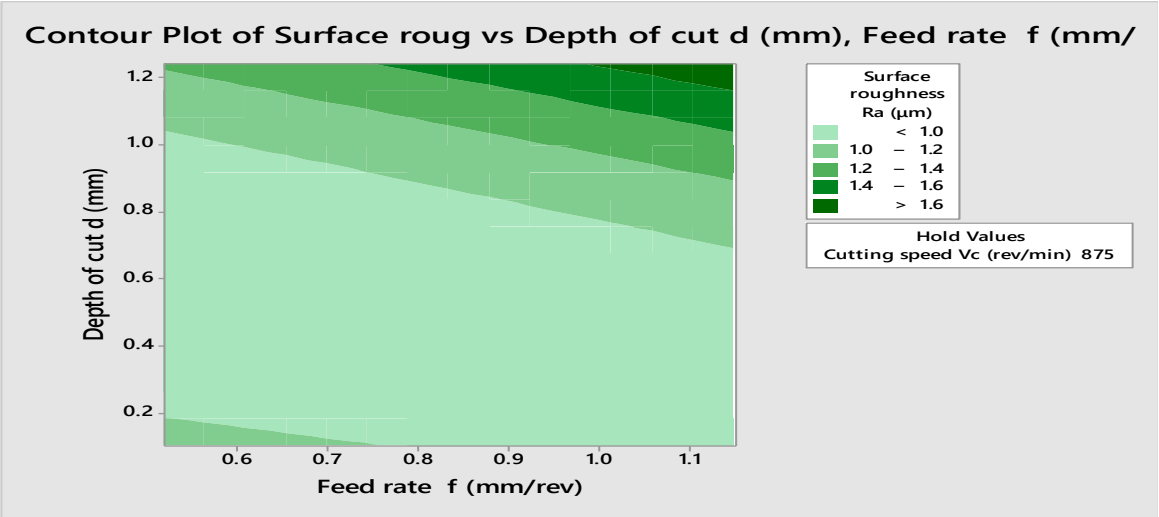

Figure 4.11: Contour plot for tool wear with JBCF

The effect of feed rate and depth of cut on the tool wear is shown using 3D surface plot in Figure 4.12. The flattened curve shape fit the design model. It is observed that as feed rate increased with depth of cut, the tool wear decrease in line with trend of the contour plot.

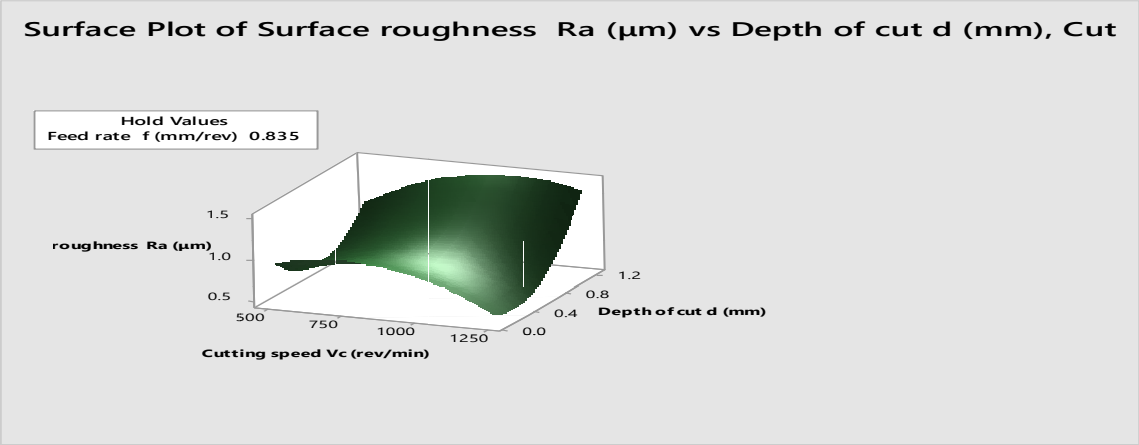

Figure 4.12: 3D surface graph for tool wear with JBCF

(b) Analysis of Variance for Tool wear Using NBCF

The ANOVA statistics as shown in Table 4.18 was employed to study the significance of the input parameters on the tool wear when cutting with NBCF. The significant effect of cutting speed, feed and depth of cut on the tool wear during cutting with NBCF are as follows: cutting speed (CS) of (40.41%), feed rate (FR) of (16.46%) and depth of cut (DOC) of (38.72%). These results show that cutting speed has significant impact on the tool wear, followed by depth of cut. This indicated that cutting speed and depth of cut are more significant than feed on the tool wear when NBCF is employed.

Table 4.18: ANOVA for tool wear, Tw (mm)

Factor	DOF	SS	MS	F	P
CS (m/min)	4	0.09	0.02	16.05	40.41
FR (mm/rev)	4	0.04	0.00	6.54	16.46
DOC (mm)	4	0.08	0.02	15.38	38.72
Error	7	0.01	0.00		4.41
Total	19	0.22	0.01		100

Figure 4.13 shows the contour plots of the effect of cutting speed (m/min) and depth of cut (mm) on surface roughness, Ra (µm). It was observed that as cutting speed increase with decrease in depth of cut, the tool wear decrease when NBCF is employed.

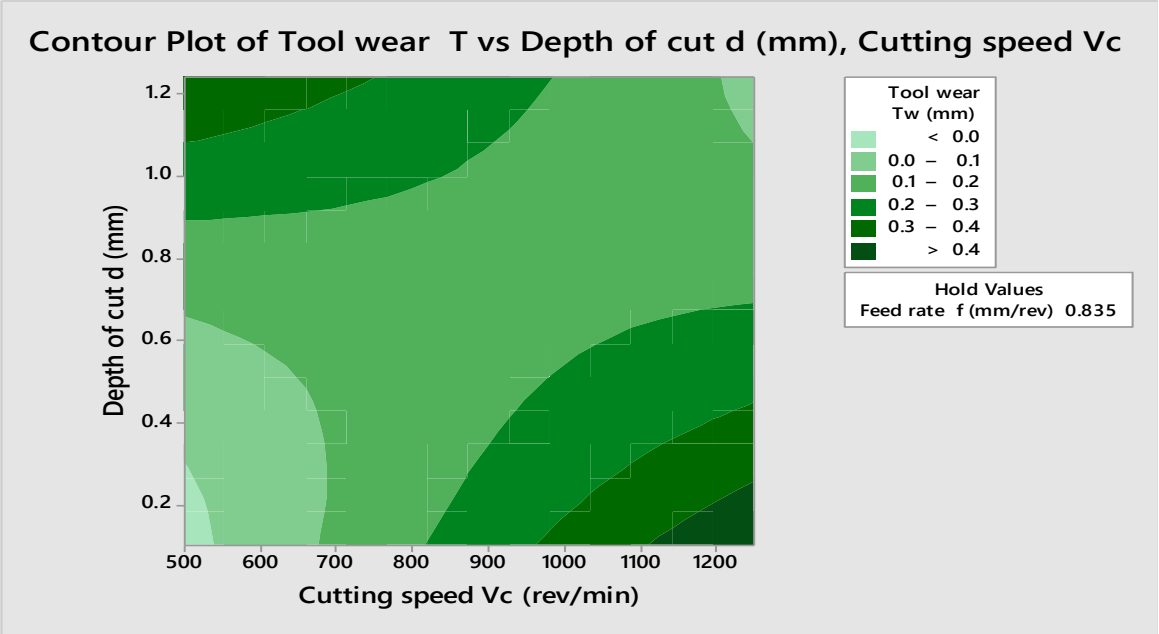

Figure 4.13: Contour plot for tool wear with NBCF

The 3D surface plot in Figure 4.14 shows the effect of cutting speed and depth of cut on the surface roughness with a flattened curve shape design model. It is observed that as cutting speed increased with depth of cut, the surface roughness increase in line with the contour plot.

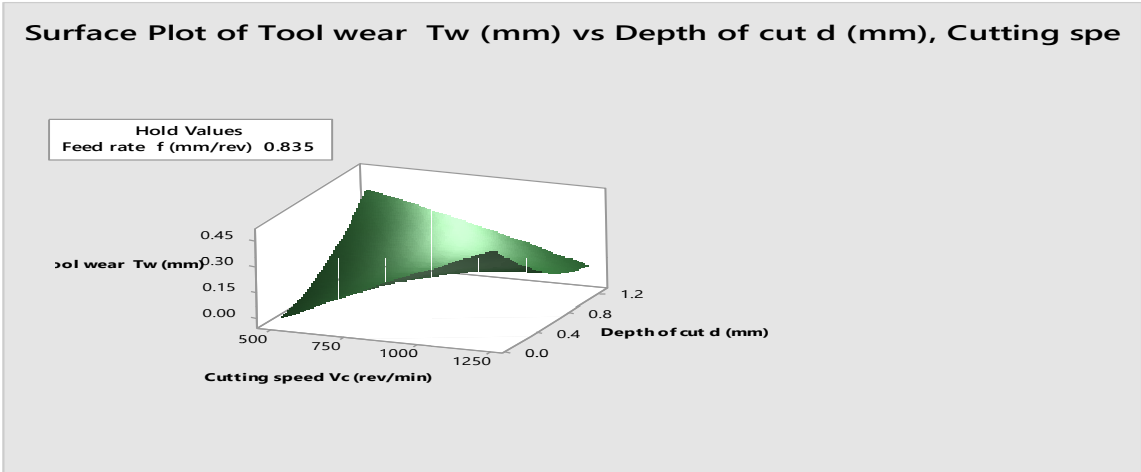

Figure 4.14: 3D surface graph for tool wear with NBCF

(c) Analysis of Variance for Tool wear Using MBCF

The ANOVA statistics as shown in Table 4.19 was employed to study the significance of the input parameters on the tool wear when cutting with MBCF. The significant effect of cutting speed, feed and depth of cut on the tool wear during cutting with NBCF are as follows: cutting

speed (CS) of (20.25%), feed rate (FR) of (20.82%) and depth of cut (DOC) of (58.37%). These results show that depth of cut has significant impact on the tool wear, followed by feed rate and cutting speed that arefound to be at close range. This indicated that depth of cut is far more significant than feed rate and cutting speed on the tool wear when turning with MBCF, and may result to poor surface roughness.

Table 4.19: ANOVA for tool wear, Tw (mm)

Factor	DOF	SS	MS	F	P
CS (m/min)					
	4	0.20	0.05	62.80	20.25
FR (mm/rev)	4	0.21	0.05	64.56	20.82
DOC (mm)	4	0.58	0.14	181.00	58.37
Error	7	0.01	0.00		0.56
Total	19	0.99	0.05		100

Figure 4.15 shows the contour plots of the effect of depth of cut (mm) and feed rate (mm/rev) on surface roughness, Ra (μm). It was observed that as depth of cut increase with decrease in feed rate, the tool wear decrease when MBCF is employed.

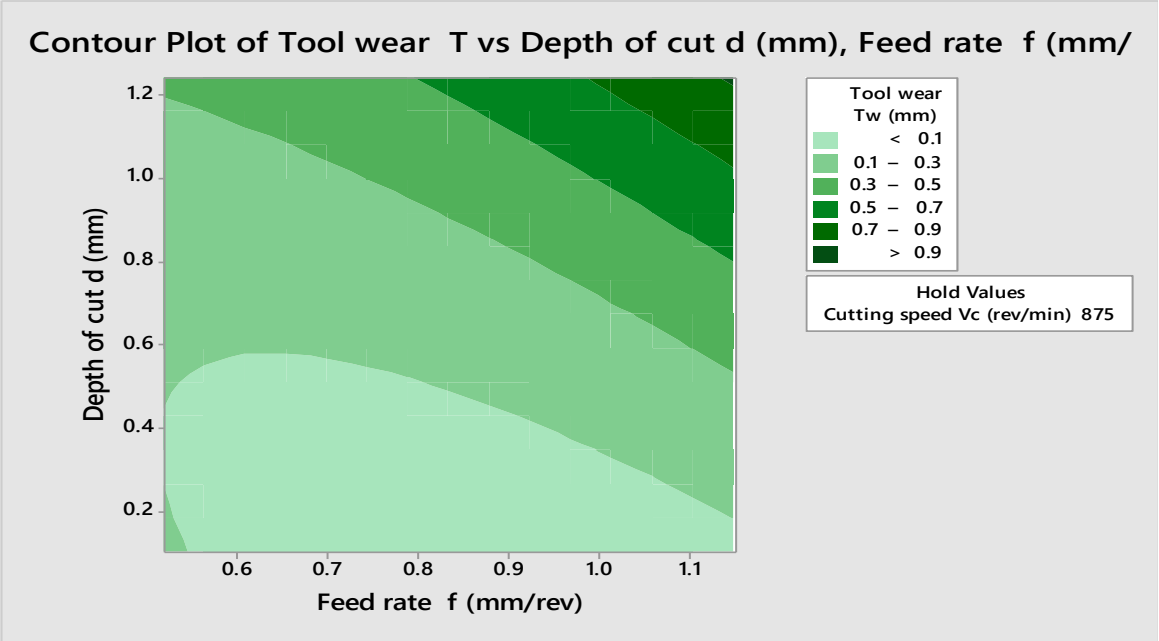

Figure 4.15: Contour plot for tool wear with MBCF

The effect of cutting speed and depth of cut on the tool wear with a flattened curve shape design model is shown in the 3D surface plot in Figure 4.16. It is observed that as depth of cut increased with feed rate, the tool wear increase in agreement with the contour plot.

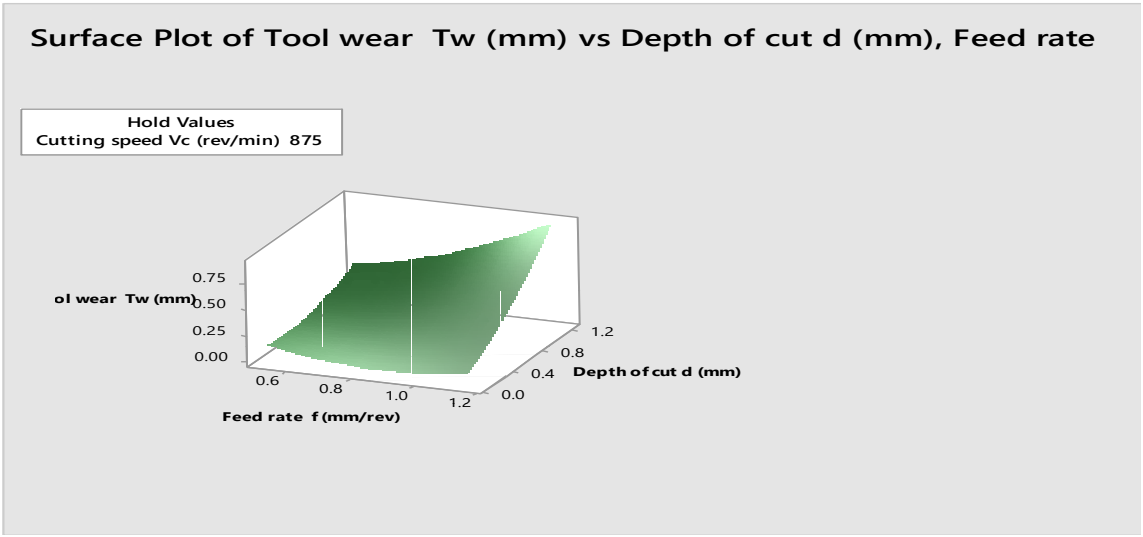

Figure 4.16: 3D surface graph for tool wear with MBCF

4.8 Interaction plot obtained from the output variables

In this study, three variables at two level (2^3) orthogonal design were studied. It is expected that 27 possible combinations of these three variables at two levels are possible; the application of

RSM method, simplified and reduced the required number of runs to 20 selected combinations that were investigated. As a result, the interaction plots obtained for output variables (surface roughness and tool wear) shows RSM method given 5 level output, explains the phenomenon of the process.

4.8.1 Interaction plot from surface roughness, Ra (μm)

The interaction plots between the cutting conditions as they affect the surface roughness are shown in Figures 4.17, 4.18 and 4.19 for JBCF, NBCF and MBCF respectively. One of the observations in the interaction plots shows that for cutting speed of 630 and 800 m/min, an interaction occurred at 1.00 mm/rev feed. An interaction between cutting speed of 800 and 1000 m/min was observed at 0.82 mm/rev feed. The different machining condition from the effect of cutting fluids shows that at lower cutting conditions: cutting speed of 630 m/min, feed of 0.65mm/rev and depth of cut of 0.30mm, there is difference in the surface roughness for all the cutting fluids. This is unconnected to the properties of cooling and lubrication of the cutting fluids at lower cutting conditions compared to cutting speed at 800 m/min, feed at 0.82 mm/rev and depth of cut at 0.65 mm at higher cutting conditions. It was found that surface roughness is below 10 % at cutting speed of 630m/min, feed of 0.65mm/rev and depth of cut of 1.00 mm machining condition for JBCF cutting fluid over mineral oil at same input parameters. Interaction plot for NBCF and MBCF are shown in Figures 4.18 and 4.19 respectively, while, the interraction plot for tool wear for the individual cutting fluids are presented in Appendix A.

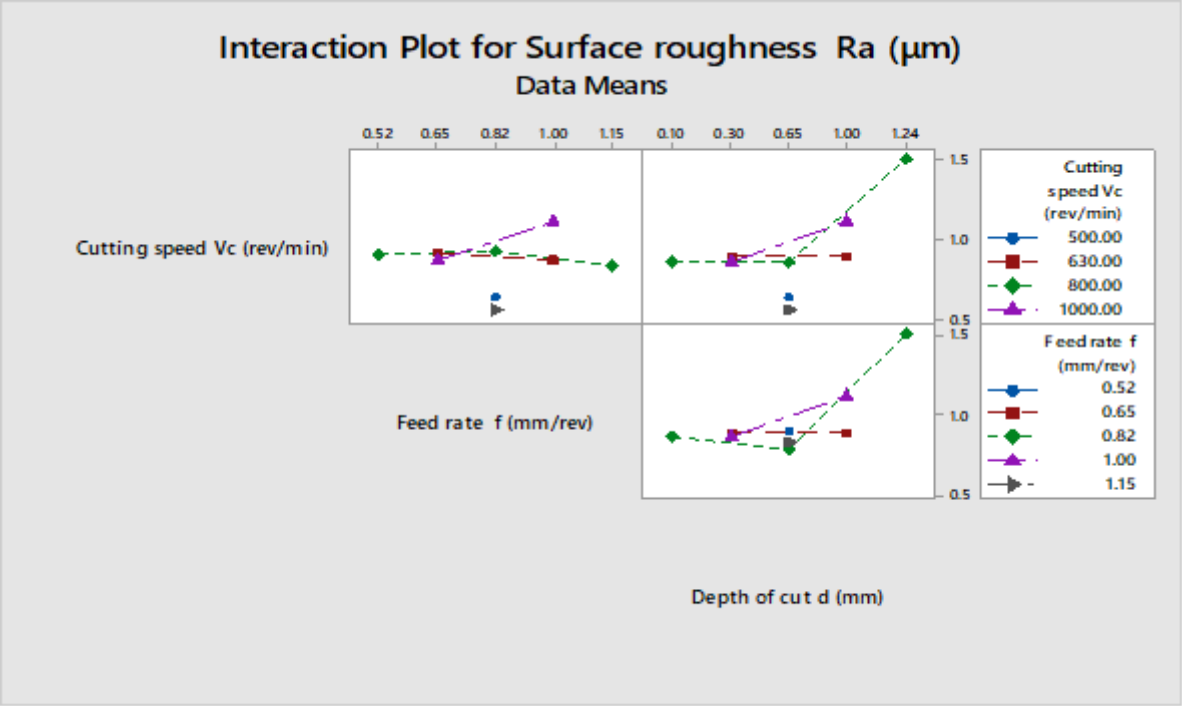

Figure 4.17: Interaction plot for surface roughness with JBCF

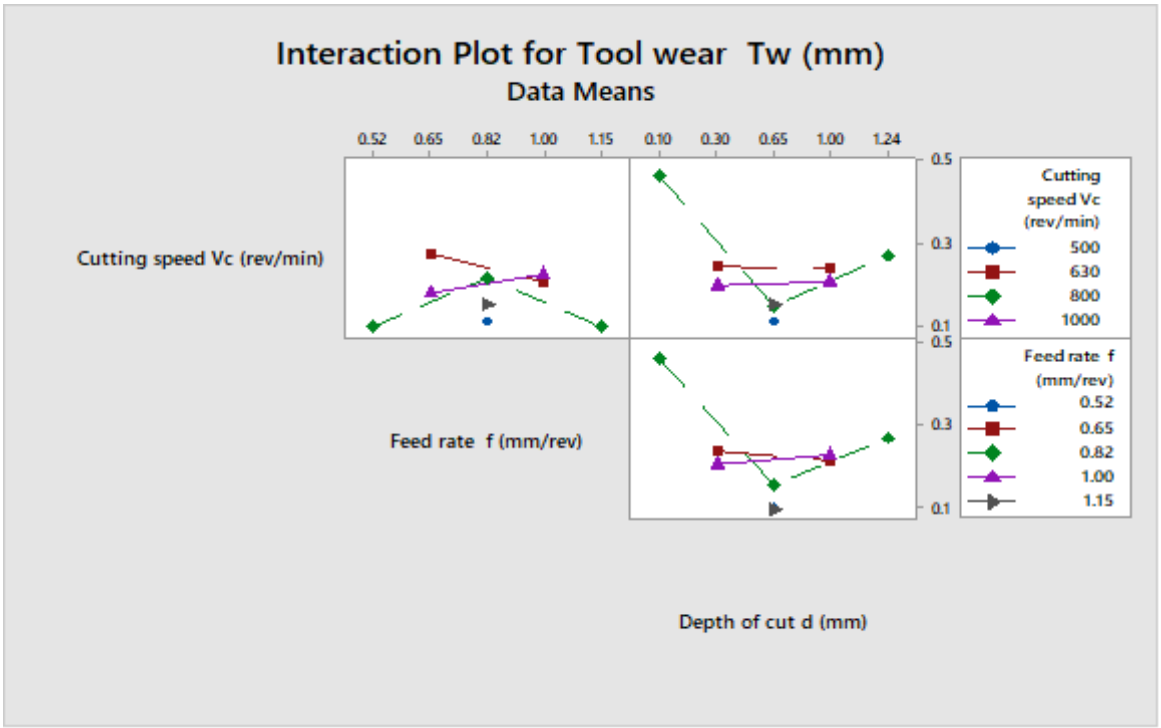

Figure 4.18: Interaction plot for surface roughness with NBCF

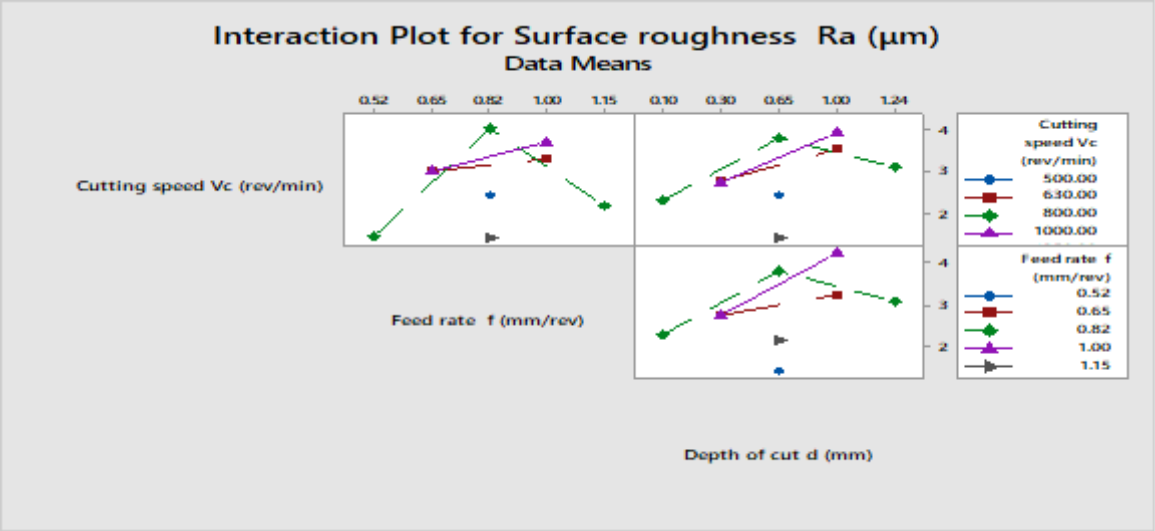

Figure 4.19: Interaction plot for surface roughness with MBCF

4.9 Grey relational analysis of the experimental results

Grey relational analysis (GRA) was conducted on the response values with the aim of compressing the multi-response parameters into a single response. The first stage of GRA involved the experimental design using RSM technique, followed by signal-to-noise (S/N) ratio calculation of responses using smaller-the better quality characteristics shown in Equation 4.3 (the smaller-the-better). The results are shown in Table 4.13. S/N ratio calculation was followed by calculation of grey relational generating (GRG) using Equation (4.4) (smaller-the-better attributes). GRG was conducted to normalize the S/N ratio values in the range between 0 and 1 (Abutu *et al.,* 2019).

$$\text{Smaller-the-better attributes} = \frac{x_{ij} - x_{ij}}{\overline{x_j} - \underline{x_j}} \qquad (4.4)$$

Where, x_{ij} is the individual response value and $\overline{x_j}$ = max $\{x_{ij}, i= 1, 2, \ldots, m\}$ and $\underline{x_j}$ = min$\{x_{ij}, i= 1, 2, \ldots, m\}$.

The GRG procedure is followed by the calculation of grey relational coefficient (GRC) using Equation (4.5)

GRC= $\frac{\Delta_{min} + \lambda\Delta_{max}}{\Delta_{ij} + \lambda\Delta_{max}}$ (i= 1, 2, ... m and j = 1, 2, . . . , n)

(4.5)

Where $\Delta_{ij} = x_{0j} - x_{ij}$ while $\Delta_{min} = \min(0)$ and $\Delta_{max} = \max(1)$

ƛ is the distinguishing coefficient, $\beta \in [0, 1]$.

Distinguishing coefficient (ƛ) is used to expand or compress the range of the GRC, leading to 0.5 is the accepted value (Abutu *et al.,* 2019).

The final stage of GRA is the calculation of grey relational grades which was obtained using Equation (4.6)

Grade = $\frac{Indivisual\ GRC}{Number\ of\ responses}$ (4.6)

The results of experimental response values along with its corresponding S/N ratio values are shown in Table 4.20 – 4.22

Table 4.21: Grey relational grade, Grey relational coefficient and Grade for JBCF

Run	Grey relational generation (GRG)		Grey relational coefficient (GRC)		Grade
	Surface roughness	Tool wear	Surface roughness	Tool wear	
X_o	1.00	1.00	0.00	0.00	0.00
1	0.43	0.14	0.47	0.37	0.42
2	0.42	0.31	0.47	0.42	0.44
3	0.14	0.09	0.37	0.36	0.36
4	1.00	0.66	1.00	0.59	**0.80**
5	0.41	0.00	0.46	0.33	0.40
6	0.43	0.35	0.47	0.43	0.45
7	0.52	0.75	0.51	0.67	0.59
8	0.43	0.36	0.47	0.44	0.45
9	0.45	0.37	0.48	0.44	0.46
10	0.40	0.40	0.46	0.45	0.46
11	0.49	0.02	0.49	0.34	0.42
12	0.48	0.57	0.49	0.54	0.51
13	0.00	0.29	0.33	0.41	0.37
14	0.46	0.58	0.48	0.54	0.51
15	0.44	0.30	0.47	0.42	0.45
16	0.42	0.34	0.46	0.43	0.45
17	0.91	0.71	0.85	0.63	**0.74**
18	0.42	0.31	0.46	0.42	0.44
19	0.44	1.00	0.47	1.00	**0.74**
20	0.47	0.62	0.49	0.57	0.53

JBCF in Table 4.21 presents the grey relational generation (GRG) using Equation (4.4) (smaller-the-better attributes) which was carried out for the 20 runs. GRG was conducted to normalize the S/N ratio values in the range between 0 and 1. The maximum value for both surface roughness and tool wear was 1.00 and minimum value of 0.00. The surface roughness and tool wear values are applicable and consistent with the research work of Abutu, (2019).

GRC value for the individual 20 runs carried with ƛ value=0.5 multiplied by the maximum changes in the individual values. The individual grade value comes from individual GRC divided by the two responses (tool wear and surface roughness for each of the runs)

Table 4.22: Grey relational generation, Grey relational coefficient and Grade for NBCF

Run	**Grey relational generation (GRG)**		**Grey relational coefficient (GRC)**		**Grade**
	Surface roughness	Tool wear	Surface roughness	Tool wear	
Xo	1.00	1.00	0.00	0.00	0.00
1	0.57	0.42	0.54	0.46	0.50
2	0.02	0.61	0.34	0.56	0.45
3	0.73	0.00	0.65	0.33	0.49
4	0.08	1.00	0.35	1.00	0.68
5	0.37	0.66	0.44	0.59	0.52
6	0.14	0.70	0.37	0.62	0.49
7	0.14	0.52	0.37	0.51	0.44
8	0.17	0.63	0.38	0.58	0.48
9	0.20	0.78	0.38	0.69	0.54
10	0.21	0.56	0.39	0.53	0.46
11	0.13	0.66	0.37	0.59	0.48
12	0.64	0.70	0.58	0.63	0.60
13	0.00	0.45	0.33	0.48	0.41
14	0.27	0.91	0.41	0.85	0.63
15	0.96	0.56	0.93	0.53	0.73
16	0.99	0.56	0.98	0.53	0.76
17	0.96	0.66	0.93	0.59	0.76
18	0.97	0.70	0.95	0.63	**0.79**
19	1.00	0.45	1.00	0.48	0.74
20	0.99	0.91	0.99	0.85	**0.92**

For the NBCF in Table 4.22, the grey relational generation (GRG) using Equation (4.4) (smaller-the-better attributes) was carried out for the 20 runs. GRG was conducted to normalize the S/N ratio values in the range between 0 and 1. The maximum value for both surface

roughness and tool wear was 1.00 and minimum value of 0.00. The surface roughness and tool wear values are consistent and applicable to the research work of (Abutu, 2019). GRC value for the individual 20 runs carried with ƛ value=0.5 multiplied by the maximum changes in the individual values as shown in Table 4.23. The individual grade value comes from individual GRC divided by the two responses (tool wear and surface roughness for each of the runs).

Table 4.23: Grey relational generation, Grey relational coefficient and Grade for MBCF

Run	**Grey relational generation (GRG)**		**Grey relational coefficient (GRC)**		**Grade**
	Surface roughness	Tool wear	Surface roughness	Tool wear	
X_o	1.000	1.000	0.00	0.00	0.00
1	0.65	0.19	0.59	0.38	0.48
2	0.45	0.01	0.48	0.34	0.41
3	0.66	0.53	0.59	0.52	0.55
4	0.59	0.17	0.55	0.38	0.46
5	0.36	0.02	0.44	0.34	0.39
6	0.80	0.56	0.71	0.53	0.62
7	0.72	0.82	0.64	0.73	0.69
8	0.95	0.20	0.91	0.38	0.65
9	0.95	0.26	0.90	0.40	0.65
10	0.94	0.21	0.90	0.39	0.64
11	0.01	0.23	0.34	0.39	0.36
12	0.58	0.15	0.55	0.37	0.46
13	0.00	0.24	0.33	0.40	0.36
14	0.51	0.24	0.51	0.40	0.45
15	0.95	0.23	0.91	0.39	0.65
16	0.95	0.25	0.90	0.40	0.65
17	1.00	1.00	1.00	1.00	**1.00**
18	0.95	0.23	0.91	0.39	0.65
19	0.40	0.00	0.46	0.33	0.39
20	0.51	0.20	0.51	0.39	0.45

GRA-Grade results along with their corresponding factor levels are shown in Table 4.24.

Table 4.24: Summary of GRA-grade values and factor levels

Run	Experimental design			GRA-Grade value		
	Cutting speed (rev/min)	Feed rate (mm/rev)	Depth of cut (mm)	Neem oil	Jathropha oil	Mineral oil
1	630.00	0.65	0.30	0.50	0.42	0.48
2	1000.00	0.65	0.30	0.45	0.44	0.41
3	630.00	1.00	0.30	0.49	0.36	0.55
4	1000.00	1.00	0.30	0.68	0.80	0.46
5	630.00	0.65	1.00	0.52	0.40	0.39
6	1000.00	0.65	1.00	0.49	0.45	0.62
7	630.00	1.00	1.00	0.44	0.59	0.69
8	1000.00	1.00	1.00	0.48	0.45	0.65
9	500.00	0.82	0.65	0.54	0.46	0.65
10	1250.00	0.82	0.65	0.46	0.45	0.64
11	800.00	0.52	0.65	0.48	0.42	0.36
12	800.00	1.15	0.65	0.60	0.51	0.46
13	800.00	0.82	0.10	0.41	0.37	0.36
14	800.00	0.82	1.24	0.63	0.51	0.45
15	800.00	0.82	0.65	0.73	0.45	0.65
16	800.00	0.82	0.65	0.76	0.45	0.65
17	800.00	0.82	0.65	0.76	0.74	1.00
18	800.00	0.82	0.65	0.79	0.44	0.65
19	800.00	0.82	0.65	0.74	0.74	0.39
20	800.00	0.82	0.65	0.92	0.53	0.45

4.10 Main Effects Factor Levels

The factor effects for jathropha oil, neem oil and mineral oil shown in Table 4.25, 4.26 and 4.27 respectively were obtained using the Grade values from GRA as presented in Table 4.24.

Table 4.25: Resulting factor effects of experimental factors (jathropha oil)

Factor level	Cutting speed (rev/min)	Feed rate (mm/rev)	Depth of cut (mm)

Level 1	0.46	0.42	0.37
Level 2	0.44	0.43	0.50
Level 3	0.51	0.51	0.52
Level 4	0.54	0.55	0.47
Level 5	0.45	0.51	0.51

Table 4.26: Resulting factor effects of experimental factors (neem oil)

Factor level	Cutting speed (rev/min)	Feed rate (mm/rev)	Depth of cut (mm)
Level 1	0.54	0.48	0.41
Level 2	0.49	0.49	0.53
Level 3	0.68	0.67	0.68
Level 4	0.52	0.52	0.48
Level 5	0.46	0.60	0.63

Table 4.27: Resulting factor effects of experimental factors (mineral oil)

Factor level	Cutting speed (rev/min)	Feed rate (mm/rev)	Depth of cut (mm)
Level 1	0.65	0.36	0.36
Level 2	0.53	0.47	0.48
Level 3	0.54	0.59	0.59
Level 4	0.53	0.59	0.59
Level 5	0.64	0.46	0.45

4.11 Main Effect Plots for GRA

The main effect plots for GRA shows Figures 4.20 – 4.22 specified the optimal factor levels of composite composition. These plots were obtained using the factor levels of main effects shown in Table 4.25-4.27.

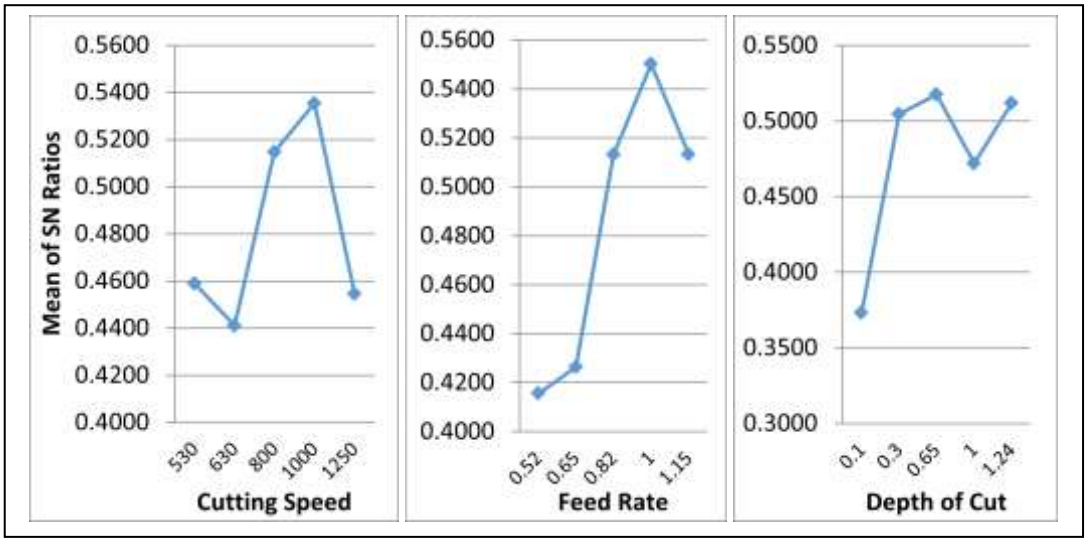

Figure 4.20: Main effect plot for GRA (jathropha oil)

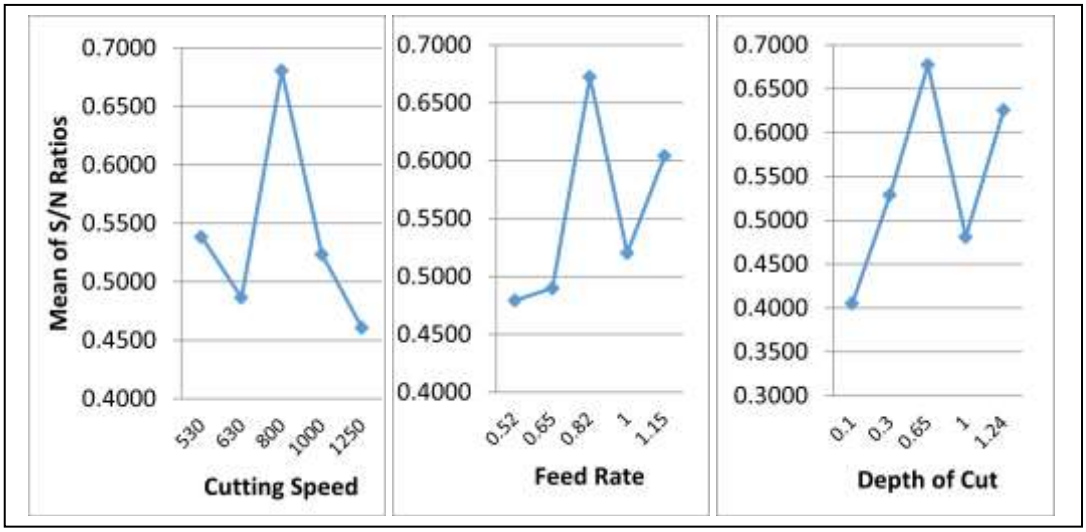

Figure 4.21: Main effect plot for GRA (neem oil)

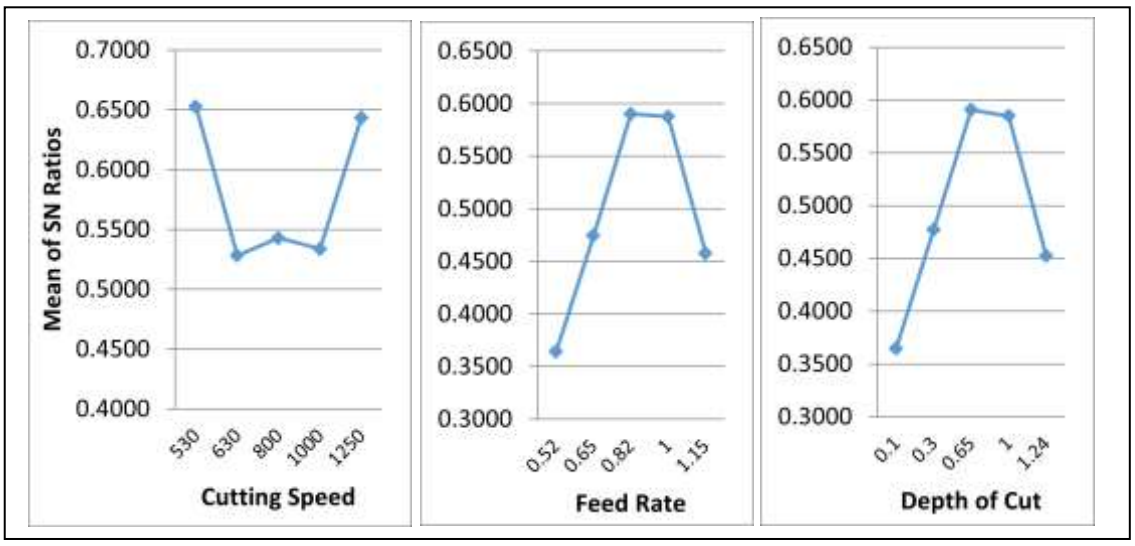

Figure 4.22: Main effect plot for GRA (mineral oil)

As shown in Figure 4.20, it can be observed that multi-response optimal factor combination for JBCF are cutting speed of 1000 rev/min, feed rate of 1 mm/rev and depth of cut of 0.65 mm while, Figure 4.21 indicates that the multi-response optimal factor combination for NBCF are cutting speed of 800 rev/min, feed rate of 0.82 mm/rev and depth of cut of 0.65 mm and finally, Figure 4.22 indicates that multi-response optimal factor combination for MBCF are cutting speed of 530 rev/min, feed rate of 0.82 mm/rev and depth of cut of 0.65 mm. Any change in the optimal factor level combination may affect the performance of the individual oil.

4.12 Confirmation test

Regression analysis through design expert statistical software were employed to obtain the mathematical models for the selected cutting parameters including cutting speed, feed rate and depth of cut. Table 4.28 present the results of the model, the values from the experiment and the percentages error.

$$Percentage\ error\ (E) = \frac{Experimental\ (Ex) value - Calculated\ (Cc)\ value}{Experimental\ (Ex)\ value} \times 100$$

Table 4.28: Percentage Error Confirmation Test

Cutting Fluids	Response	Calculated value	Experimental value	Percentage Error (%)
JBCF	Surface roughness (µm)	0.9102	0.9267	1.78
	Tool wear (mm)	0.7126	0.7333	1.10

NBCF	Surface roughness (µm)	1.2513	1.3067	2.82
	Tool wear (mm)	0.3593	0.3633	4.24
MBCF	Surface roughness (µm)	0.3724	0.3833	2.84
	Tool wear (mm)	0.5506	0.5600	1.68

The R^2 for any multiple linear regression analysis is expected to be within 0.8 and 1.0 as revealed by Montgomery *et al*, (1998). However, this work show that regression results compares favourably. The whole R^2 values from both surface roughness and tool wear agrees with the regression models for both responses in the three cutting fluids.

CHAPTER FIVE

5.0 CONCLUSION AND RECOMMENDATIONS

5.1 Conclusion

In this study, the experimental evaluation and optimisation of tool wear and surface roughness as responses in turning AISI 304 alloy steel with coated carbide using RSM has been exploited. The study can be categorised into three basic sections. The first part required formulation and characterisation of the cutting fluids from jatropha seed oil and neem seed oil needed for the evaluation of the responses. Detailed properties of these oils were carried out as it affects their uses as cutting fluids, with the water to oil ratio of 9:1 and using four different additives. The

second part employed surface roughness tester, Dinolite digital measuring microscope and RSM design of experiment (DOE) using Minitab software to simplify and minimised the needed machining runs in order to achieve the needed optimal result from the responses. The performance of the individual responses on the input parameters were accessed using RSM method through the evaluation and optimisation of the turning parameters. The findings from a comparative study of these responses are hereby summarized in this chapter. Furthermore, some recommendations have been made for future work.

The fatty acid composition results for the two oil samples shows that jatropha seed oil has an approximately 21.6% saturated fat with the main contributors being 14.2 % palmitic acid and 7% stearic acid. About 78.4% of jatropha seed oil is unsaturated fatty acid with 44.7% oleic acid and 32.8% linoleic acid. Neem seed oil has approximately 37.0% saturated fat with the main contributors being 18.1% each of palmitic acid and stearic acid. About 63.0% is unsaturated with 44.5% oleic acid and 18.3% linoleic acid. The study showcase the difference in the composition of fatty acid which affected their individual performances as cutting fluid using coated carbide tool in turning AISI 304 alloy steel.

Three samples A, B, and C were adopted for preparing oil-based cutting fluid, and were experimentally evaluated to check their individual pH, stability, viscosity and corrosion for each of the samples with the desirable optimal values for the formulation variables are as follows: anticorrosion = 10.61%; antioxidant = 0.64%; Bioxide = 0.97% and emulsifier = 9.35%;

The pH, stability, corrosion and viscosity tests were carried out for the individual adopted samples. ASTM D 445 was for standard viscosity test of 0.47 mm^2/s JSO and 0.44 mm^2/s NSO, whereas, ASTM D 4627 was for corrosion test. Stability test was carried out 72 hours for each sample with JA and NC samples highly stable, boasting 95% and 92% volume of water respectively. The pH test value for JSO and NSO were 8.36 and 8.67 respectively.

The evaluation from the Orthogonal optimal turning parameters for the surface roughness are: 1250 m/min of cutting speed (level 5), 1.15 mm/rev of feed (level 5), 0.65 mm depth of cut

(level 3) with JBCF. The surface roughness optimal turning parameters for NBCF are 1000 m/min of cutting speed (level 4), 0.52 mm/rev of feed (level 1), 0.10 mm depth of cut (level 1). Also, 1250 m/min of cutting speed (level 5), 0.52 mm/rev of feed (level 1), 0.65 mm depth of cut (level 3) was recorded for MBCF surface roughness.

The ANOVA shows the contribution of the input parameters contribution of cutting speed, feed, and depth of cut as follows: JBCF = cutting speed (CS) of 27.39%, feed rate (FR) of 6.16% and depth of cut (DOC) of 62.73% respectively for surface roughness; NBCF = cutting speed (CS) of 37.26%, feed rate (FR) of 24.78% and depth of cut (DOC) of 36.74%; MBCF = cutting speed (CS) of 33.69%, feed rate (FR) of 38.29% and depth of cut (DOC) of 24.53%.

The ANOVA show that DOC, CS and FR has more significant effect on the surface roughness with DOC (62.73%) for JBCF, follow by cutting speed (37.26%) for NBCF and, also feed rate (38.29%) for MBCF respectively.

The tool wear optimal turning parameters are 500 m/min of cutting speed (level 1), 1.15 mm/rev of feed (level 5), 0.65 mm depth of cut (level 3) for JBCF; 630 m/min of cutting speed (level 2), 1.0 mm/rev of feed (level 4), 0.10 mm depth of cut (level 1) for NBCF and 500 m/min of cutting speed (level 1), 1.15 mm/rev of feed (level 5), 0.10 mm depth of cut (level 1) for MBCF.

ANOVA was used to study the significance of the input parameters on the tool wear. The significant effects of cutting speed, feed, depth of cut and cutting fluids on the tool wear are as follow: cutting speed (CS) of 10.62%, feed rate (FR) of 15.29% and depth of cut (DOC) of 70.83% for JBCF; cutting speed (CS) of 40.41%, feed rate (FR) of 16.46% and depth of cut (DOC) of 38.72% for NBCF and cutting speed (CS) of 20.25%, feed rate (FR) of 20.82% and depth of cut (DOC) of 58.37% for MBCF.

The ANOVA show that DOC, FR and DOC has more significant effect on the tool wear with DOC (70.83%) for JBCF, follow by feed (40.41%) for NBCF and, also depth of cut (58.37%) for MBCF respectively.

The DOC in terms of ANOVA shows optimum significance in the overall performance of the

input parameters on both surface roughness and tool wear responses with the individual experimented cutting fluids.

The multiple regression analysis indicates the fitness of experimental measurements. The regression models obtained are as follow: Surface roughness R^2 = 85.14%, R^2 (adj) = 71.76%, tool wear R^2 = 71.24%, R^2 (adj) = 56.35% for JBCF; surface roughness (R^2 = 82.88%) R^2 (adj) = 67.46%, tool wear (R^2 = 63.75 %) R^2 (adj) = 57.13% for NBCF and surface roughness (R^2 = 84.44%) R-sq (adj) = 70.43%, tool wear (R^2 = 70.48 %) R-sq (adj) = 55.92% for MBCF. These measurements gave a close fit with the experimental data.

The regressional models obtained proved that JBCF with surface roughness and tool wear of R^2 of 85.14%, R^2 (adj) = 71.76% and 71.24%, R^2 (adj) = 56.35% respectively, performs better in machining process than NBCF. This is followed by MBCF employed in the machining operation.

The multi-response optimal factor combinations are as follows: for the JBCF are cutting speed (1000 rev/min), feed rate (1 mm/rev) and depth of cut (0.65 mm), while, for the NBCF are cutting speed (800 rev/min), feed rate (0.82 mm/rev) and depth of cut (0.65 mm) and for the MBCF are cutting speed (530 rev/min), feed rate (0.82 mm/rev) and depth of cut (0.65 mm). The performance of the individual oil may be affected if there is any change in the optimal factor level combination.

The experimental study shows that: JBCF and NBCF could be used in machining process with potential ability to reduce related health risks, better performance rate compared to MBCF, and lower costs towards waste treatment due to their higher bio-degrability.

5.2 Recommendation

There is need for extended study to evaluate and optimise formulated JBCF, NBCF with MBCF and to address other machining variables like cutting force, coefficient of friction, cutting temperature, chip formation which will further contribute to the machining industries achieving

suitable machining products.

5.3 Contribution of the Study to Knowledge

This study has contributed to knowledge in the following aspects:

The JBCF optimum values of 1250 m/min of cutting speed (level 5), 1.15 mm/rev of feed (level 5), 0.65 mm depth of cut (level 3), and the NBCF optimum values of 1000 m/min of cutting speed (level 4), 0.52 mm/rev of feed (level 1), 0.10 mm depth of cut (level 1) can be used as cutting fluids during turning of AISI 304 alloy steel, as both shows improved performance over MBCF. The two formulated cutting fluids are indigenous vegetable cutting fluids that can be used to replace the conventional mineral based cutting fluid. The optimal combined multi-response performance of JBCF (0.740µm and 0.800mm) and NBCF (0.920µm and 0.79mm) shows minimal surface roughness and tool wear respectively compared to MBCF (1.00µm and 1.00mm).